Technische Universität München
Max-Planck-Institut für Biochemie
Abteilung für Molekulare Strukturbiologie

Structural Studies of Tripeptidylpeptidase II: Expression and Crystallization Trials

Gönül Seyit

Vollständiger Abdruck der von der Fakultät für Chemie der Technischen Universität München zur Erlangung des akademischen Grades eines Doktors der Naturwissenschaften (Dr. rer. nat.) genehmigten Dissertation.

Vorsitzende:	Univ.-Prof. Dr. Johannes Buchner
Prüfer der Dissertation:	1. Hon.-Prof. Dr. Wolfgang Baumeister
	2. Univ.-Prof. Dr. Sevil Weinkauf

Die Dissertation wurde am 28.09.2006 bei der Technischen Universität München eingereicht und durch die Fakultät für Chemie am 05.12.2006 angenommen.

1. Summary

Tripeptidylpeptidase II (TPP II) exists as a spindle-shaped, 6 MDa homo-oligomeric complex composed of two segmented strands. The segments of each strand contain two monomers in a head-to-head orientation. TPP II is an amino peptidase of the subtilisin type, which is fully active only in its fully assembled state. The enzyme cleaves proteasome-generated peptides and is considered a key component of the proteolytic cascade in eukaryotes. Presently, understanding the function of TPP II on the molecular level awaits determination of a high-resolution structure.

In the present study, the recombinant expression of *Drosophila* TPP II in *Escherichia coli* was established. In *E. coli,* TPP II assembled autonomously into the fully active spindles, a quaternary structure that apparently confers stability to the enzyme. By MBP-tagging, the N-terminal region of TPP II monomers was shown to be essential for holocomplex formation.

The concatameric architecture of TPP II leads to a plethora of size variants *in vitro*, depending on the enzyme concentration. This inherent heterogeneity has probably been the major obstacle hampering both, accurate biochemical characterization and the crystallization of the enzyme since its discovery more than two decades ago. In the present work, a novel, highly efficient purification method was developed, and a systematic approach was used to generate homogeneous and stable fragments of the complex. Mutational approaches generally led to the formation of soluble aggregates, whereas physical disassembly methods resulted in reversible disassembly of the complex. TPP II disassembled irreversibly only when chemically modified. In the presence of the non-ionic detergent β-octyl glucoside, the complexes were dissected into stable tetramers and preliminary crystals of TPP II were obtained.

2. Introduction

2.1 Cellular Proteolysis

Cellular proteins are in a dynamic state of constant renewal – that is, they are continuously degraded and synthesized (Schoenheimer, 1942). Protein degradation in the cytosol is a regulated process and it is involved in controlling a broad array of biological processes, such as cell cycle, apoptosis, signal transduction, antigen presentation, transcription, DNA repair, stress response and protein quality control. The ubiquitin-proteasome cascade is the major proteolytic system in the cytosol of eukaryotic cells. The majority of the substrates are targeted for degradation by ubiquitination (Ciechanover, 2005; Ciehanover et al., 1978). The ubiquitinated proteins are bound by the 26S proteasome, unfolded and degraded into oligopeptides of 3-22 amino acids (Baumeister et al., 1998; Kisselev et al., 1999). The majority of the proteasome-generated oligopeptides then need to be further processed by peptidases. Tripeptidylpeptidase II (TPP II), a subtilisin-like serine peptidase displaying both exo- and endo-peptidolytic activities (Balow et al., 1983; Geier et al., 1999; Seifert et al., 2003), cleaves the proteasome products (Reits et al., 2004; York et al., 2006) to produce antigenic peptides and short peptides that can be used as substrates by other exopeptidases.

2.2 Cellular roles of TPP II

In eukaryotes TPP II has a broad tissue and species distribution (Balow and Eriksson, 1987; Balow et al., 1986; Tomkinson, 1994; Tomkinson, 1995), but little is known about its physiological function. TPP II has been shown to play key roles in major histocompatibility complex class I (MHC class I) antigen presentation and in general intracellular protein turnover.

It is now well established that the correct size of antigenic peptides is necessary for a stable binding to MHC class I molecules. Proteasomes degrade proteins to produce either polypeptides with the correct size for presentation or antigenic precursors with N-terminal extensions. Subsequently, the aminopeptidases in the endoplasmic reticulum or in the cytosol trim the N-terminal extensions of these proteasome-generated antigenic precursors. Recently, several studies suggested a role of TPP II in the processing of antigenic peptides

in the cytosol (Kloetzel, 2004; Kloetzel and Ossendorp, 2004; Saveanu et al., 2005). Using the specific inhibitor butabindide and RNA interference experiments, Reits et al. showed that inhibition of TPP II inhibited the export of MHC class I molecules to the cell surface (Reits et al., 2004). The same effect was observed when proteasome inhibitors were used, suggesting that the two proteases functioned in the same pathway (Reits et al., 2004). TPP II is the major peptidase capable of processing proteasome products of 14-17 amino acids *in vivo* (York et al., 2006). However, only a minority of the proteasome-generated peptides fall into this class and TPP II, unlike the proteasome, is not essential for generation of most presented peptides (York et al., 2006). Additional experimental evidence for the role of TPP II in antigen processing has been provided by Levy et al. The authors reported the involvement of TPP II in generation of the $RU1_{34-42}$ epitope by N - terminal trimming of its proteasome-generated precursor. Depending on the N - terminal extension of the precursor peptide, TPP II acted either sequentially or redundantly with puromycin-sensitive aminopeptidase (PSA), and inhibition of these peptidases abolished the CTL-mediated recognition of antigen expressing cells (Levy et al., 2002).

Although involved in N-terminal trimming of some antigenic peptide precursors, TPP II does not cleave within the antigenic peptides. Therefore, TPP II may also play a role in protecting antigenic peptides from their complete degradation in the cytosol (Burri et al., 2002).

Besides its role in post-proteasomal antigen processing, TPP II can generate the human immunodeficiency virus (HIV) epitope Nef_{73-82}, by two endo-peptidolytic cleavages, independently of the proteasome (Herberts et al., 2003; Seifert et al., 2003). This antigenic peptide, which can be generated *in vitro* by purified TPP II alone, but not by proteasomes, has a lysine at the C-terminus. Since, as an endo-peptidase, TPP II has a preference for cleavage after lysine residues (Geier et al., 1999; Seifert et al., 2003), it may be involved in the generation of antigenic ligands with a C-terminal lysine residue, which are not produced by proteasomes (Tenzer et al., 2005).

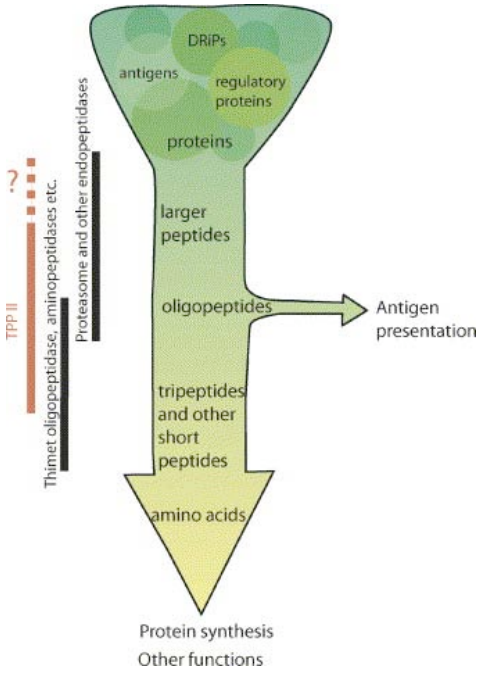

Figure 2.1. The role of TPP II in cytosolic protein degradation (Tomkinson and Lindas, 2005). Majority of the cellular proteins are degraded by cytosolic peptidases to produce free amino acids, whereas only a small fraction of peptides are processed for antigen presentation. The proteasome and other endopeptidases initiate the degradation of targeted proteins such as DRiPs (defective ribosomal products), some rapidly degraded regulatory proteins (e.g. cyclins) and potential antigens. The role of TPP II in this process is not well established. TPP II may cleave proteasome products and generate short peptides, which can be recognized by other exopeptidases. Additionally, TPP II may also assume some of the functions of the proteasome.

Recently, TPP II has been suggested to compensate for the loss of some of the proteasome activities. Cells adapted to lethal concentrations of the proteasome inhibitor 4-hydroxy-5-iodo-3-nitrophenylacetyl-Leu-Leu-leucinal-vinyl sulfone (NLVS) displayed high TPP II activity (Glas et al., 1998). Also, over-expression of TPP II in NLVS-selected EL-4 cells apparently prevented the accumulation of polyubiquitinated proteins and partially restored peptide loading to MHC class I molecules (Wang et al., 2000). However, proteasomes purified from the NLVS-adapted cells lack the chymotryptic-like activity, but still exhibited residual activity to degrade longer peptide substrates (Wang et al., 2000). Apparently, the NLVS-resistant cells still depended on this residual proteasome activity for the degradation of polyubiquitinated proteins, antigen presentation and cell viability (Princiotta et al., 2001). An up-regulation of TPP II activity accompanied by decreased proteasomal activity was observed in apoptosis resistant tumour cells (Hong et al., 2003). Also, in Burkitt's lymphoma (BL) cells, which are resistant to apoptosis, TPP II was

upregulated. Its inhibition led to apoptosis suggesting that the enzyme is required for the survival of BL cells (Gavioli et al., 2001). Taken together, a general proteasome-backup role of TPP II does not appear likely. Nevertheless, TPP II seems to be one of the proteases that are critical for cell survival when the proteasome activity is sub-optimal.

An increased activity and expression of TPP II, accompanied by high proteasome activity, was found during sepsis and cancer cachexia (Chand et al., 2005; Hasselgren et al., 2002; Wray et al., 2002). Therefore, in accordance with the assumed role of TPP II in general protein turnover, it appears to be involved in substantial proteolytic degradation taking place in these pathological conditions.

TPP II purified from human cerebral cortex has been shown to cleave tripeptides from several naturally occurring neuropeptides, with a broad specificity (Wilson et al., 1993). Aside from soluble TPP II, a membrane-bound variant of the enzyme was identified, which degrades the neuropeptide choleocystokinin (Rose et al., 1996). This TPP II-variant is thought to be anchored in the lipid bilayer by a covalent glycosyl phosphatidyl inositol (GPI) link, since there is no membrane-spanning region in the sequence. The membrane-bound form, like the cytosolic TPP II, is widely distributed in various tissue types, but it is less abundant (Rose et al., 1996).

Is TPP II essential for cell survival? Book et al. aimed at finding an answer to this question through T-DNA disruption of the TPP II gene in *Arabidopsis* (Book et al., 2005). Although the TPP II gene is broadly expressed in various tissue types in *Arabidopsis*, and homologues are present in other plant genomes, it is apparently not essential (Book et al., 2005). Therefore, in plants, TPP II may act redundantly with other peptidases, which can compensate for its absence. Knockout flies and mice lacking TPP II expression would reveal whether TPP II is essential in animals.

2.3 Peptidase activity of TPP II

The major activity of TPP II is successive cleavage of tripeptides from the free N-termini of oligopeptides (Tomkinson, 2004). The enzyme requires a free α-amino group of the substrate, since it can not cleave succinyl-Ala-Ala-Phe-paranitroanilide (Suc-AAF-pNA). The pH optimum is in the neutral range. The substrate specificity is broad, although the rate of cleavage may vary more than 100-fold between different substrates (Balow et al., 1983; Balow et al., 1986). *In vitro* TPP II has the highest activity towards the fluorogenic

tripeptide H-Ala-Ala-Phe-aminomethyl-coumarin (AAF-AMC) (Geier et al., 1999). As an exo-peptidase, TPP II can not cleave peptide bonds before or after a proline residue (Balow et al., 1983; Balow et al., 1986). Interestingly, as an endo-peptidase, TPP II can cleave after proline residues (Seifert et al., 2003). The largest polypeptide used as TPP II substrate thus far, is an ovalbumin fragment of 41 amino acids, which was cleaved by TPP II both exo- and endo-proteolytically (Geier et al., 1999). The peptides generated by TPP II ranged from 7 to 27 amino acids. The endo-proteolytic cleavage sites are frequently located at the carboxyl side of Lys (K) or Arg (R) residues, suggesting a predominant trypsin like activity (Geier et al., 1999; Seifert et al., 2003). I*n vitro*, purified TPP II has been shown to cleave peptides ranging between 6 to 30 residues at similar rates (York et al., 2006), whereas *in vivo,* TPP II degrades peptides longer than 15 amino acids (Reits et al., 2004).
No natural inhibitors of TPP II have been identified thus far. Butabindide was designed as a potent, highly specific, competitive inhibitor (IC_{50} = 7 nM) of TPP II (Rose et al., 1996). Also analogues of butabindide were designed as TPP II inhibitors with higher stability (Breslin et al., 2003; Breslin et al., 2002; Ganellin et al., 2005).

2.4 Structure of TPP II

The atomic-resolution structure of TPP II has not yet been determined. Presently, the information about the structure of TPP II comes from the homology alignments of the amino acid sequence, modelling studies and from single-particle electron microscopy and 3D reconstruction studies.
Based on the sequence similarities to the subtilases in the N-terminal domain, TPP II has been classified as a serine protease of the subtilisin-type (Siezen and Leunissen, 1997; Tomkinson and Jonsson, 1991; Tomkinson et al., 1987). According to the homology modelling with known crystal structures of other subtilases, the catalytic domain has been predicted to contain the N-terminal approximately 528 residues (De Winter et al., 2005). The active site serine residue has been identified by sequence analysis of the ^{3}H-labeled tryptic fragments of human TPP II (Tomkinson et al., 1987). Through site-directed mutagenesis studies, Asp-44, His-264 and Ser-449 were shown to form the catalytic triad of human TPP II, and Asn-362 to potentially stabilize the oxyanion in the transition state (Hilbi et al., 2002).

Sequence alignments revealed an insert of ~200 residues between the catalytic Asp and His of TPP II, which is not present in subtilisin (L1 in Figure 2.2). This insert was suggested to be involved in complex formation, since a G252R mutation in this region led to interference in oligomerization and to inactivation (Tomkinson et al., 2002). Interestingly, an insert of ~150 amino acids between the catalytic Asp and His residues is also present in Pyrolysin, which is a membrane-bound subtilase from the hyperthermostable archaeon *Pyrococcus furiosus* and the closest homolog of TPP II on amino acid level (de Vos et al., 2001).

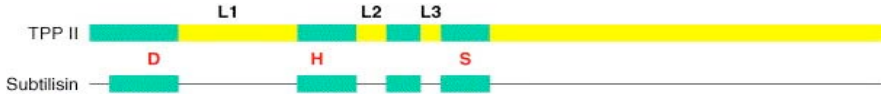

Figure 2.2. Schematic overview of the sequence alignment between TPP II and subtilisin (De Winter et al., 2005). Green boxes represent regions of homology; yellow boxes are regions within the TPP II sequence for which there is no sequence similarity to subtilisin. The approximate positions of the three catalytic residues (D, H and S) are indicated along both sequences.

In addition to the insert in the catalytic, N-terminal domain, TPP II has a long C-terminal extension (Figure 2.2), which is not homologous to any protein in the database. This C-terminal part is conserved among the TPP II homologues, except that insect, worm, plant and fungal forms carry additional inserts as compared to mammalian TPP II.

Electron microscopic investigations have shown that TPP II forms giant "double-bow" oligomers (Harris and Tomkinson, 1990; Macpherson et al., 1987). The 3D structure of the TPP II complex from *Drosophila* has been extensively studied by single-particle cryo-electron microscopy and thus far it has been resolved to 2.2 nm (Rockel et al., 2005). *Drosophila* TPP II assembles into a 6 MDa complex of 60 x 28 nm (Figure 2.3). The spindle-shaped holocomplex is composed of two twisted strands (bows), each containing 10 segments. Each segment is composed of two, head-to-head oriented monomers of 150 kDa (Rockel et al., 2005).

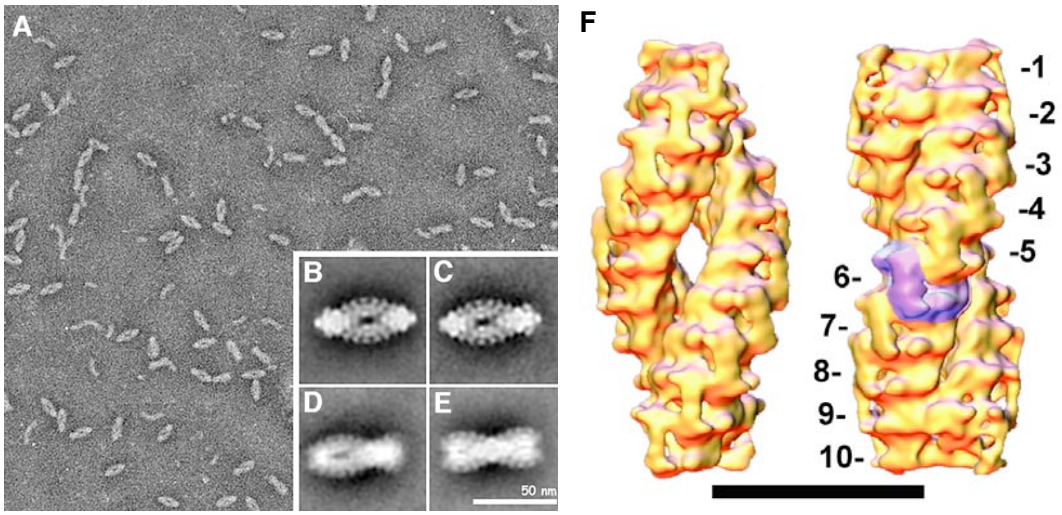

Figure 2.3. Structure of TPP II (Rockel et al., 2002; Rockel et al., 2005). A, Electron micrograph of TPP II purified from *Drosophila melanogaster*. B-E, class averages of the TPP II holocomplexes: B, spindle view; C and D, views with off-center constrictions; E, dumbbell view. F, Surface representations of TPP II model as obtained by single-particle electron microscopy and 3D reconstruction; left, spindle orientation; right, dumbbell orientation. Segments of one of the strands are numbered. Segment six is highlighted in purple. Scale bar: 30 nm.

In the TPP II preparations obtained from human erythrocytes (Macpherson et al., 1987) or from *Drosophila* (Rockel et al., 2002), the spindles are the predominant oligomeric form (Figure 2.3A). The spindles were thus suggested to have an enhanced stability owing to a dimerization motif called "double clamp" at the spindle poles as shown in Figure 2.4 (Rockel et al., 2005).

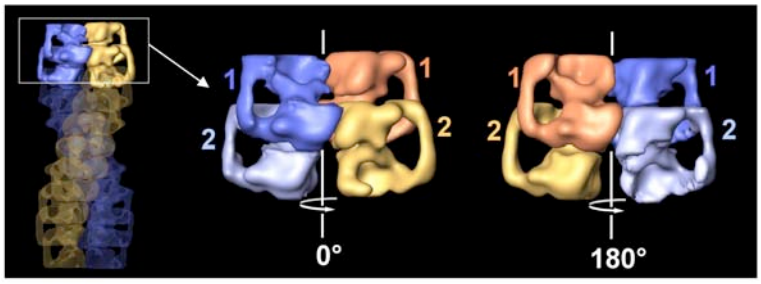

Figure 2.4. The double clamp stabilizing the TPP II spindles (Rockel et al., 2005). The terminal dimer (1) of one strand "locks" the two terminal dimers (1 and 2) of the counterpart strand.

In contrast to the single strands, the spindles have a defined length. Thus, the double clamp might also be crucial for length determination (Rockel et al., 2005).

Although the spindle seems to be the preferred state *in vivo*, the size of the TPP II oligomers is variable *in vitro*, as shown by size exclusion chromatography (Renn et al.,

1998; Tomkinson, 2000) and electron microscopy (Macpherson et al., 1987; Rockel et al., 2005; Seyit et al., 2006). TPP II can form extended spindles, or disassemble into single bows or lower oligomers, depending on the conditions. This inherent heterogeneity is attributable to the linear concatameric architecture of TPP II and is fundamentally different from that of the other oligomeric proteases which form discrete structures such as the 20S proteasome, which has a barrel-shaped structure composed of up to four rings (Baumeister et al., 1998); TET protease, forming tetrahedral oligomers (Borissenko and Groll, 2005); or the *archaeal* functional homologue of TPP II, tricorn protease, which forms icosahedral capsids composed of hexamers (Walz et al., 1997).

2.5 Size-activity relationship

Spindle formation is a prerequisite for full activity of TPP II (Macpherson et al., 1987; Tomkinson, 2000). The dimers have specific activity of about 1/10th of the spindle activity, and are assumed to be the smallest active form (Seyit et al., 2006; Tomkinson, 2000), although one report indicates that monomers also have proteolytic activity (Wilson et al., 1993).

In a recent study, the specific activity of *Drosophila* TPP II was shown to be correlated with strand length in a hyperbolic fashion and a mechanism of assembly and activation was proposed (Seyit et al., 2006). According to this mechanism, upon addition of a new dimer to a strand, two adjoining monomers each belonging to the consecutive dimers are activated, probably due to a conformational change upon contact formation (Figure 2.5). The model explains why tetramers have more than half of the spindle activity. According to the model the single strands are expected to be 91% active, but whether contacts between two strands lead to 100% activation is presently unknown (Seyit et al., 2006).

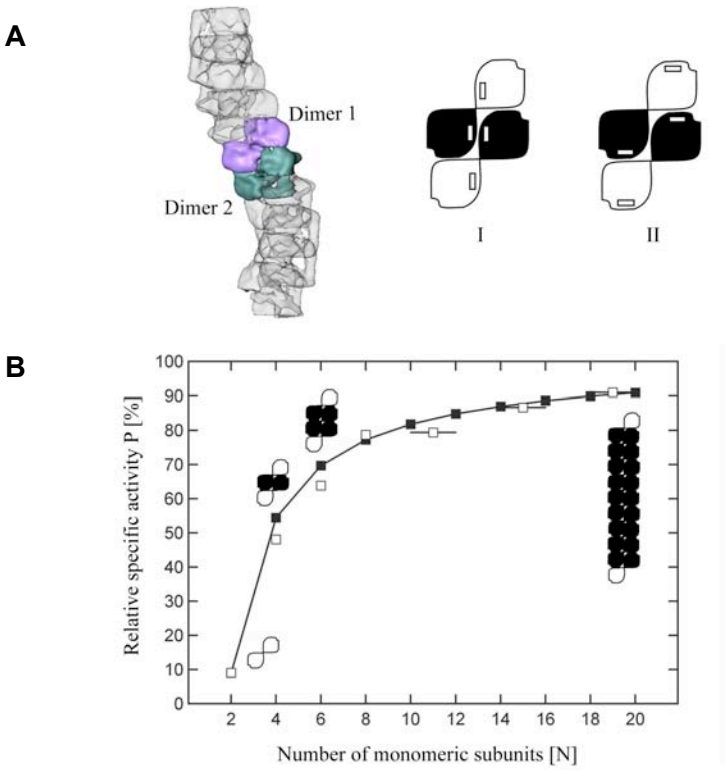

Figure 2.5. Activation of TPP II upon assembly (Seyit et al., 2006). A, Left: structure of a single strand obtained by cryo-electron microscopy (see also (Rockel et al., 2005). Two adjacent dimers are highlighted in color. I, and II, two possible arrangements of active sites (white boxes) in a tetramer. B, comparison of the experimentally obtained specific activity data (empty squares) with a function ($P = 100(N-2)/N + 2P_{basal}/N$) derived from the activation model proposed (filled squares). The activation status of monomers in selected oligomeric states is indicated; white, basal activity (P_{basal}); black, fully activated (100%).

The two strands composing the TPP II holocomplex contain a channel along their longitudinal axis that traverses each segment. This channel with lateral openings resembles an arcade, and appears to be a novel variant of a proteolytic nanocompartment (Rockel et al., 2005). The route substrates might take through the complex has not yet been determined.

2.6 Preparation of TPP II

TPP II has been purified to apparent homogeneity from rat liver and human erythrocytes (Balow et al., 1986), human brain (Wilson et al., 1993), rat brain (Rose et al., 1996), fly (Renn et al., 1998; Rockel et al., 2002; Rockel et al., 2005) and plant (Book et al., 2005). The native expression levels of TPP II are fairly low (about 0.05 mg/ml in *Drosophila* eggs and human erythrocytes, Dr. Jürgen Peters unpublished data). Thus, to obtain sufficient

amounts of the enzyme, Tomkinson et al. established a method for recombinant expression of TPP II in human embryonic kidney 293 cells (Tomkinson et al., 1997). TPP II from mouse, human and *Drosophila* were expressed using this expression system. The yield of recombinant TPP II obtained was about 4-10 fold of the endogenously expressed enzyme, as determined from the increase in activity and densitometric measurements (Renn et al., 1998; Tomkinson et al., 1997). In addition to the low expression levels achieved with the HEK 239 system, the major disadvantage was the endogenous TPP II expression, which led to some complications, especially in mutational studies (Hilbi et al., 2002; Tomkinson et al., 2002). Therefore, mutational studies need to be carried out in alternative expression systems lacking endogenous TPP II expression.

2.7 The aims of this study

The crucial role that TPP II plays in the proteolytic cascade in the eukaryotic cytosol has recently become evident, but the mode of action of this extraordinary peptidase still remains an enigma. Understanding the functional significance of the unique structural organization of the enzyme requires a high-resolution structure. Thus far, TPP II has resisted crystallization probably owing to its low expression/purification yields and its inherent conformational heterogeneity *in vitro*. As crystallization depends on obtaining large quantities of homogeneous material, the aims of this study were: i) to develop a system for high yield expression/purification and ii) to dissect the oligomeric complex into homogeneously sized, stable sub-complexes, which would enable the crystallization and structure determination of TPP II at atomic level.

3. Materials and methods

3.1 Growth and maintenance of *Escherichia coli*

3.1.1 *E. coli* host strains

Chemically competent *E. coli* strains DH5α (Novagen) and XL10-Gold® (Stratagene) were used for cloning. Strain BL21(DE3) (Stratagene) was used for the expression of the wild type and the His_6-tagged TPP II; strain TB1 (New England Biolabs) was used for the expression of maltose-binding protein tagged TPP II.

3.1.2 Storage of *E. coli* cultures

0.8 ml of logarithmic-phase (OD_{600} ~0.5) *E. coli* culture was added to 0.2 ml of sterile glycerol in a 1.8-ml screw-cap vial and vortexed vigorously to ensure even mixing. The culture was frozen in liquid nitrogen and stored at –80°C (modified from (Sambrook et al., 2001).

3.1.3 Growing starter cultures of *E. coli*

From glycerol stock cultures, *E. coli* cells were streaked onto selective LB-agar plates containing the appropriate antibiotic, 100 μg/ml Ampicillin or 30 μg/ml Kanamycin, and incubated at 37°C overnight. 10 ml of selective LB broth was inoculated with a single colony. The starter cultures were grown in 50 ml tubes with loose lids to allow aeration, through vigorous shaking at 37°C overnight.

3.1.4 Preparation of competent *E. coli* cells

TFB1	**TFB2**
100 mM RbCl	10 mM MOPS
50 mM $MnCl_2$	10 mM RbCl
30 mM KAc	75 mM $CaCl_2$
10 mM $CaCl_2$	15% glycerol
15% glycerol	The pH was adjusted to 6.8 with KOH.
The pH was adjusted to 5.8.	TFB1 and TFB2 were sterile-filtered.

Competent cells of strains DH5α, BL21(DE3) and TB1, were prepared according to the procedure described in QIAexpressionist (Qiagen, 2003). Starter cultures were grown as described in Section 3.1.3, except that LB medium without antibiotics was used. 100 ml of LB was inoculated with 1 ml starter culture. Cells were grown in a 250-ml baffled Erlenmeyer flask, with rapid shaking at 37°C. When an OD_{600} of ~0.5 was reached, the cultures were cooled on ice for 5 min. Cells were harvested by centrifugation (5 min, 4000 x *g*, 4°C) and resuspended gently in 30 ml of ice-cold TFB1 buffer. The suspension was kept on ice for 90 min. Then cells were collected by centrifugation (5 min, 4000 x *g*, 4°C) and resuspended in 4 ml of ice-cold TFB2 buffer. Single use aliquots of 40 μl competent cells were prepared in sterile microcentrifuge tubes and frozen in liquid nitrogen. The cells were stored at –80°C. The XL10-Gold Ultracompetent cells were purchased as ready to use.

3.1.5 Transformation of competent *E. coli* cells

Aliquots of 40 μl of competent cells were thawed on ice. Following addition of plasmid DNA, the cells were incubated on ice for 30 min. The cells were subjected to heat shock at 42°C for 45 sec, then cooled on ice for 2 min. 260 μl of NYZ^+ medium were added and cells were grown at 37°C with shaking for 1 h. 100 μl of the transformation mix were spread to LB plates containing the appropriate antibiotic (30 μg/ml Kanamycin for the pET constructs or 100 μg/ml Ampicillin for the pMAL-c2X constructs). The cells were grown 37°C overnight.

3.2 Nucleic acid techniques

3.2.1 Isolation of plasmid DNA from *E. coli*

For the isolation of plasmids, a QIAprep Spin Miniprep Kit of QIAGEN was used. The procedure is based on alkaline lysis of bacterial cells followed by selective adsorption of DNA onto silica-gel membrane in high-salt buffer and elution in low-salt buffer. *E. coli* cultures were grown at 37°C, with shaking, for up to 16 h (Section 3.1.3). Plasmid purification was performed according to the manufacturer's instructions, with the following modifications: 12.5 ml of *E. coli* culture and a double volume of P1 (500 μl), P2 (500 μl) and N3 (700 μl) buffers were used per QIAprep spin column. Washing steps with Buffer PB and Buffer PE were repeated once. DNA was eluted as described in the kit protocol using 50 μl of Buffer EB (10 mM Tris-Cl, pH 8.5) and stored in the same buffer.

3.2.2 Restriction enzyme digestion of DNA

Restriction digestion reactions were carried out in 20 μl of 1 x NEBuffer (New England Biolobs) as recommended by the manufacturer. Resulting DNA fragments were separated by agarose gel electrophoresis (Section 3.2.3).

3.2.3 Agarose gel electrophoresis

Samples containing DNA were loaded to 0.8% w/v agarose gels in 1xTAE buffer. Following electrophoresis the gels were incubated with ethidium bromide (0.5 μg/ml) for 15 min. DNA bands were visualized on a UV-transilluminator.

3.2.4 Isolation of DNA from agarose gels

DNA fragments obtained by enzymatic cleavage or PCR amplification were isolated from agarose gels using a QIAquick Gel Extraction Kit of QIAGEN. The purification was performed as recommended by the manufacturer, except that the washing steps were repeated once. The DNA was eluted using 50 μl of Buffer EB (10 mM Tris-Cl, pH 8.5) and stored in the same buffer.

3.2.5 Quantitation of DNA

DNA-containing samples were diluted 25-fold in MilliQ H_2O and the absorption spectrum between 250 nm and 350 nm was measured using quartz cuvettes (1 cm path length). For pure DNA samples the absorption is maximal at 260 nm and according to the Beer-Lambert law, for double stranded DNA, one A_{260} unit corresponds to a concentration of 50 μg/ml.

3.2.6 Cloning of *Drosophila melanogaster* TPP II cDNA in *E. coli*

The 4065 base pair cDNA (GenBank accession number: AF035251) of *Drosophila melanogester*, coding for the 1354 amino acid (~150 kDa) TPP II (Renn), was cloned in pET28a (Novagen, Section 3.2.6.1), pET30b (Novagen, Sections 3.2.6.2 and 3.2.6.3) and pMAL-c2X (New England Biolabs, Section 3.2.6.4) plasmid vectors.

3.2.6.1 Clone dTPP II-NHis

Clone dTPP II-NHis plasmid, harbouring the complete coding sequence for *Drosophila* TPP II with an N-terminal His_6-tag in pET28a vector, was obtained from Erika Seemüller.

3.2.6.2 Clone dTPP II-CHis

Clone dTPP II-CHis plasmid, harbouring the complete coding sequence for *Drosophila* TPP II with a C-terminal His_6-tag in pET30b vector, was obtained from Erika Seemüller.

3.2.6.3 Clone dTPP II-wt

To excise the TPP II DNA fragment, 3 µg of the dTPP II-NHis plasmid were digested with 20 units of NdeI and 10 units of NotI (Section 3.2.2). After the digestion, the resulting DNA fragments were separated by agarose gel electrophoresis (Section 3.2.3). The 4065 bp TPP II DNA fragment with NdeI-NotI cohesive ends was isolated from the gel (Section 3.2.4). 5 µg of pET30b plasmid were linearized with NdeI and NotI and isolated in the same way. As a result of the NdeI/NotI digestion, the sequence coding for a His_6-tag upstream of the multiple cloning site was excised from the plasmid. Also, the TPP II DNA

contained a termination codon, in order to prevent the expression of the His_6-tag located downstream.

For the insertion of TPP II DNA into the pET30b vector a Takara ligation kit was used. The ligation mix containing 4 μl of TPP II DNA, 6 μl of linearized vector and 10 μl Solution I (Takara) was incubated at 16°C for 40 min and transformed to *E. coli* strain DH5α (Section 3.1.5). The cells were grown on LB agar plates containing 30 μg/ml Kanamycin. One positive clone was chosen by restriction analysis of the isolated plasmids and the insertion was verified by sequencing (MWG). The recombinant construct, dTPP II-wt, was transformed to the BL21(DE3) strain of *E. coli* (Section 3.1.5) and used for the expression of the untagged, wild type *Drosophila* TPP II.

3.2.6.4 Clone dTPP II-Nmbp

In order to fuse a maltose-binding protein-tag to the N-terminus of TPP II, the dTPP II-Nmbp plasmid was constructed starting with a pMAL-c2X vector (New England Biolabs). The original pMAL-c2X vector does not contain suitable restriction sites for cloning of TPP II DNA. Thus, to enable cloning of TPP II using the NdeI/NotI restriction endonucleases, the following modifications were introduced to the pMAL-c2X vector:

I) The NdeI recognition site (outside of the multiple cloning site) was eliminated by introducing a T1527G mutation.

II) The original MCS was exchanged with a novel one containing NdeI/NotI recognition sites.

3.2.6.4.1 Elimination of the NdeI recognition site in the pMAL vector

The NdeI site in the pMAL-c2X vector was eliminated by introducing a T1527G mutation. A QuikChange XL Site-Directed Mutagenesis Kit (Stratagene) was used. The PCR reaction was set using 2.5 μl of pMAL-c2X (20 ng/μl) dsDNA template and 1 μl of each oligonucleotide primer (25 pmol/μl, Table 3.1); the rest of the reaction components were included and the thermal cycling was performed as recommended by the manufacturer.

Table 3.1. Oligonucleotide primers (Metabion) used for introducing a T1527G mutation to the pMAL-c2X vector.

Mutation	Primer
T1527G	5'-CCAACAAGGACCATAGCAGATGAAAATCGAAGAAGGTAAACTGG-3' 5'-CCAGTTTACCTTCTTCGATTTTCATCTGCTATGGTCCTTGTTGG-3'

Following amplification, 5 μl of the reaction mix were treated with 10 units of DpnI at 37°C for 1h, in order to digest the parental (i.e., the nonmutated) DNA. Subsequently, the mix was used to transform 40 μl of competent *E. coli* (TB1) cells (Section 3.1.5). One mutant clone harbouring the pMAL-c2X/NdeI$^{(-)}$ plasmid (pMAL-c2X lacking the NdeI recognition site) was chosen by restriction analysis of the isolated plasmids and the mutation was verified by sequencing (MWG).

3.2.6.4.2 Exchanging the multiple cloning site of the pMAL vector

To excise the original MCS, 3 μg of the pMAL-c2X/NdeI$^{(-)}$ vector (Section 3.2.6.4.1) were digested with 100 units of EcoRI and 100 units of HindIII (Section 3.2.2). After the digestion, the products were separated by agarose gel electrophoresis (Section 3.2.3) and the linearized vector having EcoRI/HindIII cohesive ends was isolated from the gel (Section 3.2.4).

The following oligonucleotides were synthesized (Metabion) and annealed to generate a linker with the EcoRI/NdeI/AflII/NotI/HindIII restriction sites:

5'- AATTCCATATGCTTAAGGCGGCCGCA-3'
5'-ACGTTGCGGCCGCCTTAAGCATATGG-3'

For the annealing, equal volumes (9 μl) of each oligonucleotide were mixed with 2 μl of 10 x T4 DNA Ligase buffer (New England Biolabs) and incubated at 90°C for 2 min, then the incubator (Eppendorf) was switched off to let the samples cool for 1 hour. Following annealing, the novel linker having EcoRI/HindIII cohesive ends, was ligated (Table 3.2) to the pMAL-c2X/NdeI$^{(-)}$ plasmid with EcoRI/HindIII cohesive ends. The ligation reaction was performed at 16°C overnight.

Table 3.2. Ligation of the novel MCS to the pMAL/NdeI$^{(-)}$ vector.

Component	Volume/reaction
T4 DNA Ligase buffer (10x)	2 μl
Linearized pMAL-c2X/NdeI$^{(-)}$ vector	16 μl
Linker DNA (the novel MCS)	1 μl
T4 DNA Ligase (2,000 U/μl)	1 μl
Total volume	20 μl

20 units of SalI were added after ligation, in order to digest the recircularized pMAL-c2X/NdeI$^{(-)}$ plasmids containing the original MCS. The digestion was performed at 37°C for 1 hour then the mix was used to transform 40 μl of competent *E. coli* (DH5α) cells (Section 3.1.5). True recombinant clones were chosen by restriction analysis of the isolated plasmids and the insertion of the novel MCS was verified by sequencing (MWG). One of the recombinants was named pMAL-mod (harbouring pMAL-c2X/NdeI$^{(-)}$ with a novel linker containing EcoRI/NdeI/AflII/NotI/HindIII restriction sites) and used for cloning of TPP II (see below).

3.2.6.4.3 Inserting the TPP II DNA into the pMAL vector

3 μg of the pMAL-mod vector (Section 3.2.6.4.2) were digested with 20 units of NdeI and 10 units of NotI (Section 3.2.2). After the digestion, the products were separated by agarose gel electrophoresis (Section 3.2.3) and the linearized vector having NdeI/NotI cohesive ends was isolated from the gel (Section 3.2.4). The TPP II DNA fragment with NdeI/NotI cohesive ends was prepared as described in Section 3.2.6.3 and ligated to the vector using T4 DNA Ligase (2,000 U/μl, New England Biolabs) according to the manufacturer's instructions. 30 units of AflII were added after ligation, in order to linearize the pMAL-mod plasmids, which do not have a TPP II insert. The digestion was performed at 37°C for 1 hour, then the mix was used to transform 40 μl of competent *E. coli* (TB1) cells (Section 3.1.5). In the plasmids isolated form selected recombinant clones, the insertion of the TPP II DNA fragment was verified by sequencing (MWG). One of the recombinants, named dTPP II-Nmbp, was used for the expression of TPP II with an N-terminal MBP-tag.

3.2.7 Introducing point mutations to the TPP II DNA

3.2.7.1 Single residue exchange by site-directed mutagenesis

The point mutants were generated using a QuikChange XL Site-Directed Mutagenesis Kit (Stratagene) as recommended by the manufacturer. dTPP II-Nmbp plasmid (Section 3.2.6.4.3) was used as a template for the mutations indicated in Table 3.3. Only the *G260R* mutation was also introduced to the dTPP II-wt plasmid (Section 3.2.6.3). 50 ng of plasmid template, and 1 μl of the forward and reverse oligonucleotide primers (25 pmol/μl) shown in Table 3.3 were used per 50 μl of PCR reaction mix. The PCR reactions were set and the thermal cycling was performed according to the manufacturer's instructions.

Table 3.3. The primers (Metabion) used to introduce point mutations into the TPP II DNA. The mutated nucleobases are indicated in bold type and the corresponding codons are underlined.

Mutation	Primer
G260R	5'-GGTAAACGTCCACGACGAG**C**GCAACGTACTGGAGG-3' 5'-CCTCCAGTACGTT**GCG**CTCGTCGTGGACGTTTACC-3'
E182A	5'-CCTGGGACAAGAAGATATTGAAA**GCG**AATCTAGACTTTGAGC-3' 5'-GCTCAAAGTCTAGATT**CGC**TTTCAATATCTTCTTGTCCCAGG-3'
E923A	5'-GACTGCAGGTGCGTCAC**GCG**AAGCGCGACCTGCTG-3' 5'-CAGCAGGTCGCGCTT**CGC**GTGACGCACCTGCAGTC-3'
E929A	5'-CGCGACCTGCTG**GCG**AAGATCTCGGAG-3' 5'-CTCCGAGATCTT**CGC**CAGCAGGTCGCG-3''
E1313A	5'-GGTTAAGCTAATCGAG**GCG**AAGCGAACCCGCGATC-3' 5'-GATCGCGGGTTCGCTT**CGC**CTCGATTAGCTTAACC-3'

3.2.7.2 Double residue exchange by site-directed mutagenesis

A QuikChange XL Site-Directed Mutagenesis (Stratagene) was used, but since the primers for these mutations were relatively long, a modified protocol consisting of two stages was applied (Wang and Malcolm, 1999) to ensure high mutagenesis efficiency. In stage one, single primer extension reactions were performed separately using 100 ng of dTPP II-Nmbp plasmid per reaction and 1 μl of the forward or reverse primers (25 pmol/μl) shown in Table 3.4.

Table 3.4. The primers (Metabion) used to introduce double mutations into the TPP II DNA. The mutated nucleobases are indicated in bold type and the corresponding codons are underlined.

Mutation	Primer
E161K *E163A*	5'-ACGCCAGTCGCAAGATTGTT**A**AATTTG**CG**TC ACAAAATCCAGGAGAAGC-3' 5'-GCTTCTCCTGGATTTTGTGA**CG**CAAATT**T**AA CAATCTTGCGACTGGCGT-3'
E224A *D227K*	5'-GGCTGACAATCGTCGACACCACG**GCG**CAGGGC**AAA**CT GGATCAGGCTCTGCGCATTGG-3' 5'-CCAATGCGCAGAGCCTGATCCAG**TTT**GCCCTG**CGC**CG TGGTGTCGACGATTGTCAGCC-3'

The thermal cycling was performed as described by Wang and Malcom (Wang and Malcolm, 1999). Subsequently, 25 μl of both single primer extension reactions were mixed together with 1 μl of *Pfu*Turbo DNA polymerase (Stratagene, 2.5 U/μl) and the standard QuikChange XL Site-Directed Mutagenesis procedure was carried out. 10 μl of DpnI treated PCR product was transformed into 40 μl of competent *E. coli* (TB1) cells (Section 3.1.5). Plasmids isolated from the transformants were sequenced (Medigenomix) to verify the mutations. Two mutant clones were named dTPP II-Nmbp-*E161K-E163A* and dTPP II-Nmbp-*E224A-D227K*.

3.2.7.3 Multiple residue exchange by site-directed mutagenesis

Multiple point mutations were introduced using a QuikChange Multi Site-Directed Mutagenesis Kit (Stratagene), according to the kit protocol, as suggested for generating mutant clone collections. 400 ng of dTPP II-Nmbp-*E224A-D227K* plasmid template (Section 3.2.7.2), and 2.5 μl of each of the forward primers (25 pmol/μl) shown in Table 3.3 were used per 100 μl of PCR reaction mix. The PCR reactions were set and the thermal cycling was performed according to the manufacturer's instructions. 1.5 μl of DpnI treated PCR mix, were used to transform 20 μl of XL10-Gold® ultracompetent *E. coli* cells as described in the standard kit procedure. The mutations were verified by sequencing (Medigenomix) and the mutant plasmids were transformed to competent BL21(DE3) *E. coli* cells (Section 3.1.5) for expression (Section 3.3.1).

3.2.7.4 C-terminal truncations

The truncation mutants were generated by introducing a termination codon to the TPP II DNA, by a single nucleobase exchange as described in Section 3.2.7.1. The primers shown in Table 3.5 were used. The dTPP II-Nmbp plasmid (Section 3.2.6.4.3) was used as a template for the mutations.

Table 3.5. The primers (Metabion) used to generate truncation mutants of TPP II. The mutated nucleobases are indicated in bold type and the termination (Ter) codons are underlined.

Mutation	Primer
Y1295Ter	5'-GCTCTGTGGCACGCCTA**A**GCCCATGGCCACTACG-3' 5'-CGTAGTGGCCATGGGC**T**TAGGCGTGCCACAGAGC-3'
Y1272Ter	5'-GCTGAGATCAACGAGCTGTA**A**ACCGAGATTATCAAGTTCG-3' 5'-CGAACTTGATAATCTCGGT**T**TACAGCTCGTTGATCTCAGC-3'
Y1216Ter	5'-GGCACTGCTCTCCTACTA**A**GGTCTGAAGAACG-3' 5'-CGTTCTTCAGACC**T**TAGTAGGAGAGCAGTGCC-3'
E526Ter	5'-GGCATTCGAGCATTTGACG**T**AGCACCGCCAGTCCAAGG-3' 5'-CCTTGGACTGGCGGTGCTA**A**CGTCAAATGCTCGAATGCC-3'

The clones harbouring the *Y1295Ter*, *Y1272Ter*, and *Y1216Ter* mutations were named clone dTPP II-Nmbp-ΔC59, clone dTPP II-Nmbp-ΔC82, and clone dTPP II-Nmbp-ΔC138, respectively. The clone with the *E526Ter* mutation was used for the expression of the N-terminal domain of TPP II.

3.2.8 Cloning of the C-terminal domain of TPP II

The DNA fragment coding for the C-terminal domain of TPP II (from the S1095 codon until the termination codon) was amplified using the primers indicated in Table 3.6. The PCR reaction was set and the thermal cycling performed as indicated in Table 3.7.

Table 3.6. The primers (Metabion) used for the amplification of the C-terminal domain fragment of TPP II DNA. The matching sequence is indicated in bold type and the cloning (NdeI/NotI) sites are underlined.

Fragment	Primer
TPP II C-terminal domain	5'-ATATATCATATG**TCACCCAAAAAGGGCAAG**-3' 5'-**AGTGCGGCCGCTGCTCAGAACAAAC**-3'

Table 3.7. PCR amplification of the C-terminal domain fragment of TPP II DNA.

PCR reaction components			
Reaction buffer (10x)	5 μl		
dTPP II-NHis plasmid (~100 ng/μl)	1 μl		
Forward primer (10 pmol/μl)	2 μl		
Reverse primer (10 pmol/μl)	2 μl		
dNTP mix (40 mM)	1 μl		
MilliQ H_2O	38 μl		
PfuTurbo DNA polymerase (2.5 U/μl)	1 μl		
Total volume	50 μl		
Cycling parameters			
Segment	**Cycles**	**Temperature**	**Time**
1	1	95°C	2 min
2	30	95°C	30 sec
		60°C	30 sec
		72°C	1 min/kb of plasmid length
3	1	72°C	10 min

The PCR reaction products were separated by agarose gel electrophoresis (Section 3.2.3) and the C-domain fragment was isolated from the gel (Section 3.2.4). The DNA fragment was concentrated by evaporation, and digested with NdeI/NotI (Section 3.2.2) to generate cohesive ends for cloning. After the digestion, the sample was incubated at 65°C for 20 minutes in order to inhibit the endonucleases. The fragment was ligated into a pMAL-mod vector (Section 3.2.6.4.2) having NdeI/NotI cohesive ends, using T4 DNA Ligase (2,000 U/μl, New England Biolabs) according to the manufacturer's instructions. The ligation mix was used to transform 40 μl of competent *E. coli* (TB1) cells (Section 3.1.5). In the

plasmids isolated form selected recombinant clones, the presence of the insert was verified by sequencing (Medigenomix). One of the recombinants, named mbp-dTPP II_C, was used for the expression (Section 3.3.1) of the C-terminal domain of TPP II with an N-terminal MBP-tag.

3.2.9 Cloning of *Homo sapiens* TPP II cDNA in *E. coli*

A pCMV6-XL4 (~4.7 kb) vector harbouring the coding sequence of *Homo sapiens* TPP II (atypical, having a G252R mutation, GenBank accession: NM_003291) was purchased from Origene. The plasmid was cloned in *E. coli* (Section 3.1.5), purified (Section 3.2.1) and used as a template for the PCR amplification of hTPP II. The PCR primers (Table 3.8) were designed to insert an NdeI recognition site upstream of the initiation codon and a NotI site downstream of the termination codon of the hTPP II coding sequence. The PCR reaction was set as described in Section 3.2.8 except that pCMV6-XL4-hTPP II plasmid (200 ng/μl) was used as a template. The thermal cycling was performed as described above (Section 3.2.8).

Table 3.8. The primers (Metabion) used for the amplification of hTPP II DNA. The matching sequence is indicated in bold type and the cloning (NdeI/NotI) sites are underlined.

Template	Primer
pCMV6-XL4-hTPP II	5'-ATATAT<u>CAT</u>**ATG**GCCACCGCTGCGACTGAGG-3' 5'-TA<u>GCGGCCGC</u>**TTAGAATACGCAATAATCGGGAGG**-3'

The PCR reaction products were separated by agarose gel electrophoresis (Section 3.2.3) and the hTPP II DNA fragment was isolated from the gel (Section 3.2.4). The fragment was digested with NdeI/NotI (Section 3.2.2) to generate cohesive ends for cloning. Following digestion, the hTPP II DNA fragment was purified using a PCR Purification Kit (Qiagen), according to the manufacturer's instructions. In order to inhibit possible residual endonuclease activity, the sample was incubated at 65°C for 20 minutes. The fragment was inserted into a pET30b (Novagen) vector having NdeI/NotI cohesive ends as described in Section 3.2.6.3. 30 units of Kpn I were added after ligation, in order to digest the recircularized pET30b vector and minimize the number of false positives. The digestion was performed at 37°C for 1 hour, then 10 µl of the mix were used to transform 40 μl of

competent BL21(DE3) *E. coli* cells (Section 3.1.5). In the plasmids isolated form selected recombinant clones, the presence of the insert was verified by sequencing (Medigenomix). One of the recombinants harbouring the pET30b-hTPP II plasmid was selected and named hTPP II-*G252R*.

3.3 Recombinant expression

3.3.1 Over-expression of TPP II in *E. coli*

Starter cultures were prepared as described in Section 3.1.3. Fresh TB medium containing the appropriate antibiotic, 100 μg/ml Ampicillin or 30 μg/ml Kanamycin, was inoculated with 1/100th volume of starter culture. Cells were grown with vigorous shaking at 37°C until an OD_{600} of ~2.5 was reached. The cultures were then cooled down to 18°C. Subsequently, 0.1 mM IPTG was added for induction and cell were grown with vigorous shaking at 18°C for 24h.

3.3.2 Cell disruption methods

3.3.2.1 Sonication

In all pilot expression experiments for small-scale purification, cells harvested from 10-15 ml culture were resuspended in 3 ml of phosphate cell-disruption buffer and homogenised by sonication (Bransonic Sonicator, tip diameter 1 cm, 2 x 10 pulses, setting "8" at 50% pulse duration). Samples were kept in ice-water bath during homogenization. Soluble fractions of the lysates were obtained by centrifugation (10 min, 18000 x *g*, 4°C) and used in further analysis or purification.

3.3.2.2 Lysozyme treatment combined with sonication

E. coli cells were harvested by centrifugation (10 min, 3500 x *g* , 4°C) and resuspended in one volume of phosphate cell-disruption buffer (Section 3.3.2.3). EDTA was added from a 200 mM stock solution to a final concentration of 5 mM and subsequently, the cell extract was aliquoted. An aliquot was subjected to a freeze-thawing step. The other two aliquots

were kept on ice for 15 min. Then lysozyme was added from a 50 mg/ml stock solution to a final concentration of 1.5 mg/ml or 3 mg/ml, and incubated at 25°C for 30 min. Subsequently, $MgCl_2$ was added, from a 200 mM stock solution to final concentration of 10 mM, to all three of the cell extract aliquots. This was followed by the addition of 20 mg/ml DNase to a final concentration of 0.25 mg/ml. After incubation at 25°C for 10 min, the cell lysates were centrifuged (10 min, 18000 x *g*, 4°C) to separate the supernatant (1st cell extract). To determine whether the cell disruption was complete, the pellet was resuspended in 3 ml of phosphate cell-disruption buffer and homogenized by sonication (Bransonic Sonicator, tip diameter 1 cm, 2 x 10 pulses, setting "8" at 50% pulse duration) in 15 ml tubes placed in a water-ice bath. Subsequently, the homogenate was centrifuged (10 min, 18000 x *g*, 4°C) to obtain the soluble fraction ("2nd cell extract"). The 1st and the 2nd cell extracts were analyzed by SDS-PAGE (Section 3.4.3).

3.3.2.3 High-pressure homogenisation

Phosphate cell-disruption buffer

40 mM K_2HPO_4/KH_2PO_4, pH 7.5

10 mM DTT

5 % glycerol

Cells were harvested by centrifugation (15 min, 3500 x *g*, 4°C) and resuspended in 1 volume of phosphate cell-disruption buffer. The cell suspension was passed twice through a high-pressure homogenizer (Avestin) at 15000-20000 psi. After this first disruption step, the homogenate was centrifuged (10 min, 48 000 x *g*, 4°C) to separate the soluble fraction, named "1st cell extract". The pellet was resuspended in phosphate cell-disruption buffer and homogenized again as described above. Subsequently, the lysate was centrifuged (30 min, 48 000 x *g*, 4°C) and the soluble fraction, named "2nd cell extract", was collected. This 2nd cell extract was used for the purification of untagged and His_6-tagged TPP II. For the purification of MBP-tagged TPP II, the 1st cell extract was used.

3.4 Protein-chemical methods

3.4.1 Activity measurements

Activity assay buffer

100 mM K_2HPO_4/KH_2PO_4, pH 7.5
0.2 mM AAF-AMC
0.1 mM bestatin
1 mM DTT
5% glycerol

Stopping buffer

100 mM Tris-HCl, pH 9.5
1% SDS

AMC-standard solution

0.1 mM AMC in DMSO
Prior to use, the solution was diluted with stopping buffer to a final concentration of 2 μM AMC.

For the exopeptidase activity measurements of TPP II, the fluorogenic substrate alanyl-alanyl-phenylalanyl-7-amino-4-methylcoumarin (AAF-AMC) was used routinely at a concentration of 0.2 mM. Bestatin was included in the assay buffer to inhibit aminopeptidases such as aminopeptidase B, leucine aminopeptidase and tripeptide aminopeptidase. TPP II samples were added to 50 μl of assay buffer aliquots preheated to 30 °C. The reactions were stopped after 30 sec to 10 min by adding stopping buffer to a final volume of 500 μl. The release of AMC was measured in a SFM25 fluorometer at λ^{ex}360 nm and λ^{em}460 nm, in quartz cuvettes. The fluorometer was calibrated using free aminomethyl coumarin (AMC).
For the determination of the kinetic constants, the activity measurements were performed using substrate concentrations of 0.15, 0.2, 0.3, 0.4, 0.5, 1 and 2 mM. K_m and V_{max} values were calculated from the Lineweaver-Burk reciprocal plot.

3.4.2 Determination of protein concentration

The concentration of soluble protein was determined using the BIORAD Protein Assay Dye Reagent, as recommended by the manufacturer. Assays were prepared in duplicates. The absorbance was measured at λ 595 nm and the protein concentration was calculated according to a standard curve obtained with bovine serum albumin.

3.4.3 Denaturing polyacrylamide gel electrophoresis (SDS-PAGE)

SDS-PAGE sample-buffer (5x)

100 mM Tris-HCl, pH 8.5
5 mM PMSF
50 mM DTT
50% glycerol
5% (w/v) SDS
0.04 % (w/v) bromphenolblue

For SDS-PAGE, the buffer system of Schägger and Jagow (Schagger and von Jagow, 1987) was used. The acrylamide concentration was 9%. Protein samples were mixed with 0.2 volume of sample-buffer and solubilized at 70 °C for 5 min. The electrophoresis was performed in a vertical electrophoresis apparatuses at 90 V, until the dye front reached the bottom of the resolving gel.

3.4.4 Non-denaturing electrophoresis (Native PAGE)

Native PAGE sample-buffer (2x)

80 mM Tris-HCl, pH 6.8
10% glycerol
5% ß-mercaptoethanol
0.04 % (w/v) bromphenolblue,

Tris/glycine native running buffer

25 mM Tris-HCl, pH 8.5
190 mM glycine

Protein samples were mixed with one volume of 2x sample-buffer and subjected to electrophoresis on Novex® Pre-Cast 4-12% Tris/glycine Gels (Invitrogen) using Tris/glycine native running buffer. The electrophoresis was performed at 80 V, overnight at 4 °C.

3.4.5 Staining of proteins after electrophoresis

Proteins separated by electrophoresis (Sections 3.4.3 and 3.4.4) were stained using colloidal Coomassie (Bio-Rad) dye, which binds non-specifically to proteins but not to the polyacrylamide gel. The gels were rinsed with MilliQ H_2O after electrophoresis and immersed in Coomassie dye for 1-2 h. Then the excess dye was removed by incubation in MilliQ H_2O for several hours.

3.4.6 Immunoblotting

1x TBS	**Blocking solution**
50 mM Tris-HCl, pH 7.5	1x TBS buffer
150 mM NaCl	1.5% Gelatin
	0.1% NaN_3

All steps of immunoblotting were performed at room temperature. Protein samples separated by SDS-PAGE (Section 3.4.3) were electrophoretically transferred from gel to a nitrocellulose membrane by the Western blotting technique (Sambrook et al., 2001). Starting from the anode plate of the transfer apparatus, the transfer stack was assembled in the following order: four sheets of Whatman 3MM paper saturated with anode buffer, nitrocellulose membrane soaked in anode buffer, the gel (rinsed with MilliQ H_2O after PAGE) and four sheets of Whatman 3MM paper saturated with cathode buffer. The cathode plate was placed on top and the transfer performed applying 2 mA per cm^2 of gel for 4h. Following transfer, the membrane was rinsed with H_2O_{MilliQ} and proteins stained using Ponceau S solution (Sigma). Full-Range Rainbow™ Molecular Weight Marker (250 kDa to 10 kDa, Amersham) was used.

For the immunological detection of TPP II, the membrane was rinsed with MilliQ H_2O to reverse the Ponceau S stain. All incubation steps were performed on a platform shaker. The membrane was incubated in blocking solution overnight, and subsequently, in 10 ml of fresh blocking solution containing 200 μl of serum with anti-TPP II rabbit IgG (Eurogentec) for 1h. Following five 5-min rinsing steps with 1 x TBS buffer, the membrane was incubated in 10 ml blocking solution containing 15 µl alkaline phosphatase

conjugated anti-rabbit IgG (Sigma) for 1.5 h. After hybridization the membrane was rinsed with 1 x TBS buffer and TPP II bands were detected using an alkaline phosphatase chromogen BCIP/NBT (Sigma).

3.4.7 Size exclusion chromatography

Superose 6 eluent buffer

80 mM K_2HPO_4/KH_2PO_4, pH 7.5
1 mM DTT
5 % glycerol
filtered and degased

Superose™ 6 columns (Amersham), with bed volumes of 2.4 ml (Superose™ 6 PC 3.2/30), 24 ml (Superose™ 6 10/300 GL - Tricorn™) and 330 ml (Superose™ 6 XK 26/70) were used for high performance size exclusion chromatography of proteins, according to the manufacturers instructions. Superose 6 is a highly cross-linked, 6% agarose-based medium. The molecular mass range, for optimal separation is 5 000 - 5 x 10^6. The exclusion limit for globular proteins is a molecular mass of 4 x 10^7. Prior to use, the Superose 6 columns were treated with 0.2 column volumes of 6 M GdnHCl to remove protein precipitates and ensure a rigorous cleaning. The columns were washed with at least 2 column volumes of Superose 6 eluent buffer. The equilibration was performed using additional 2-column volumes of eluent buffer.
An HPLC System (Beckman) or an ÄKTA™ System (Amersham) was used to operate the 24 ml Superose 6 column at a flow rate of 0.4 or 0.5 ml/min respectively. The 330 ml Superose 6 column was operated at 1.2 ml/min flow rate. A SMART™ System (Amersham) was used to operate the 2.4 ml Superose 6 column at flow rate of 0.05 ml/min. The columns were calibrated using a Molecular Weight Marker Kit for size exclusion chromatography (Sigma, Carbonic anhydrase 29 000, Albumin 66 000, Alcohol Dehydrogenase 150 000, β-Amylase 200 000, Apoferritin 443 000, Thyroglobulin 669 000 and Blue Dextran 2 000 000 M_r).

3.4.8 Purification of TPP II from *E. coli* (approach I)

Q-binding buffer (IEC)

40 mM K_2HPO_4/KH_2PO_4, pH 8

1 mM DTT

5 % glycerol

Q-elution buffers

100-400 mM K_2HPO_4/KH_2PO_4, pH 7

1 mM DTT

5 % glycerol

P-binding buffer (HIC)

40 mM K_2HPO_4/KH_2PO_4, pH 7

900 mM $(NH_4)_2SO_4$

1 mM DTT

5 % glycerol

P-elution buffers

40 mM K_2HPO_4/KH_2PO_4, pH 7.5

900-100 mM $(NH_4)_2SO_4$

1 mM DTT

5 % glycerol

E. coli cells expressing TPP II were induced as described in Section 3.3.1 . The cells were resuspended in phosphate-cell-disruption buffer and homogenized as described in Section 3.3.2.3 to obtain the 2nd cell extract. The 2nd cell extract was filtered and its pH adjusted to 7.9. Subsequently, the extract was subjected to ion exchange chromatography (IEC) using three connected to each other HiTrap Q FF (3 x 5ml) columns. The columns were equilibrated with 60 ml of Q-binding buffer and the 2nd cell extract loaded. After binding, the columns were washed with 20 ml of Q-binding buffer. The protein was eluted by a step gradient using the same buffer at increasing ionic strengths. 100, 150, 200, 250, 300, 350 and 400 mM K_2HPO_4/KH_2PO_4, pH 7 buffers containing 1 mM DTT and 5 % glycerol were used for elution. 3 ml of each buffer were applied sequentially to the column. Eluate fractions of 1.5 ml were collected and analysed for AAF-AMC hydrolysing activity (Section 3.4.1). 4 fractions with highest activity were pooled and concentrated by hydrophobic interaction chromatography (HIC) using a 1 ml HiTrap Phenyl HP column. The HiTrap Phenyl column was equilibrated with P-binding buffer. To the HiTrap Q eluate pool, 4M $(NH_4)_2SO_4$ was added slowly with continuous stirring to a final concentration of 900 mM. The sample was then loaded to the HiTrap Phenyl column. After binding, the column was washed with 2 column volumes of P-binding buffer. The protein was eluted with a step gradient using 40 mM K_2HPO_4/KH_2PO_4 buffer pH 7.5, 1 mM DTT, 5 % glycerol with decreasing $(NH_4)_2SO_4$ concentrations of 900, 800, 600, 400, 200, and 100

mM. 10 drops (~360 μl) of each buffer, starting with the highest $(NH_4)_2SO_4$ concentration, were applied sequentially to the column and the eluate fractions of 5 drops (~180 μl) were collected. The two fractions with the highest TPP II activity were pooled and separated on a 24 ml Superose 6 column (Section 3.4.7). The activity (Section 3.4.1) and concentration (Section 3.4.2) of TPP II in the peak Superose 6 eluate fractions were determined and the specific activity of purified TPP II was calculated. TPP II particles were visualized by electron microscopy (Section 3.5.2).

3.4.9 Purification of TPP II from *E. coli* (approach II)

E. coli cells expressing TPP II were induced as described in Section 3.3.1. The cells were resuspended in phosphate-cell-disruption buffer and homogenized as described in Section 3.3.2.3 to obtain the 2nd cell extract. The 2nd cell extract was treated with polyethyleneimine (PEI) at a concentration of 0.2 % for 10 minutes on ice. After centrifugation (15 min, 30000 x *g*, 4°C), the sediment was discarded and 1.5 volumes of saturated $(NH_4)_2SO_4$ were added to the supernatant. After incubation on ice for 1-2h the sample was centrifuged (10 min, 30000 x *g*, 4°C), the supernatant was removed completely in a brief second centrifugation step and discarded. The sediment was resuspended in 80 mM K_2HPO_4/KH_2PO_4, pH 7.5 buffer containing 10 mM DTT and 5 % glycerol. The concentrated sample was subjected to size exclusion chromatography on a 24 ml Superose 6 column (Section 3.4.7). The activity (Section 3.4.1) and concentration (Section 3.4.2) of TPP II in the peak Superose 6 eluate fractions were determined and the specific activity of purified TPP II was calculated. TPP II particles were visualized by electron microscopy (Section 3.5.2).

3.4.10 GdnHCl titration

TPP II was purified as described in Section 3.4.9. 6 M GdnHCl was added dropwise to a final concentration of 550 mM during 20 min. The sample was then subjected to size exclusion chromatography on a Superose 6 column (Section 3.4.7) and TPP II particles in the peak eluate fractions were visualized by electron microscopy (Section 3.5.2).

3.4.11 Purification of MBP-tagged TPP II by affinity chromatography

Amylose column buffer I

20 mM K_2HPO_4/KH_2PO_4, pH 7.5
200 mM NaCl,
1 mM EDTA
10 mM DTT
5% glycerol

Amylose column buffer II

100 mM K_2HPO_4/KH_2PO_4, pH 7.5
1 mM EDTA
10 mM DTT
5% glycerol

E. coli cells expressing MBP-tagged TPP II were induced as described in Section 3.3.1. The harvested cells were resuspended in amylose column buffer and homogenized as described in Section 3.3.2.3. Either amylose column buffer I or II were used for the affinity purification of MBP-tagged TPP II, giving the same results. A column packed with amylose resin (supplied with the pMAL Protein Fusion and Purification Kit, New England Biolabs) to give a bed volume of 5 ml was used. Prior to use, the column was equilibrated with 10 column volumes of amylose column buffer. The cell extract was diluted five fold with cooled amylose column buffer and loaded to the column. Subsequently, the column was washed with 10 column volumes of column buffer and the MBP-tagged TPP II eluted with column buffer containing 10 mM maltose. Fractions of 1 ml were collected and the protein concentration determined (Section 3.4.2). To determine the assembly state of the fusion protein, the amylose eluate fractions with highest protein concentration were pooled and subjected to size exclusion chromatography on a 2.4 ml Superose 6 column (Section 3.4.7). The Superose 6 eluate fractions were assayed for AAF-AMC hydrolyzing activity (Section 3.4.1). MBP-tagged TPP II particles were visualized by electron microscopy (Section 3.5.2).

3.4.12 Purification of His_6-tagged TPP II by affinity chromatography

IMAC binding buffer

40 mM K_2HPO_4/KH_2PO_4, pH 7.5
20 mM Imidazole
25 mM NaCl
1 mM DTT
5% glycerol

The Immobilized Metal Affinity Chromatography (IMAC) was performed using a 1 ml HisTrap HP (Amersham) column. The column was equilibrated with 8 ml of IMAC binding buffer without DTT and subsequently, with 2 ml of binding buffer containing 1 mM DTT (the column is compatible with 5 mM DTT). *E. coli* cells expressing His_6-tagged TPP II were induced as described in Section 3.3.1. The cells were resuspended in phosphate cell-disruption buffer and homogenized as described in Section 3.3.2.3 to obtain the 2nd cell extract. Imidazole and NaCl were added to the 2nd cell extract to final concentrations of 20 mM and 25 mM respectively. The imidazole was included at low concentrations to minimize the binding of the non-tagged *E. coli* proteins. After loading the cell extract, the HisTrap HP column was washed with IMAC binding buffer. A step gradient ranging between 100 mM and 500 mM imidazole was used for elution. The eluate fractions of 5 drops (180 μl) were collected. The fraction with the highest TPP II activity was subjected to size exclusion chromatography on a 24 ml Superose 6 column (Section 3.4.7). TPP II particles in the Superose 6 eluate fractions were visualized by electron microscopy (Section 3.5.2).

3.4.13 Disassembly of TPP II by dialysis

Dialysis buffer

25 mM Tris-HCl, pH 7.5
2 mM DTT
5% glycerol

The dialysis was carried out in 10000 MWCO Slide-A-Lyzer dialysis cassettes (Pierce), at 4°C overnight. The effect of dialysis on disassembly was assessed by size exclusion chromatography on a 2.4 ml Superose 6 column (Section 3.4.7). The disassembled TPP II particles in the peak Superose 6 eluate fractions were visualized by electron microscopy (Section 3.5.2).

3.4.14 Disassembly of TPP II by methylation

Selective methylation of lysine residues was performed using a JBS Methylation Kit (Jena Bioscience). The method is based on the chemical replacement of the protons in the ε-amino group of the lysines of a protein, with methyl groups. The aim was to chemically modify the surface of the TPP II subunits and prevent their oligomerization. Purified TPP II complexes (≥6 MDa) were used at concentrations of 0.6 - 1 mg/ml. The procedure was applied as recommended by the manufacturer, except that $1/5^{th}$ of the recommended reagent concentration was used, since the TPP II concentration was low. The effect of methylation on disassembly was assessed by native PAGE (Section 3.4.4) and by size exclusion chromatography, on a 2.4 ml Superose 6 column (Section 3.4.7). The disassembled TPP II particles in the peak Superose 6 eluate fractions were visualized by electron microscopy (Section 3.5.2).

3.4.15 Disassembly of TPP II by β-octyl glucoside treatment

Purified TPP II complexes (≥6 MDa, 0.6 - 1 mg/ml), were treated with the non-ionic detergent, β-octyl glucoside ($C_{14}H_{28}O_6$, CMC ~15 mM, Roche). TPP II was incubated in the presence of 20, 40 or 60 mM β-octyl glucoside, on ice for 1 to 8 days. The effect of β-octyl glucoside on disassembly was assessed by size exclusion chromatography, using a 2.4 ml Superose 6 column as described in Section 3.4.7, except that 40 mM β-octyl glucoside was included in the eluent buffer. TPP II particles in the peak Superose 6 eluate fractions were visualized by electron microscopy (Section 3.5.2).

3.4.16 Large-scale purification of TPP II for crystallization

Wild type TPP II was purified from 50 g of *E. coli* cells (clone dTPP II-wt) as described in Section 3.4.9, except that a preparative-scale Superose 6 column with bed volume of 330

ml was used (Section 3.4.7). Fractions of 2 ml, eluting between 116 and 148 ml were collected. The eluate fractions were assayed for TPP II activity (Section 3.4.1) and protein concentration (Section 3.4.2) and combined in two pools, p1 and p2, according to the elution profile and specific activity. p1 and p2 were frozen and stored at -80°C until further use. Both p1 and p2 were used in the crystallization trials, but only the experiment where p1 was used is described here, since this particular preparation yielded TPP II crystals. 10.5 ml of p1 were thawed and to disassemble the TPP II complexes 0.5 M β-octyl glucoside (OG) was added drop wise to a final concentration of 40 mM. The sample was incubated in the presence of OG on ice for eight days. The disassembly state was assessed via size exclusion chromatography as described before (Section 3.4.15). Disassembled TPP II was further purified and concentrated by ion exchange chromatography using a 1 ml HiTrap Q FF column (Amersham). Prior to use, the column was equilibrated with column buffer containing 40 mM Tris-SO_4 pH 7.8, 1 mM DTT, 5 % glycerol and 40 mM OG. In order to reduce the potassium phosphate concentration (to 40 mM) and ensure efficient binding, the protein sample was diluted with one volume of 10 mM DTT, 5 % glycerol and 40 mM OG solution. After adjusting the pH to 7.8, the sample was loaded to the HiTrap Q column. The column was washed with 3 ml of column buffer and subsequently TPP II was eluted with 250 mM Tris-SO_4 pH 7.5 buffer containing 10 mM DTT, 5 % glycerol and 40 mM OG. Eluate fractions of 5 drops (~180 μl) were collected and assayed for TPP II activity (Section 3.4.1) and protein concentration (Section 3.4.2). The peak fractions were combined in two pools, ep3-6 and ep7-13, and dialysed in 10000 MWCO Slide-A-Lyzer dialysis cassettes against 25 mM Tris-SO_4 pH 7.5, 10 mM DTT, 5 % glycerol and 40 mM OG, in order to remove the excess buffer. The dialysis was carried out at 4°C for two days. Both ep3-6 and ep7-13 were used in the crystallization trials, but only the ep7-13 preparation described below yielded TPP II crystals. Following dialysis, an aliquot ep7-13 was subjected to size exclusion chromatography (Section 3.4.7) to ensure that no re-assembly of the tetramers occurred. The sample was further concentrated using 100K MWCO centrifugal devices (PALL) by centrifugation at 9000 x *g*/ 4°C until the sufficient concentration was reached. After each centrifugation step, the sample was mixed using a micropipette, to avoid local concentration on the membrane. After the final concentration step, the sample was analysed by native PAGE (Section 3.4.4) and by size exclusion chromatography on a 2.4 ml Superose 6 column (Section 3.4.7). TPP II particles were

visualized by electron microscopy (Section 3.5.2). The ep7-13 preparation was used for setting crystallization drops as described in Section 3.5.1.

3.5 Biophysical methods

3.5.1 Crystallization

The hanging drop vapour diffusion technique was used for crystallization trials of wild type TPP II (Section 3.4.9), disassembled wild type TPP II ep3-6 (Section 3.4.16), TPP II-Nmbp (Section 3.4.11), and the C-terminal domain of TPP II (purified as described in Section 3.4.11) using Crystal Screen 1™, Crystal Screen 2™ and Index™ crystallization screens (Hampton Research). No crystals were observed at these conditions.
Ep7-13, containing tetrameric TPP II (Section 3.4.16) was used to set droplets containing 100 nl protein solution and 100 nl mother liquor with 576 crystallization solutions. The droplets were set using a crystallization robot at Sirenade Pharmaceuticals AG.

3.5.2 Electron microscopy

Electron microscopy images of the negatively stained specimen were recorded by Mrs. Brigitte Kühlmorgen (MPI of Biochemistry, Martinsried). For negative staining, carbon-coated copper grids were incubated for 1 min on a drop of protein sample solution and then consecutively transferred to two drops of MilliQ H_2O or 40 mM ammonium sulphate, pH 7.5 for washing. Staining was performed by incubation on a drop of 2 % uranyl acetate for 1 min.

Table 3.9. Electron Microscope Settings

Voltage	120 kV
Magnification	28000x
Defocus	-3 μm
Pixel size (on the specimen level)	4.36 Å

3.6 Materials

3.6.1 Media

Terrific Broth (TB) Medium

Part 1:

12 g Bacto Tryptone

24 g Bacto Yeast Extract

4 ml glycerol

Deionised H_2O to 0.9L final volume

Part 2:

2.3 g KH_2PO_4

16.4 g K_2HPO_4

Deionised H_2O to 0.1L final volume

Part 1 and Part 2 were sterilized separately at 121°C for 20 min, and combined to make 1L prior to use.

LB (Luria-Bertani) Broth Medium

10 g Bacto Tryptone

5 g Bacto Yeast Extract

10 g NaCl

Deionised H_2O to 1L final volume

Sterilization: 121°C / 20 min.

LB Agar

LB Broth

15 g/L Bacto Agar

Sterilization: 121°C / 20 min.

The appropriate antibiotic was added after cooling the LB Agar to ~45 °C.

NYZ^+ Broth

10 g of NZ amine (casein hydrolysate)

5 g of yeast extract

5 g of NaCl

Deionised H_2O to 1L final volume

The pH was adjusted to 7.5 using NaOH.

The NYZ^+ Broth was sterilized at 121°C for 20 min.

The following filer-sterilized supplements were added prior to use:

12.5 ml of 1 M $MgCl_2$

12.5 ml of 1 M $MgSO_4$

10 ml of 2 M glucose

3.6.2 Enzymes, kits, standards, chromatography media and columns

3.6.2.1 Enzymes

Dpn I (10 U/μl)	Stratagene
Lysozyme	Sigma
PfuTurbo DNA polymerase (2.5 U/μl)	Stratagene
Restriction endonucleases and buffers	New England Biolabs
Solution I (containing Ligase)	Takara
T4 DNA Ligase (2,000 U/μl) and buffer	New England Biolabs

3.6.2.2 Kits

JBS Methylation Kit	Jena Bioscience
pMAL Protein Fusion and Purification Kit	New England Biolabs
QIAprep Spin Miniprep Kit	Qiagen
QIAquick Gel Extraction Kit	Qiagen
QIAquick PCR Purification Kit	Qiagen
QuikChange Multi Site-Directed Mutagenesis Kit	Stratagene
QuikChange XL Site-Directed Mutagenesis Kit	Stratagene

3.6.2.3 Standards

Full-Range Rainbow™ Molecular Weight Marker (250 kDa to 10 kDa)	Amersham
HMW Calibration Kit for Native Electrophoresis (669 kDa to 69 kDa)	Amersham
MWGF1000 Kit for Molecular Weights 29,000-700,000	Sigma
PageRuler™ Protein Ladder (200 kDa to 10 kDa)	Fermentas

3.6.2.4 Chromatography media and columns

Amylose resin	New England Biolabs
HisTrap HP column (1ml)	Amersham
HiTrap Phenyl HP column (1ml)	Amersham

HiTrap Q FF column (5ml)	Amersham
Superose™ 6 10/300 GL - Tricorn™ (24 ml)	Amersham
Superose™ 6 PC 3.2/30 (2.4 ml)	Amersham
Superose™ 6 XK 26/70 (330 ml)	Amersham

3.6.3 Chemicals

Ammonium sulfate	Merck
Acetic acid	Merck
Agarose	Biomol
Alanyl-alanyl-phenylalanyl-7-amino-4-methylcoumarin (AAF-AMC)	Bachem
Alkaline phosphatase chromogen BCIP/NBT	Sigma
Aminomethyl coumarin (AMC)	Bachem
Ampicillin	Sigma
Bacto Agar	Difco
Bacto Tryptone	Difco
Bacto Yeast Extract	Difco
Bestatin	Sigma
Bromphenolblue	Serva
$CaCl_2$	Merck
Coomassie	Biorad
DMSO	Merck
DTT	Merck
EDTA	Merck
EtBr	Merck
Gelatin	Sigma
Glucose	Merck
Glycerol 86-88% pure	Riedel-de Haen
Glycine	Merck
Guanidine	Merck
HCl	Merck
Imidazole	Merck
IPTG	Biomol
K_2HPO_4	Merck
KAc	Merck
Kanamycin	Amersham
KH_2PO_4	Merck
KOH	Merck
Maltose	Merck
$MgCl_2$	Merck
$MgSO_4$	Merck
$MnCl_2$	Merck
MOPS	Merck
NaCl	Merck
NaOH	Merck
n-Octyl-beta-D-glucopyranoside ($C_{14}H_{28}O_6$)	Roche
NZ amine	Difco
Phosphoric acid	Merck
PMSF	Sigma

Polyethyleneimine (PEI)	Sigma
Ponceau S concentrate	Sigma
Protein Assay Dye Reagent Concentrate	Biorad
RbCl	Sigma
SDS solution	Biorad
TCA	Merck
Tris	Merck
Uranyl acetate	Merck

3.6.4 Consumables

Butane cartridges CV360	Campingaz
Centrifugal ultrafiltration devices 100K MWCO	Pall
Centrifuge bottles	Beckman
Cryotubes 1.8 ml	Nunc
Crystallization consumables	Hampton Research
Cuvettes 1.5 ml PMMA	Roth
Dialysis cassettes (Slide-A-Lyzer 10000 MWCO)	Pierce
Filter unit Millex-GS 0.22 μm	Millipore
Filter Steriltop 0.22 μm	Millipore
Gels (Novex® Pre-Cast 4-12% Tris/glycine)	Invitrogen
Microcentrifuge tubes	Eppendorf
Nitrocellulose membrane	Schleicher&Schnell
Pipette tips	Peske

3.6.5 Equipment

Autoclave		Tecnomara
Bunsen burner	Fireboy plus	Integra
Cell-disrupter	EmulsiFlex-C5	Avestin
Centrifuges	5417R	Eppendorf
	Avanti J-25 (JA25.50, JA10)	Beckman
	Rotanta 46 RS	Hettich
	Sorvall RC-5B (SS-34)	DuPont
Electron microscope	CM 12	Philips
Electrophoresis apparatuses		MPI Workshop
Fluorometer	SFM 25	Kontron
FPLC	ÄKTA Purifier 10	Amersham
	SMART	Amersham
Freezer	- 86C ULT	Forma
Fridges/freezers		Liebherr
Gel dryer		BioRad
HPLC	System Gold®	Beckman
Ice machine		Ziegra
Incubator		Heraeus
Incubator shaker	Minitron	Infors
Cellstar		Nunc
Magnetic Stirrer	Combimag RCT	Ika
Mixer/incubator	Thermomixer 1.5 ml	Eppendorf
PCR-thermocycler	PCR System 2400	Perkin Elmer
Peristaltic pump	Minipuls 2	Gilson

pH meter	744	Metrohm
Photometer	UV/Vis Spectrometer Lambda 40	Perkin Elmer
Pipettes	Pipetman 5 ml	Gilson
	2, 10, 20, 100, 1000 μl	Eppendorf
Platform shaker	Rockomat	Tecnomara
Quartz cuvettes 10 mm		Hellma
Scanner	Scan Maker 6100	Microtek
Ultra pure water system	MilliQ PLUS	Millipore
Ultrasonic bath	Sonorex Super RK 156	Bandelin
UV transilluminator/camera		Herolab
Vacuum concentrator	BA-VC-300H	Bachofer
Vortexer	VF2	Ika

4. Results

4.1 Recombinant expression of *Drosophila* TPP II in *E. coli*

Since the aim of this study was the characterisation of TPP II in terms of activity and structure, it was crucial to obtain large quantities of the enzyme. Previously, TPP II was purified from *Drosophila* eggs (Rockel et al., 2002; Rockel et al., 2005). This procedure produced relatively low amounts of enzyme, which were not sufficient for elaborate studies. Therefore, TPP II was cloned and expressed recombinantly in *E. coli*. In addition to the advantages of rapid growth and easy handling, *E. coli* was chosen for its lack of endogenous TPP II expression. This would prevent the contamination of the recombinant protein with native material, a problem often encountered in eukaryotic expression systems.

4.1.1 Optimization of TPP II expression in *E. coli*

To determine the optimal expression conditions for TPP II, various parameters like induction temperature, length of induction, inducer concentration and type of growth medium were investigated. *E. coli* clone dTPP II-NHis (Section 3.2.6.1 and Figure 4.1), expressing *Drosophila* TPP II with an N-terminal His_6-tag was used in the expression optimisation experiments.

Figure 4.1. dTPP II-NHis plasmid used for expression of the full length *Drosophila* TPP II with an N-terminal His_6-tag. Arrows denote the NdeI and NotI restriction sites and the termination codon (*Ter*).

The first parameter investigated was the induction temperature. At 30°C, low amounts of soluble TPP II were obtained, whereas the yield of soluble protein increased significantly when lower induction temperatures such as 18°C, were used (Figure 4.2A). Indeed, even

higher amounts of soluble TPP II were observed when cells were induced at 12°C and 9°C for 36 h and 72 h respectively. However, since a significantly shorter time period (24h) was needed for growth of *E. coli* at 18°C, this temperature was used routinely for TPP II expression. The effect of different inducer (IPTG) concentrations – 0.025, 0.1 and 1 mM – was also investigated (Figure 4.2B). Since the best results were obtained when cells were induced with 0.1 mM IPTG, this concentration was used routinely for expression.

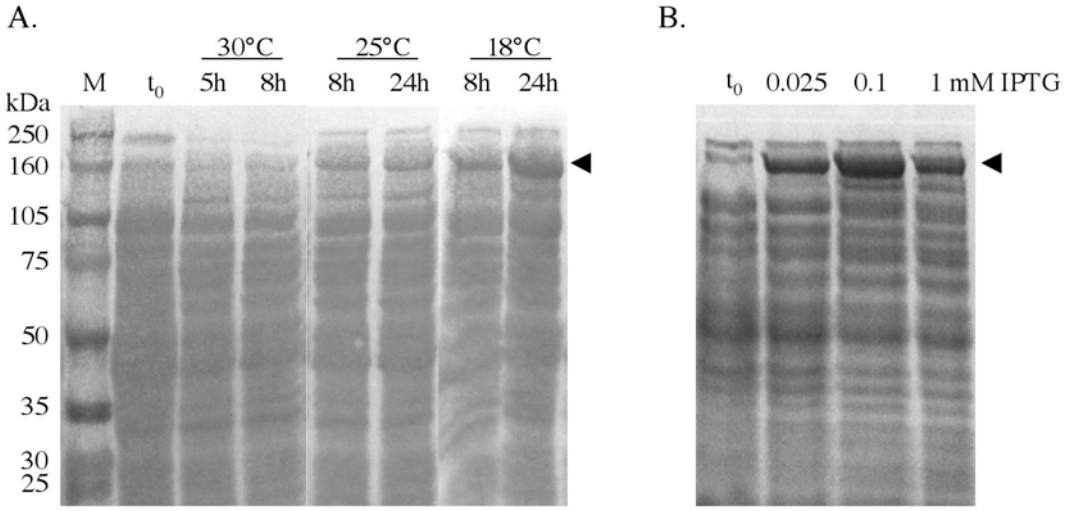

Figure 4.2. Optimization of TPP II expression in *E. coli.* A, Ponceau stained blot of an SDS-gel showing the effect of induction temperature and length on expression of soluble TPP II. *E. coli* cells were induced with 1mM IPTG for 5 – 24h at 30 – 18°C, as indicated. B, SDS-gel showing the effect of IPTG concentration on the expression of soluble TPP II. The cells were induced at 18°C for 24h. Cell extracts containing equal amounts of total protein were loaded on each lane. The arrows denote the 150 kDa TPP II band. In the cell extract harvested before induction (t_0), a weak TPP II band is observed due to leaky expression.

Higher yields of cells were obtained when *E. coli* was grown in Terrific Broth (TB, containing potassium phosphate buffer, pH 7.5), instead of LB. TB was the optimal growth medium due to its buffering capacity, preventing the acidification of the cultures even after long growth periods. When grown in TB, *E. coli* cultures induced with 0.1 mM IPTG and grown at 18°C for 24 h, reached an OD_{600} of 15, on average.

4.1.2 Enrichment of TPP II in the "2nd cell extract" of *E. coli*

Initially, it was not known whether the harsh procedures used for disruption of *E. coli* cells would destabilize the TPP II complexes. Therefore, the mildest approach, cell lysis with

lysozyme was used (Section 3.3.2.2). Subsequently, the cell extract, named“ 1st cell extract”, was separated by centrifugation. To ensure that cell disruption was complete, the pellet was resuspended, homogenized by sonication, and subsequently centrifuged to separate the extract named “ 2nd cell extract”. The SDS-gel in Figure 4.3 shows that the cells were efficiently lysed in the first disruption step, since the majority of *E. coli* proteins were released into the 1st cell extract. Increasing the lysozyme concentration two-fold or an additional freezing-thawing step did not improve the lysis.

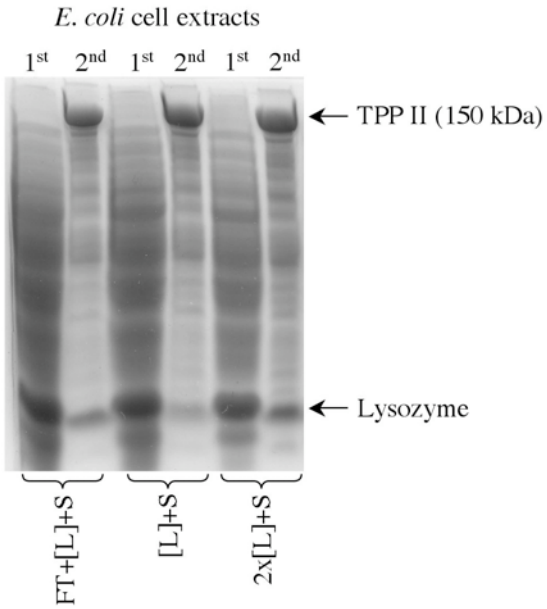

Figure 4.3. SDS-gel of the 1st and 2nd cell extracts of *E. coli.* The 1st cell extract represents the supernatant obtained after mild cell disruption using lysozyme (1.5 or 3 mg/ml final concentration), with or without a preceding freezing-thawing step. The pellet was then resuspended, homogenized via sonication and centrifuged to separate the supernatant named 2nd cell extract. The same amount of total protein was loaded on each lane. FT, freezing-thawing; [L], treatment with 1.5 mg/ml of lysozyme; 2x[L], treatment with 3 mg/ml of lysozyme; S, sonication.

Surprisingly, a large amount of TPP II was detected in the 2nd cell extract (Figure 4.3). Moreover, since the major part of the native proteins was separated in the 1st cell extract, the 2nd cell extract was significantly enriched in TPP II. This enrichment is due to a weak association of TPP II with the cell debris. Thus, a harsher disruption step, such as sonication, was needed for the release of TPP II into the 2nd cell extract.

4.2 Purification of TPP II from *E. coli*

To obtain a maximum yield of TPP II, two different purification approaches were compared.

4.2.1 Purification of recombinant TPP II: approach I

The purification of TPP II using approach I was performed as described in Section 3.4.8. *E. coli* clone dTPP II-wt (Figure 4.4) was used for expression.

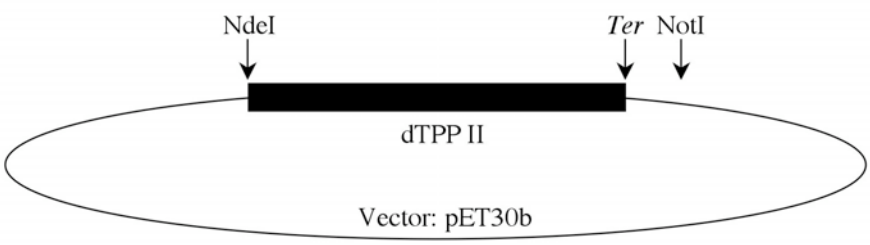

Figure 4.4. dTPP II-wt plasmid used for expression of the wild type *Drosophila* TPP II in *E. coli*. Arrows denote the NdeI and NotI restriction sites and the termination codon (*Ter*).

After the first homogenisation of *E. coli* cells, a significant amount of native proteins and part of the nucleic acid content was discarded by separating the 1st supernatant. This served as the first purification step since TPP II activity was 2.4-fold enriched in the 2nd supernatant (Table 4.1). To measure the peptidase activity of TPP II, the chromogenic substrate AAF-AMC was used in the presence of the amino-peptidase inhibitor Bestatin.

Table 4.1. Enrichment of TPP II in the 2nd cell extract of *E. coli*. AAF-AMC-hydrolysing activity was measured at 30°C and 0.2 mM substrate concentration. The specific activity was determined in relation to total protein. The TPP II content of total protein (in percent) was calculated according to the specific activity of purified TPP II complexes (6500 pmol x min^{-1} x μg^{-1}, see Table 4.2).

	Total protein ($\mu g/\mu l$)	Volume Activity (pmol x min^{-1} x μl^{-1})	Specific Activity (pmol x min^{-1} x μg^{-1})	TPP II (% of total protein)
1st cell extract	20.56	5160	251	4%
2nd cell extract	11.25	6770	602	9%

The 2nd cell extract was subjected to ion exchange chromatography, followed by hydrophobic interaction chromatography (HIC). Peak HIC fractions were pooled and separated by size exclusion chromatography on a Superose 6 column. The specific activities determined after each purification step are listed in Table 4.2.

Table 4.2. Purification of TPP II from *E. coli*. After each chromatographic step, the AAF-AMC-hydrolysing activity in the peak fractions was measured at 30°C and 0.2 mM substrate concentration. The specific activity was determined in relation to total protein. After Superose 6 chromatography TPP II was pure (Figure 4.5). Thus, 6500 pmol x min^{-1} x μg^{-1} is the specific activity of TPP II at 0.2 mM substrate concentration.

Purification Step	Protein (µg/µl)	Volume Activity (pmol x min^{-1} x μl^{-1})	Specific Activity (pmol x min^{-1} x μg^{-1})
2nd cell extract	11.25	6770	602
Q-Sepharose HP	1.25	2522	2018
Phenyl-Sepharose FF	0.79	3881	4913
Superose 6	0.04	238	6500

In the SDS-gel (Figure 4.5A), recombinant TPP II is represented by a major band corresponding to a molecular mass of ~ 150 kDa. The weak additional band at ~ 115 kDa was also observed in native TPP II purified from *Drosophila* (Renn et al., 1998; Rockel et al., 2002; Rockel et al., 2005). This ~ 115 kDa band, which is always present in the purified TPP II samples, will be shown below to be a TPP II fragment (Section 4.7.2).

In Superose 6 chromatography the enzyme eluted between 7.2 - 8.8 ml, corresponding to an apparent M_r of about 6 x 10^6 and higher, which indicated the presence of assembled TPP II. It was demonstrated by electron microscopy that TPP II formed spindle shaped complexes in *E. coli* (Figure 4.5). Those complexes exhibited full peptidolytic activity towards AAF-AMC (see table 4.2).

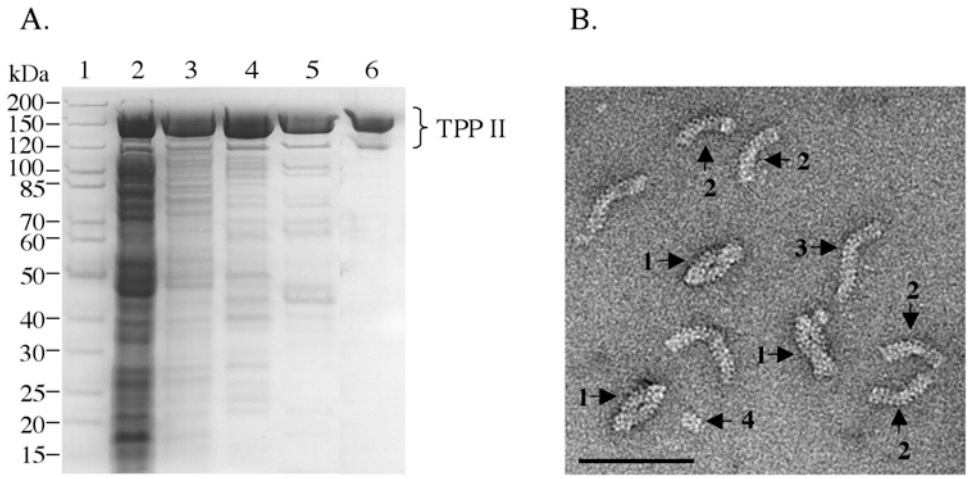

Figure 4.5. Purification of recombinant TPP II from *E. coli* using approach I. A, SDS-gel; lane 1, marker; lane 2, 1st cell extract; lane 3, TPP II-enriched 2nd cell extract; lane 4, Q-Sepharose HP eluate; lane 5, Phenyl-Sepharose FF eluate; lane 6, Superose 6 eluate containing pure TPP II. Sample volumes having the same TPP II activity were loaded on each lane. B, electron micrograph of purified recombinant TPP II complexes (Superose 6 eluate in panel A). Different oligomeric forms such as: 1, spindles; 2, bows (single strands); 3, extended (over-long) single strands and 4, lower oligomers were observed. Scale bar: 100 nm.

In the electron micrographs of purified TPP II, besides fully assembled spindles, bows (single strands) and lower assembly states were also observed (Figure 4.5). Since the purification procedure described above resulted in relatively low yields of TPP II, an alternative purification approach was established (approach II in Section 4.2.2.).

4.2.2 High-yield purification of recombinant TPP II: approach II

High degree of disassembly of the TPP II complexes during purification with approach I, led to loss of material in the final size exclusion chromatography step, and resulted in low yields. Therefore, purification approach II, which provided a fast and efficient purification of TPP II, was established (Section 3.4.9). *E. coli* clone dTPP II-wt (Figure 4.4) was used for expression. The TPP II-enriched 2nd cell extract of *E. coli* was treated with 0.2 % final concentration of PEI, which efficiently precipitated the nucleic acids in the cell extract. Addition of PEI increased the pH to 8.9 and resulted in disassembly of TPP II into small oligomers consisting of mainly tetramers, as shown by size exclusion chromatography in Figure 4.6B. When the protein was concentrated by ammonium sulphate precipitation, the concentration led to the reconstitution of the TPP II spindles. Due to their high apparent M_r

($\geq$ 6 x 10^6), the reconstituted TPP II complexes were efficiently separated from all *E. coli* proteins by a single size exclusion chromatography step (Figure 4.6B). The specific activity of purified TPP II (Table 4.3) was in good agreement with that of the enzyme obtained in the alternative purification approach I (Section 4.2.1).

Table 4.3. Purification of TPP II from *E. coli*. AAF-AMC-hydrolysing activity was measured after each purification step, at 30°C and 0.2 mM substrate concentration. The specific activity was determined in relation to total protein. After Superose 6 chromatography TPP II was pure (Figure 4.6). Thus, 6576 pmol x min^{-1} x μg^{-1} is the specific activity of TPP II at 0.2 mM substrate concentration.

Purification Step	Protein ($\mu g/\mu l$)	Volume Activity (pmol x min^{-1} x μl^{-1})	Specific Activity (pmol x min^{-1} x μg^{-1})
2^{nd} cell extract	11.25	6770	602
PEI Precipitation	6.42	2050	319
AS Precipitation	17.79	33225	1868
SEC Superose 6	0.62	4090	6576

The electron micrographs of the Superose 6 fractions eluting at 7.2 - 8.0 ml, revealed the presence of single strands, elongated single strands and spindles with extensions at the spindle poles, in addition to the spindles (Figure 4.6C). The fraction eluting at 8.0 - 8.8 ml (Figure 4.6D) contained mainly spindles that were morphologically indistinguishable from the native TPP II complex isolated from *Drosophila* (Figure 4.6E).

Approach II was used routinely for TPP II purification, since it provided large yields of fully active TPP II complexes. The concentration of TPP II after the final purification step was at least 16-fold of that obtained with purification approach I (Tables 4.2 and 4.3). It is important to obtain high concentrations of TPP II after chromatography, since the enzyme can not be concentrated by ultrafiltration, due to precipitation.

The yield of purified TPP II was 15-20 mg per litre of *E. coli* culture, or 1.5-2 mg protein per g of cells.

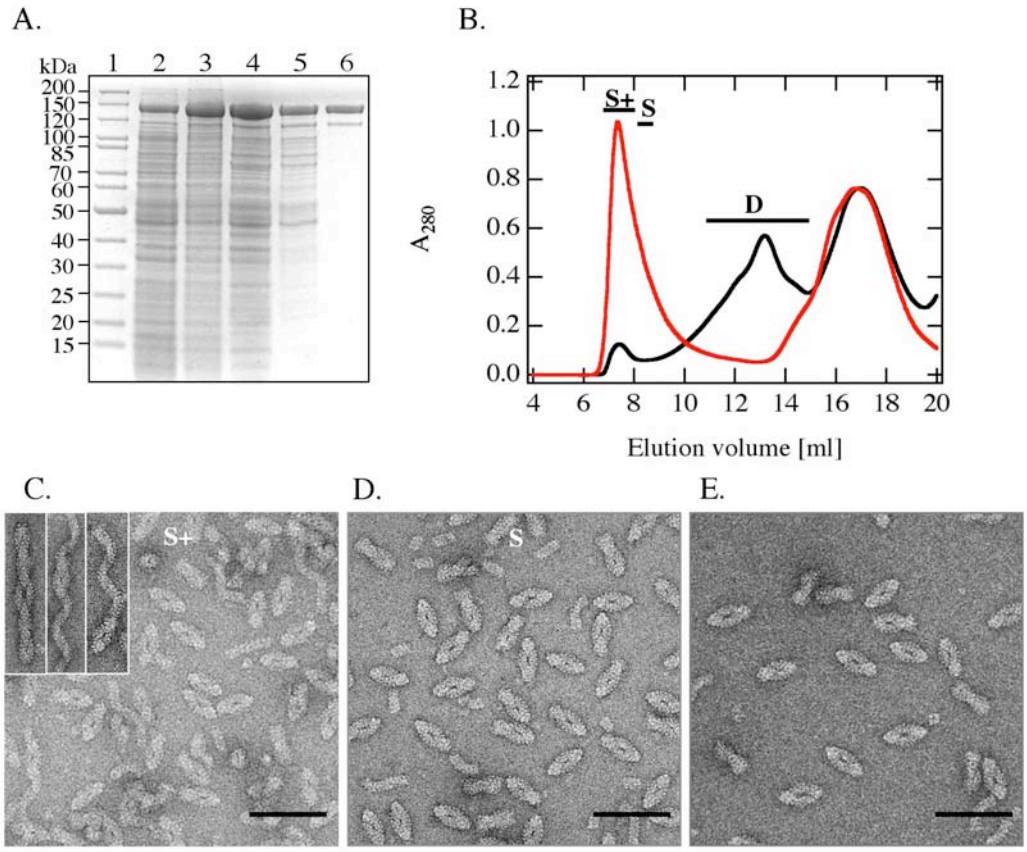

Figure 4.6. Purification of recombinant TPP II from *E. coli* using approach II. A, SDS-PAGE; lane 1, marker; lane 2, 1st cell extract; lane 3, TPP II-enriched 2nd cell extract; lane 4, supernatant after polyethyleneimine treatment; lane 5, ammonium sulfate precipitate; lane 6, complete high molecular mass peak (7.2–8.8 ml elution volume) of Superose 6 eluate. The same activity of TPP II was loaded on each lane. The TPP II preparation was homogeneous as verified by mass spectrometry. B, size exclusion chromatography on Superose 6. Black line, sample as in A, lane 4; D: disassembly products. Red line, ammonium sulfate precipitate; S(+): spindles plus extended complexes; S: spindles. *E. coli* proteins elute at 15–19 ml. C, electron micrograph of negatively stained particles of the S(+) fraction in B. The inset shows selected extended complexes. D, electron micrograph of the spindle fraction (S). E, native TPP II purified from *Drosophila* eggs. Scale bar: 100 nm.

4.3 Enzymological characterisation of recombinant TPP II

The recombinant TPP II spindles were characterized with respect to their peptidolytic activity towards the synthetic substrate AAF-AMC, and compared to the native enzyme. The Superose 6 eluate between 8.0 - 8.8 ml (Section 4.2.2) containing predominantly spindles was used and the activity measurements were carried out at AAF-AMC concentrations ranging between 0.15 and 2 mM, as described in Section 3.4.1.

From the Lineweaver-Burk plot (1/*v* versus 1/[S]) (Figure 4.7), the K_m of the recombinant TPP II was determined as 0.44 +/- 0.05 mM. This value is in good agreement with the K_m of the native enzyme, which was determined as 0.47 +/- 0.07 mM (Seyit et al., 2006).
Since the K_m was very high, a saturating substrate concentration could not be used. Instead, a concentration of 0.2 mM was used and V_{max} was determined as described below: According to the Henri-Michaelis-Menten equation $v/V_{max} = [S]/ K_m + [S]$, at $[S] = 0.45\ K_m$, $v/V_{max} = 0.31$ and $v = 6576$ pmol x min^{-1} x μg^{-1} (see Table 4.3), thus, V_{max} is 21,000 ± 1,000 pmol x min^{-1} x μg^{-1}. To ensure that the measured velocity represented the true v_0, the measurements were performed over a short enough time (depending on the enzyme concentration), so that [S] remained essentially constant (no more than 3% of the substrate was cleaved over the assay periods). Recombinant TPP II exhibited the highest AAF-AMC-hydrolyzing activity at pH ranging between 7.5 and 8.0 (data not shown).

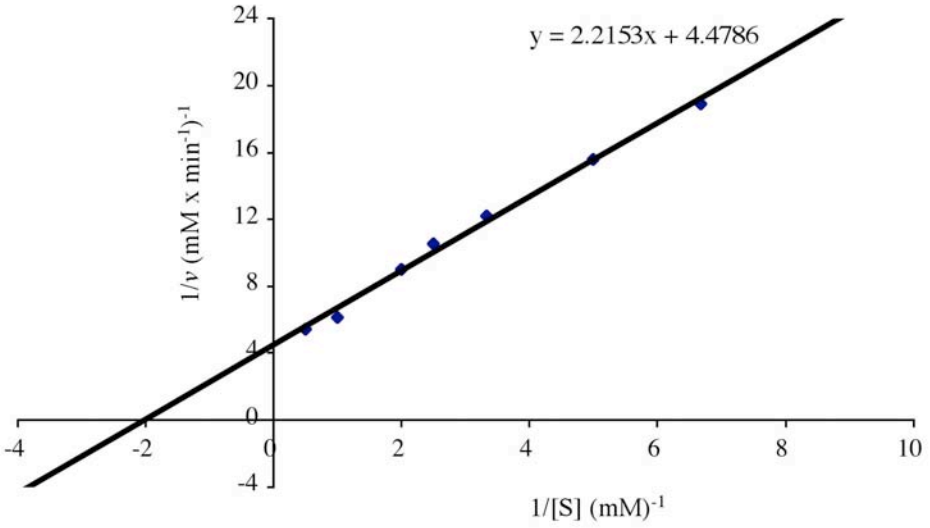

Figure 4.7. Lineweaver-Burk plot. TPP II spindles were used to determine the velocity (*v)* of AAF-AMC cleavage at 30°C.

4.4 Guanidine titration of TPP II complexes

In native TPP II preparations obtained from *Drosophila* eggs the spindles are the dominating form of TPP II (Rockel et al., 2002; Rockel et al., 2005). Therefore, the spindles were interpreted to be the most stable oligomeric form of TPP II *in vivo*. To probe the stability difference between single strands and spindles, purified TPP II (eluting between 7.2 - 8.0 ml from Superose 6 in Section 4.2.2) consisting of bows, unpaired

elongated strands, spindles and spindles with extensions was titrated with the chaotropic agent guanidine hydrochloride (GdnHCl, Section 3.4.10). At 0.55 M GdnHCl, the activity decreased to about one half. Subsequent size exclusion chromatography on a Superose 6 column gave disassembly peaks corresponding to lower oligomeric states such as 6-, 4-, 2- and 1-mers, in addition to the peak corresponding to the high molecular weight complexes of >6 MDa (Figure 4.8A). The high molecular weight peak contained essentially spindle-shaped holocomplexes (Figure 4.8B), which were resistant to disassembly under these conditions. On the other hand, previously present unpaired strands and the single stranded extensions disassembled into lower oligomers, mainly tetramers (Figure 4.8C). The degree of disassembly depended on the GdnHCl concentration used and on the incubation time. For example, at a GdnHCl concentration of 0.44 M, disassembly occurred to a lower extent but the same disassembly products were observed.

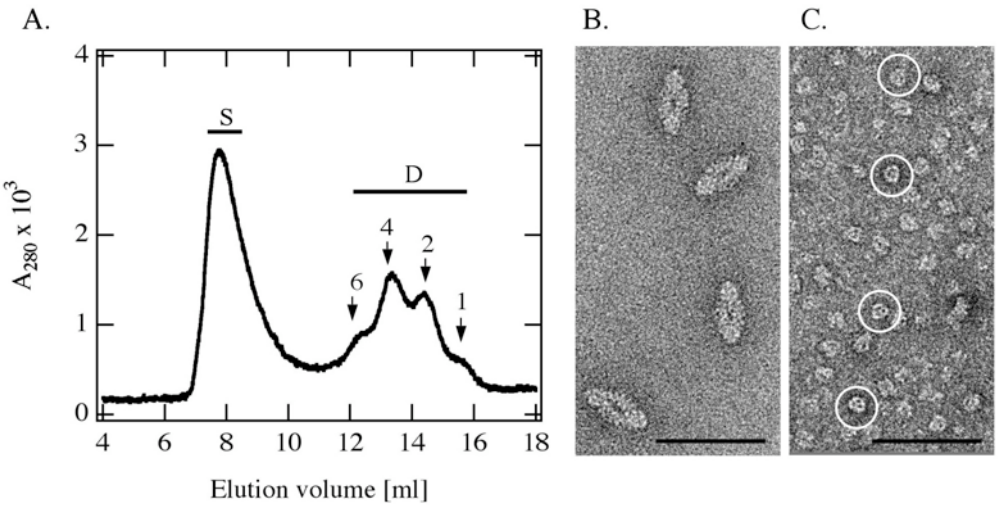

Figure 4.8. Disassembly of TPP II in the presence of GdnHCl. Intact spindles are resistant to 0.55 M GdnHCl, whereas unpaired strands disassemble into mainly tetramers. A, Superose 6 chromatogram after GdnHCl titration. S: spindles, D: disassembly products. Oligomeric states (hexamers to monomers) are denoted with arrows. B, electron micrograph of the spindle (S) fraction in panel A. C, electron micrograph of disassembly products (fraction D in panel A), tetramers are marked with circles. Scale bar: 100 nm.

According to these observations, the holocomplexes seem to be more stable than the unpaired strands. Therefore, it must be the lateral contact formation between the two strands that lends stability to the spindles.

4.5 The effect of N- and C-terminal fusions on assembly and stability of the TPP II complexes

Before establishing the high-yield purification approach II (Section 4.2.2), a His_6-tag was fused to the N- or C-terminus of TPP II to enable affinity-based purification. Metal chelate affinity purification did not produce high yields of active protein. Nevertheless, these experiments and additionally, maltose-binding protein tagging provided some insights into the structural organization of the TPP II complexes.

4.5.1 Purification and characterization of N-terminally His_6-tagged TPP II

E. coli clone dTPP II-NHis (Figure 4.1), was used for expression of *Drosophila* TPP II with an N-terminal His_6-tag (Section 3.2.6.1). The expression yield of TPP II-NHis was about the same as with untagged TPP II. TPP II-NHis also had the same specific activity as the untagged enzyme, when purified using purification approach II (Section 4.2.2). On the other hand, when purified by affinity chromatography (Figure 4.9A, see Section 3.4.12) the specific activity of TPP II-NHis decreased to about 70% in the HisTrap HP eluate. The decrease of activity was due to the presence of imidazole and NaCl (20 mM and 25 mM respectively) during the affinity purification, since full activity was recovered upon removal of the imidazole and NaCl by size exclusion chromatography using 80 mM potassium phosphate, pH 7.5 and 1 mM DTT as eluant. As determined by electron microscopy of the Superose 6 peak, TPP II-NHis formed spindles (Figure 4.9B), which had full activity. A minor peak of dimers (Figure 4.9B), exhibiting about $1/10^{th}$ of the spindle specific activity, was also observed. The full spindle and dimer activities after the removal of imidazole, show that the effect of imidazole was reversible. A similar decrease of activity upon treatment with imidazole was observed with the untagged TPP II (Section 4.5.2). Thus this effect can not be attributed to the presence of the N-terminal His_6-tag. Moreover, when purified in the absence of imidazole, TPP II-NHis displayed the same assembly and activity characteristics as the untagged TPP II. Therefore, under normal conditions, a His_6-tag at the N-terminus of TPP II subunits does not interfere with the assembly of the spindles.

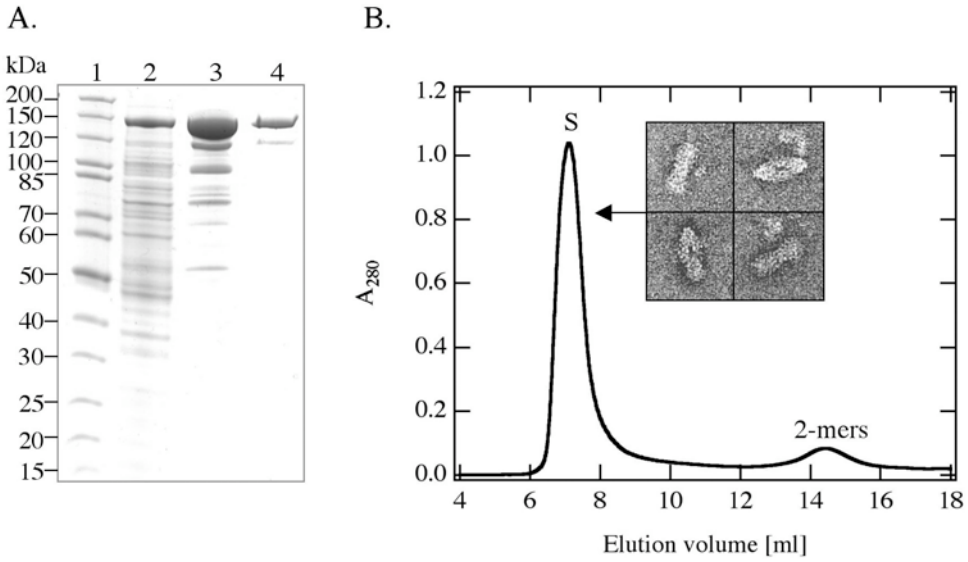

Figure 4.9. Purification of TPP II-NHis. A, SDS-gel; lane 1, marker; lane 2, 2nd cell extract of *E. coli*; lane 3, HisTrap HP eluate; lane 4, Superose 6 peak fraction (7-8 ml, S in panel B). B, Superose 6 chromatogram of HisTrap HP eluate in panel A lane 3. S, spindles; inset, gallery of TPP II-Nhis holocomplexes observed in fraction S.

4.5.2 Purification and characterization of C-terminally His_6-tagged TPP II

E. coli clone dTPP II-CHis (Figure 4.10), was used for expression of *Drosophila* TPP II with a C-terminal His_6-tag (Section 3.2.6.2).

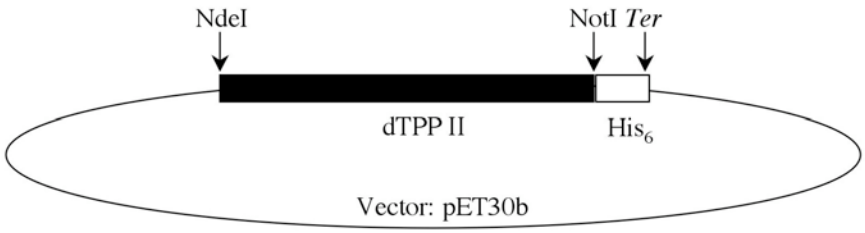

Figure 4.10. dTPP II-CHis plasmid used for expression of *Drosophila* TPP II with a C-terminal His_6-tag. Arrows denote the NdeI and NotI restriction sites and the termination codon (*Ter*).

TPP II with a C-terminal His_6-tag was purified by affinity chromatography (Section 3.4.12) to 2.2 mg/ml (Figure 4.11A, lane 3). When subjected to size exclusion chromatography on a Superose 6 column, TPP II-CHis eluted in two major peaks. The first peak corresponding to the high molecular mass complexes (Figure 4.11B) contained spindles, as shown by electron microscopy (Figure 4.11B inset). This shows that, the C-terminally His_6-tagged

TPP II subunits can assemble into holocomplexes. On the other hand, the specific activity measured in this fraction was only about 1/10th of the full spindle activity, most probably due to the presence of inactive aggregates in addition to the spindles. The presence of a prominent dimer peak (Figure 4.11B) indicated that TPP II-CHis had a higher propensity for disassembly than TPP II-NHis (Section 4.5.1).

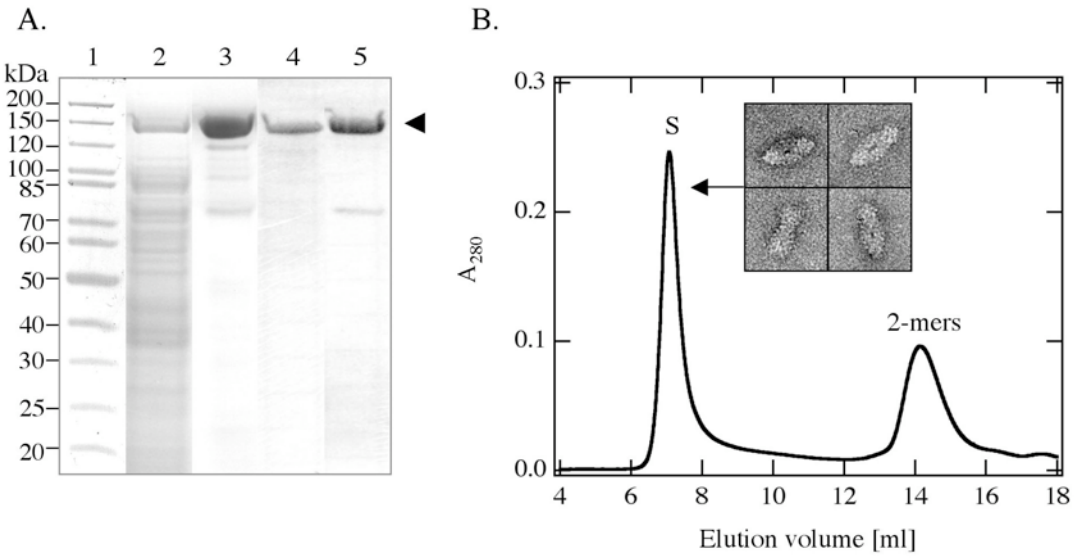

Figure 4.11. Purification of TPP II-CHis. A, SDS-gel; lane 1, marker; lane 2, 2nd cell extract of *E. coli*; lane 3, HisTrap HP eluate; lane 4, fraction S (spindles) in panel B, lane 5, 2-mer fraction in panel B, equal volumes of Superose 6 eluate were loaded in lanes 4 and 5. B, Superose 6 chromatogram of the HisTrap HP eluate in panel A lane 3; inset, gallery of TPP II-Chis holocomplexes observed in fraction S.

The effect of imidazole on TPP II was investigated in TPP II-CHis and TPP II-wt 2nd cell extracts exhibiting the same initial activity. A significant decrease of TPP II activity was monitored in both of the cell extracts after incubation for 2h in the presence of 25 mM NaCl and 20 mM imidazole (Figure 4.12). Interestingly TPP II-CHis, which retained about 1/4th of the original volume activity, was more susceptible to the destabilizing effect of imidazole than the TPP II-wt exhibiting about half of the original volume activity. Furthermore, as judged by size exclusion chromatography, incubation for 2 h with 200 mM imidazole resulted in complete disassembly of TPP II-CHis oligomers, whereas wild type TPP II, in addition to partial disassembly, still gave a peak corresponding to the elution volume of spindles (data not shown).

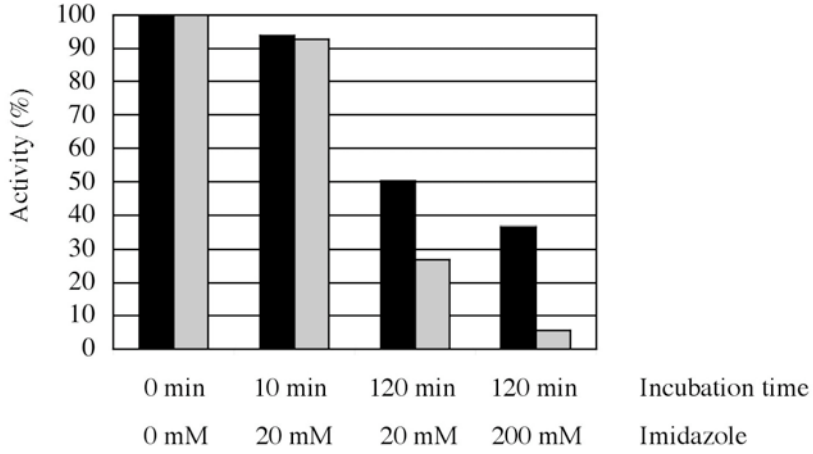

Figure 4.12. The effect of imidazole treatment on the activity of the TPP II complex. C-terminally His_6-tagged subunits (TPP II-CHis, grey bars) are more susceptible to disassembly and thus show a higher decrease of activity, compared to the untagged subunits (TPP II-wt, black bars).

These results lead to the following conclusions: i) The His_6-tag is accessible and therefore enables isolation of TPP II-CHis by affinity purification. ii) The presence of the spindles indicates that the $CHis_6$-tagged TPP II assembles. iii) When exposed to destabilizing conditions such as treatment with imidazole, the $CHis_6$-tagged complex shows reduced stability compared to the untagged and the $NHis_6$-tagged enzyme. Thus, apparently, even a short insertion (His_6) at the C-terminus can alter the stability of the enzyme. Therefore, the C-terminal region appears to be essential for complex formation.

4.5.3 An N-terminal maltose-binding protein tag prevents spindle formation

A maltose-binding protein-tag (MBP-tag) was fused to the N-terminus of TPP II with the purpose to map the catalytic (N-terminal) domain of TPP II in the oligomers, and also to determine whether a bulky tag in this region would alter oligomer assembly. MBP is a monomeric protein with a molecular mass of 42 kDa (Spurlino et al., 1991). MBP-tagged TPP II (TPP II-Nmbp) was purified from *E. coli* clone dTPP II-Nmbp (Figure 4.13) as described in Section 3.4.11.

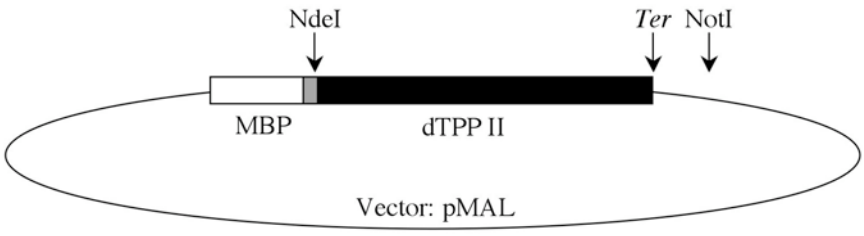

Figure 4.13. dTPP II-Nmbp plasmid used for the expression of *Drosophila* TPP II with an N-terminal MBP-tag. The grey box represents the sequence coding for a 26 amino acid linker ($TNSSSN_{10}$LGIEGRISEFH) between MBP and TPP II. Arrows denote the NdeI and NotI restriction sites and the termination codon (*Ter*).

SDS-PAGE of the *E. coli* extract revealed over-expression of TPP II-Nmbp in soluble form (Figure 4.14A lane 2). TPP II-Nmbp was purified by a single affinity chromatography step to a concentration of ~ 6 mg/ml (Figure 4.14A lane 3). The yield was ~ 25 mg protein per liter of culture. To determine the assembly state of TPP II-Nmbp, the amylose resin eluate was subjected to size exclusion chromatography on a 2.4 ml Superose 6 column. This revealed the presence of both, high oligomers of TPP II and some disassembly products (Figure 4.14B). Unpaired strands of various lengths were observed in electron micrographs of the Superose 6 peak fraction (Figure 4.14B). This shows that single strands can assemble independently and that the strand elongation is not limited to a certain length. On the other hand, no spindles were formed. Since the presence of an N-terminal MBP-tag prevented spindle formation, the N-terminal domain appears to be oriented towards the strand-to-strand interface and thus involved in strand pairing.

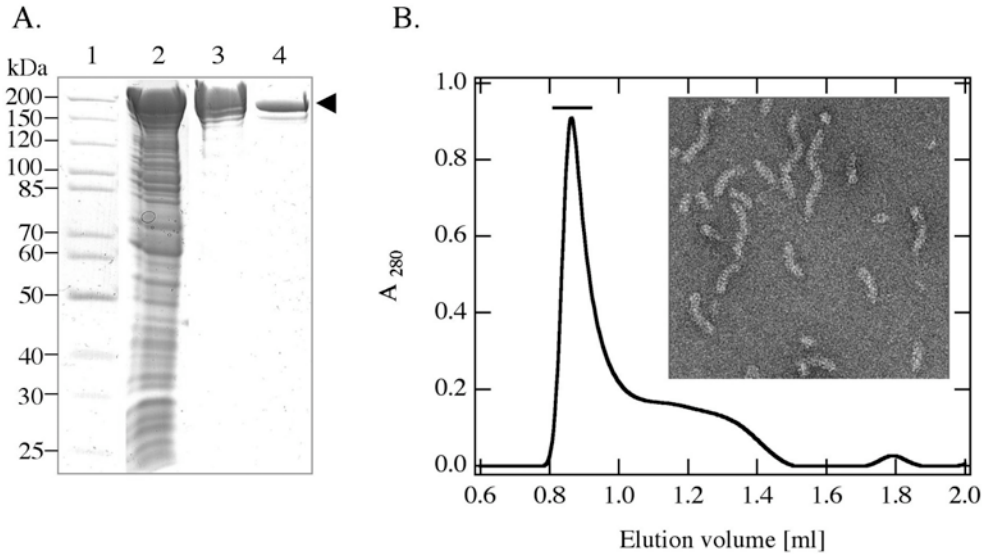

Figure 4.14. Expression and purification of N-terminally MBP-tagged TPP II. TPP II-Nmbp subunits assemble into single strands, but do not form spindles. A, SDS-gel; lane 1, marker; lane 2, *E. coli* cell extract; lane 3, amylose eluate; lane 4, Superose 6 eluate containing pure TPP II-Nmbp. The arrow denotes the 192 kDa TPP II-Nmbp band. B, Superose 6 chromatogram of the amylose eluate in panel A lane 3; inset, electron micrograph of Superose 6 fraction indicated by the bar.

The specific molar activity of TPP II-Nmbp (981 pmol x min^{-1} x μmol^{-1}) was indistinguishable from the activity of the untagged TPP II (986 pmol x min^{-1} x μmol^{-1}). The result indicates that spindle formation does not have a significant effect on the peptidase activity. However, as discussed in Section 4.4 it seems to stabilize the enzyme.

4.6 Disassembly of the TPP II complexes to obtain homogeneous and stable subunits

Every crystallization attempt requires chemically and conformationally homogenous material. By expressing TPP II in *E. coli*, it became possible to obtain chemically pure protein at high concentration. However, conformational homogeneity was difficult to achieve, since the holocomplexes could not be completely separated from the other assembly states (Figure 4.6C). Because of the concatameric structure of the enzyme, oligomerization is a dynamic process and assembly/disassembly depends on the conditions such as buffer composition, temperature (Section 4.6.3) and most significantly on the enzyme concentration (Section 4.2.2). At concentrations of ≥1 mg/ml TPP II formed multiple-spindle complexes and elongated single strands with lengths up to about 250 nm

(Figure 4.6C inset). In order to provide homogeneity, a number of approaches potentially leading to irreversible disassembly were investigated systematically. The objective was to obtain TPP II subunits, which do not reassemble even at elevated protein concentrations and which do not further disassemble.

4.6.1 Site-directed mutagenesis for disassembly of TPP II

Sequence alignments of *Drosophila* TPP II with homologues were performed and used in order to predict the individual amino acids and amino acid clusters, which might have a role in complex formation. Consequently, the effects of: i) the *G260R* mutation (Section 4.6.1.1), ii) mutations in the conserved charged clusters (Section 4.6.1.2), and iii) truncations at the C-terminus of TPP II (Section 4.6.1.3) were investigated. The mutated residues are marked in the sequence alignment in Figure 4.15.

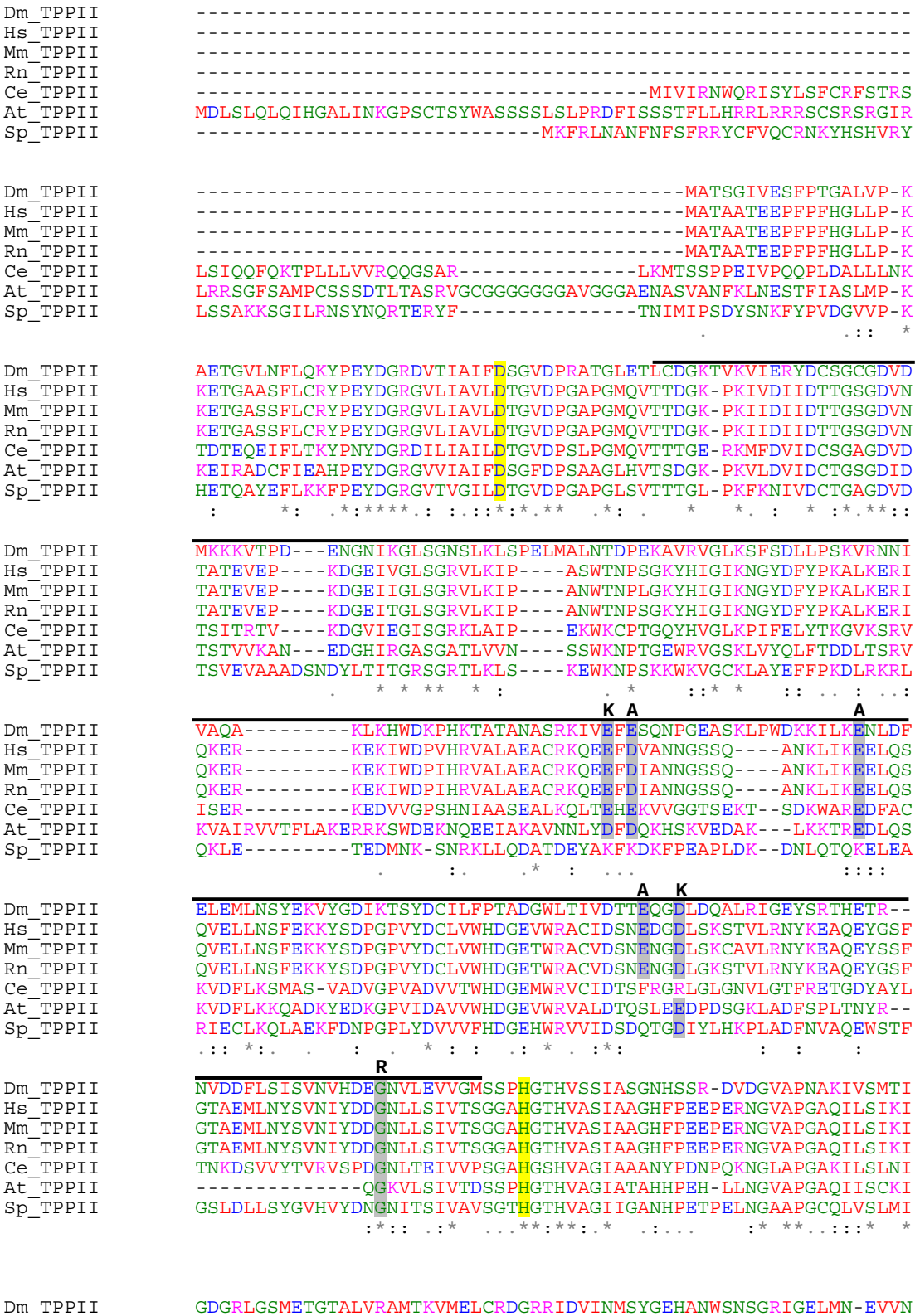
Dm_TPPII
Hs_TPPII
Mm_TPPII
Rn_TPPII
Ce_TPPII
At_TPPII
Sp_TPPII
K A
A
A K
R

```
Dm_TPPII        KYGVVWVASAGNHGPALCTVGTPPDISQPSLIGVGAYVSPQMMEAEYAMREK-LPGNVYT 421
Hs_TPPII        KHNIIYVSSAGNNGPCLSTVGCPGGTTS-SVIGVGAYVSPDMMVAEYSLREK-LPANQYT 408
Mm_TPPII        KHNTIYVSSAGNNGPCLSTVGCPGGTTS-SVIGVGAYVSPDMMVAEYSLREK-LPANQYT 408
Rn_TPPII        KHNTIYVSSAGNNGPCLSTVGCPGGTTS-SVIGVGAYVSPDMMVAEYSLREK-LPANQYT 408
Ce_TPPII        RRGVIYVCSAGNQGPALSTVGAPGGTTT-GVIGIGAYLTSESADTLYGVYKP-VESSIYP 458
At_TPPII        KRRLIFVSSAGNSGPALTTVGAPGGTTS-SIIGVGAYVSPAMAAGAHSVVEPPSEGLEYT 504
Sp_TPPII        KRNVVIVSSAGNNGPAYTTVGAPGGTTF-DVISVGAYVTSGMMQAQYNLLST-VHDTPYT 471
                :   : *.**** **.  *** * . :  .:*.:***::.      : : .       *.

Dm_TPPII        WTSRDPCIDGGQGVTVCAPGGAIASVPQFTMSKSQLMNGTSMAAPHVAGAVALLISGLKQ 481
Hs_TPPII        WSSRGPSADGALGVSISAPGGAIASVPNWTLRGTQLMNGTSMSSPNACGGIALILSGLKA 468
Mm_TPPII        WSSRGPSADGALGVSISAPGGAIASVPNWTLRGTQLMNGTSMSSPNACGGIALVLSGLKA 468
Rn_TPPII        WSSRGPSADGALGVSISAPGGAIASVPNWTLRGTQLMNGTSMSSPNACGGIALVLSGLKA 468
Ce_TPPII        WSSRGPCQDGKLGVSLVAPAAAFAGVPQYCRQSMQMMNGTSMSSPNAAGNVACMLSGLKQ 518
At_TPPII        WSSRGPTSDGDLGVCISAPGGAVAPVPTWTLQRRMLMNGTSMASPSACGAIALLLSAMKA 564
Sp_TPPII        WCSRGPTLDGDTGVSIYAPGGAITSVPPYSLQNSQLMNGTSMSSPSACGGISLILSALKA 531
                * **.*  **  ** : **..*.: ** :      :******::* ..* :: ::*.:*

Dm_TPPII        QNIEYSPYSIKRAISVTATKLGYV--DPFAQGHGLLNVEKAFEHLTEHRQSKDN------ 533
Hs_TPPII        NNIDYTVHSVRRALENTAVKADNI--EVFAQGHGIIQVDKAYDYLVQN-TSFAN------ 519
Mm_TPPII        NNVDYTVHSVRRALENTAIKADNI--EVFAQGHGIIQVDKAYDYLIQN-TSFAN------ 519
Rn_TPPII        NNVDYTVHSVRRALENTAIKADNI--EVFAQGHGIIQVDKAYDYLIQN-TSFAN------ 519
Ce_TPPII        NNLKWTPYTVRMALENTAYMLPHI--ESFSQGQGMIKIATAYEKLSEILVNKVFP----- 571
At_TPPII        EGIPVSPYSVRRALENTSTPVGDLPEDKLTTGQGLMQVDKAYEYLKQFQDYPCVFYQIKV 624
Sp_TPPII        QKKPYTAAAIKKAVMYTSKDLR----DDFNTG--MLQVDNAYEYLAQSDFQYTG------ 579
                :    :  ::: *:  *:        : :  *  :::: .*:: * :

Dm_TPPII        ----------------------------MLRFSVRVGNNA--DKGIHLRQGVQRNS-ID 561
Hs_TPPII        ----------------------------KLGFTVTVGN----NRGIYLRDPVQVAAPSD 546
Mm_TPPII        ----------------------------RLGFTVTVGN----NRGIYLRDPVQVAAPSD 546
Rn_TPPII        ----------------------------RLGFTVTVGN----NRGIYLRDPVQVAAPSD 546
Ce_TPPII        ----------------------------PRLTHFEINVSNHCKKSKGVYVREPN-WNGPQE 603
At_TPPII        NLSGKTRLPAVTLGKFPKILGFFDKQYNFLFMKILNSINAVPTSRGIYLREGTACRQSTE 684
Sp_TPPII        ---------------------------ARSFTINGNIGNS---KRGVYLRNPTEVCSPSR 609
                                                  *    .:*:::*:

Dm_TPPII        YNVYIEPIFYNDKEADPKDKFNFNVRLNLIASQP-WVQCGAFLDLSYGTRSIAVRVDPTG 620
Hs_TPPII        HGVGIEPVFPENTENS--EKISLQLHLALTSNSS-WVQCPSHLELMNQCRHINIRVDPRG 603
Mm_TPPII        HGVGIEPVFPENTENS--EKISFQLHLALTSNSS-WVQCPSHLELMNQCRHINIRVDPRG 603
Rn_TPPII        HGVGIEPVFPENTENS--EKISFQLHLALTSNSS-WVQCPSHLELMNQCRHINIRVDPRG 603
Ce_TPPII        FTIGVEPIFQNHLSDNNLPAISFEKQIILQSTAP-WVSHPQTMFVVAQERTMVVTVDASK 662
At_TPPII        WTIQVDPKFHEG-ASNLKELVPFEECLELHSTDEGVVRVPDYLLLTNNGRGFNVVVDPTN 743
Sp_TPPII        HMFNVAPKFED---GEEYEKSHFEVQLSLATTQP-WIQAPEYVMMAGTGRGIPVRVDPTA 665
                  . : * * :    .      ::  : * :.    :     : :    * : : **.

Dm_TPPII        LQPGVHSAVIRAYDTDCVQKGSLFEIPVT-VVQPHVLESDQNTPVFEPASSKGDNSVEFQ 679
Hs_TPPII        LREGLHYTEVCGYDIASPNAGPLFRVPITAVIAAKVNESSHYDLAFT--------DVHFK 655
Mm_TPPII        LREGLHYTEVCGYDIASPNAGPLFRVPITAVIAAKVNESSHYDLAFT--------DVHFK 655
Rn_TPPII        LREGLHYTEVCGYDIASPNAGPLFRVPITAVIAAKVNESSHYDLAFT--------DVHFK 655
Ce_TPPII        APKGANYTEIVGIDTADPSLGPIFRIPVTVINPEKVAVDQYTSRLVG-----------K 710
At_TPPII        LGDGVHYFEVYGIDCKAPERGPLFRIPVTIIIPKTVANQPPVISFQQMS---------FI 794
Sp_TPPII        LAPGHHFGKVLAYDASNESRRCVFEIPVTVMKPSSISNTCFSLRDVS----------FE 714
                   * :   : . *    .   :*.:*:* :    :

Dm_TPPII        PNTIQRDFILVPERATWAELRMRITDPNRGEDIGKFFVHTNQLLPKQSCRKLETMKIVSV 739
Hs_TPPII        PGQIRRHFIEVPEGATWAEVTVCSCSS---EVSAKFVLHAVQLVKQRAYRSHEFYKFCSL 712
Mm_TPPII        PGQIRRHFVEVPEGATWAEVTVCSCSS---EVSAKFVLHAVQLVKQRAYRSHEFYKFCSL 712
Rn_TPPII        PGQIRRHFVEVPEGATWAEVTVCSCSS---EVSAKFVLHAVQLVKQRAYRSHEFYKFCSL 712
Ce_TPPII        SGVTERRFVEVPSWATSAKITLRSTNK---DEMDRFTLHTVYIEDDKCSRNTETQKIQGP 767
At_TPPII        SGHIERRYIEVPHGATWAEATMRTSGF---DTTRRFYIDTLQVCPLR--RPIKWESAPTF 849
Sp_TPPII        PTLIKRHFLVPPKGATYVEIRVKATSEL--ESTNMLWISVNQTIPQTKLNEASTELIMPV 772
                .   .* ::  *  ** .:  :   .    :    : : .          .  .

Dm_TPPII        GSENESIMAFKVKSGRILELCIAKYWSN----YGQSHLKYSLRFRGVEAHNPNAYVMHAG 795
Hs_TPPII        PEKGTLTEAFPVLGGKAIEFCIARWWAS----LSDVNIDYTISFHGIVCTAP-QLNIHAS 767
Mm_TPPII        PEKGTLIEAFPVLGGKAIEFCIARWWAS----LSDVNIDYTISFHGIVCTAP-QLNIHAS 767
Rn_TPPII        PEKGTLIEAFPVLGGKAIEFCIARWWAS----LSDVNIDYTISFHGIVCTAP-QLNIHAS 767
Ce_TPPII        IG-NEWSKSITVQGGKTLEACVVRAWSRG---KNPVDVDMTIDFFGVKKPTS-ISLIHGA 822
At_TPPII        ASPSAKSFVFPVVSGQTMELAIAQFWSSGLGSREPTIVDFEIEFHGVGVDKE-ELLLDGS 908
Sp_TPPII        TQNEVTTKLVSIDDSYTLELCMAQWWSS----LEPMVLDIDVNFHGIKVVNGKEINLISS 828
                          . : ..  :* .:.: *:          :.  : * *:         : ..
```


Dm_TPPII RGIHKLEIEA-LVAEDVQPQLQLKNAEVVLKPTEAKISPLSATRDVIPDGRQVYQNLLAF 854
Hs_TPPII EGINRFDVQSSLKYEDLAPCITLKNWVQTLRPVSAKTKPLGS-RDVLPNNRQLYEMVLTY 826
Mm_TPPII EGINRFDVQSSLKYEDLAPCITLKSWVQTLRPVNAKTRPLGS-RDVLPNNRQLYEMVLTY 826
Rn_TPPII EGINRFDVQSSLKYEDLAPCITLKSWVQTLRPVNAKTRPLGS-RDVLPNNRQLYEMVLTY 826
Ce_TPPII TNTPIRFQAAPTKSIDVSPSISLKSLVVSLKPQSAKVEPLGPRDMFLTSGLQINRLLLTY 882
At_TPPII EAPIKVEAEALLASEKLVPIAVLNKIRVPYQPIDAQLKTLSTGRDRLLSGKQILALTLTY 968
Sp_TPPII QGLKRVDCAS-IRRENFKPDITLKDYVDSFKPTNTVIKPLGD-RDIMPDGQQLFELMATY 886
NLNVAKAADVSIYAPIFNDLLYEAEFESQMWMLFDANKALVATGDAHSHTSFTKLDKGEY 914
NFHQPKSGEVTPSCPLLCELLYESEFDSQLWIIFDQNKRQMGSGDAYPHQYSLKLEKGDY 886
SFHQPKSGEVTPSCPLLCELLYESEFDSQLWIIFDQNKRQMGSGDAYPHQYSLKLEKGDY 886
SFHQPKSGEVTPSCPLLCELLYESEFDSQLWIIFDQNKRQMGSGDAYPHQYSLKLEKGDY 886
QLKVQKPSEVQLQLAGLTPYLYESPVDCVLFQIFGANKSFVGASSSYPDRWTQKLEKGDY 942
KFKLEDSAEVKPYIPLLNNRIYDTKFESQFFMISDTNKRVYAMGDVYP--ESSKLPKGEY 1026
SVEISEKTELKADFAVPHN-MYDNGFNGLFFMVFDSQKQRVHYGDMY--TSSHTLEKGEY 943
A A
TIRLQVRHEKRDLLEKISEANLVASFKLTSPLTLDFYENYNQCIVGGR-KYVSSPLR-LS 972
TIRLQIRHEQISDLERLKDLPFIVSHRLSNTLSLDIHENHSFALLGKK-KSSNLTLPPKY 945
TIRLQIRHEQISDLDRLKDLPFIVSHRLSNTLSLDIHENHSLALLGKK-KSSSLTLPPKY 945
TIRLQIRHEQISDLDRLKDLPFIVSHRLSNTLSLDIHENHSLALLGKK-KSSSLTLPPKY 945
TIQAQIRYPDDQVLQGMKELPLLVHVKLGNKISVDLAASASDATLGKECKFAGKALLPNQ 1002
KLQLYLRHENVELLEKLKQLTVFIERNMG-EIRLNLHSEPDGPFTGNG-AFKSSVLMPGV 1084
LYKFQLLSVDPSTLERFRNVTLRLTKKLKKPITLPLYADHIDFCDNKT---YERENIDAG 1000
TRVLYIAPITQERLTKANLPAQCAWLSGNLVFPQDEVGRRVAQHPFTYILNPAEKKSHTN 1032
NQPFFVTSLPDDKIPKG--AGPGCYLAGSLTLSKTELGKKADVIPVHYYLIPPPTK---- 999
NQPFFVTSLPDDKIPKG--AGPGCYLAGSLTLSKTELGKKADVIPVHYYLIPPPTK---- 999
NQPFFVTSLPDDKIPKG--AGPGCYLAGSLTLSKTELGKKADVIPVHYYLIPPPTK---- 999
EMTVYAMNIADDKLPKTIVPTSGSFLAGTFSALKDSDLSDVDKSEVIYFLSEYSTR---- 1058
KEAFYLGPPTKDKLPKN--TPQGSMLVGEISYGKLSFDEKEGKNPKDNPHRLVKLD---- 1138
VVESFVVGTNIEGEQYASELKENSLLTGELKFGDCEKG----TVPVTLVLPPKIST---- 1052
GSSNGSSAAGSTATAAAVTTANGAKPKAPATPQAATSVTNPAAGDGISVQNDPPVDSSGS 1092
----------TKNGSKDKEKDS---------- 1011
----------IKNGSKDKEKDS---------- 1011
----------TKNGSKDKEKDS---------- 1011
----------PTKGLSMVTT---------- 1068
----------APEEDKKAASAP---------- 1150

PASPKKGKANADDYAESFRDFQCSQIVKCELE------MAEKIYNDVVAAHPKHLQANLL 1146
----EKEKDLKEEFTEALRDLKIQWMTKLD---------SSDIYNELKETYPNYLPLYVA 1058
----EKEKDLKEEFTEALRDLKIQWMTKLD---------STDIYNELKETYPAYLPLYVA 1058
----EKEKDLKEEFTEALRDLKIQWMTKLD---------STDIYNELKETYPAYLPLYVA 1058
----KKDTNQNQEMTDAIRDLEVSWVQKLTDEK-----AAKEFFEACLQKYPDHLPLLQN 1119
----TCSKSVSERLEQEVRDTKIKFLGNLKQETEEERSEWRKLCTCLKSEYPDYTPLLAK 1206
-----KEDTKLGEKCANIVQLQVDLLSKLADQ------EKEKHLKYLQSSYKNSLEVQLA 1101
LIQNIESNQLKSQLPLTFVNAQKTSPPEAGESADKQKEDQKKVRSALERIVKLADKVIQE 1206
RLHQLDAE----------KERMKRLN----EIVDAANAVISH 1086
RLHQLDAE----------KERMKRLN----EIVDAANAVISH 1086
RLHQLDAE----------KERMKRLN----EIVDAANAVISH 1086
RVKQLMQAKLVDQTPENVQKIIELCG---------QILQITKPNETLQFSSVKQEHDDDL 1170
ILEGLLSRS----------DAGDKISHHEEIIEAANEVVRS 1237
KLDIVKETN----------ERLSTADSILSL 1122
TDSEALLSYYGLKN---DTRADAAKIKTNMDKQKNTLIEALSKKGIAVAKLAVLDDCIK- 1262
IDQTALAVYIAMKT---DPRPDAATIKNDMDKQKSTLVDALCRKGCALADHLLHTQAQDG 1143
IDQTALAVYIAMKT---DPRPDAATIKNDMDKQKSTLIDALCRKGCALADHLLHTQPHDG 1143
IDQTALAVYIAMKT---DPRPDAATIKNDMDKQKSTLVDALCRKGCALADHLLHAQPHDG 1143
LTVDKWLALTGGSE---DQRKDVVKLISQFEERKKSIILALQALSSLEQDIEVRKSKFDV 1227
VDVDELARFLLDKTE--PEDDEAEKLKKKMEVTRDQLADALYQKGLAMARIENLKGEKEG 1295
IDTEALSRYYSCQQKVEDTIPRDVVLEKKMALQRDAFIRALVVKCETFSTQGHKD----- 1177

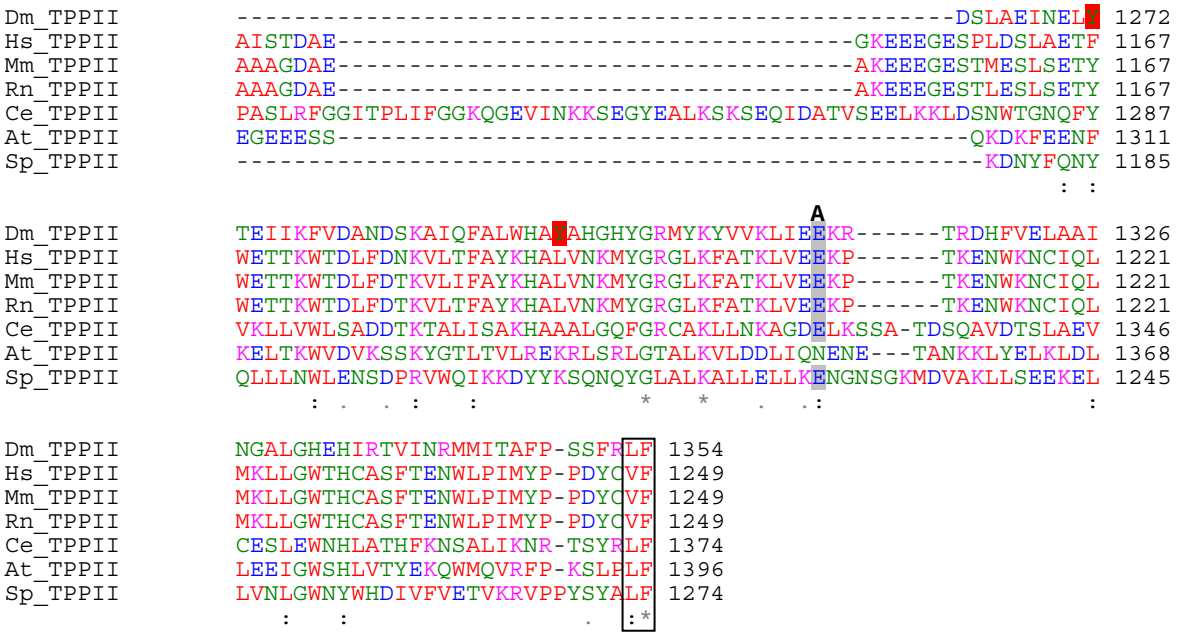

Figure 4.15. Sequence alignment of TPP II from *Drosophila melanogaster* (Dm, GenPept accession: AAC28563) with its homologues from *Homo sapiens* (Hs, AAH39905), *Mus musculus* (Mm, AAH58239), *Rattus norvegicus* (Rn, NP_112399), *Caenorhabditis elegans* (Ce, NP_495221), *Arabidopsis thaliana* (At, CAB79085), and *Schizosaccharomyces pombe* (Sp, CAB55179), using CLUSTAL W (version 1.83, at http://www.ebi.ac.uk/clustalw/). The identical residues are marked with asterisks; colons indicate the conserved residues; dots indicate the semi-conserved residues. Active site residues of TPP II are highlighted in yellow; mutated residues are highlighted in grey and the mutation is indicated above each in black bold type. The residues exchanged with a termination codon (to generate truncated proteins) are highlighted in red. The black line marks the ~ 200 residue insert between the catalytic D and H residues, which is not present in subtilisin; the grey line marks the non-conserved region in *Drosophila* TPP II; black box: the highly conserved LF residues on the C-terminal end.

4.6.1.1 *G260R* mutation

Compared to other subtilases, TPP II has an insert of ~200 amino acids between the catalytic Asp and His residues in its N-terminal domain (Figure 4.15). This region was reported to play a role in the formation of the active holocomplexes (Tomkinson et al., 2002). In the same study, it was concluded that a *G252R* mutation in the insert sequence of human TPP II resulted in a non-assembled and inactive enzyme.

According to the sequence alignment in Figure 4.15, G252 in human TPP II corresponds to G260 in the *Drosophila* enzyme. The *G260R* mutation was introduced into the wild type *Drosophila* TPP II sequence as described in Section 3.2.7.1 (clone dTPP II-*G260R*, Figure 4.16)

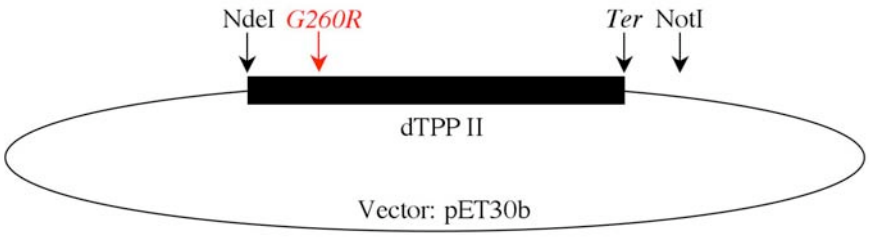

Figure 4.16. dTPP II-*G260R* plasmid used for expression of *Drosophila* TPP II with a *G260R* mutation, in *E. coli*. Black arrows denote the NdeI and NotI restriction sites and the termination codon (*Ter*), the red arrow denotes the mutation site in *Drosophila* TPP II gene.

The recombinant protein was expressed in *E. coli* in soluble form and AAF-AMC-hydrolysing activity was detected in the cell extract. In the cell extract, the mutant exhibited a reduced activity of 146 pmol x min^{-1} per µg of total protein, as compared to the wild type enzyme (602 pmol x min^{-1} per µg of total protein). The mutant TPP II expression level was roughly the same as in the wild type, as judged from the intensity of the 150 kDa band on the SDS-gels. Consequently, the cell extract contained about the same amount of TPP II per µg of total protein as the wild type cell extract. Therefore, the mutant activity of 146 pmol x min^{-1} per µg of total protein, corresponded to about 25% of the wild type TPP II activity in the cell extract and was taken as an indication for disassembly. The cell extract was subjected to size exclusion chromatography on a Superose 6 column, and volume activities in the eluate fractions were measured. As shown in Figure 4.17, the distribution of activity revealed the presence of various oligomeric states, and no

prevalence of spindles was observed, indicating that the G260R mutation interfered with complex formation.

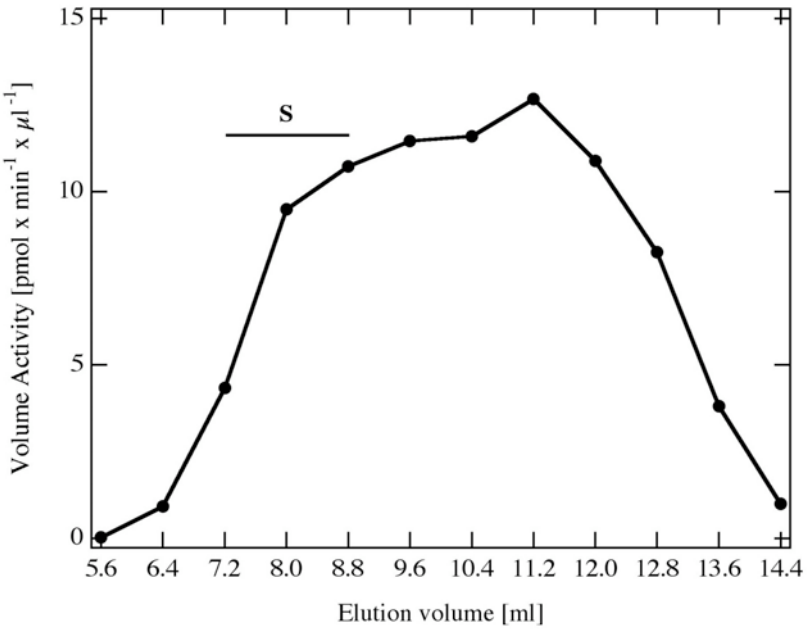

Figure 4.17. Activity distribution of TPP II-G260R mutant enzyme in *E. coli* cell extract. The cell extract was subjected to size exclusion chromatography on Superose 6 and AAF-AMC hydrolysing activity of eluate fractions was measured. The wide distribution of activity revealed the presence of TPP II-G260R at various stages of assembly. But the spindles were not the prevailing form in the dTPP II-G260R cell extract, indicating that the mutation led to disfavoured complex formation. The bar denotes the elution volume corresponding to spindles (S).

To find out whether the effect of the G260R mutation can be overcome at high enzyme concentrations, the purification procedure involving an ammonium sulphate precipitation step (purification approach II in Section 4.2.2) was used. Upon concentration to ≥10 mg/ml, fully assembled spindles indistinguishable from the native ones in morphology were formed (Figure 4.18). The specific activity of the purified spindles was about the same as that of the wild type enzyme.

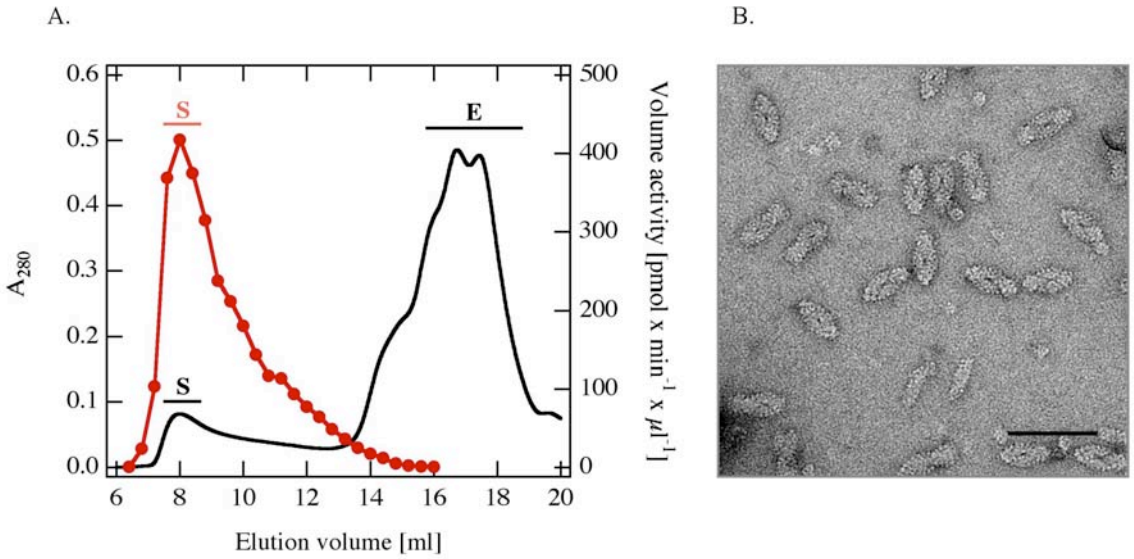

Figure 4.18. Characterization of TPP II-G260R. A, Size exclusion chromatography on Superose 6 of TPP II-G260R cell extract, after PEI precipitation and subsequent ammonium sulphate precipitation. Black line, A_{280}; red line, volume activity measured in eluting fractions. Upon concentration, intact and active spindles (S) were formed, giving a prominent activity peak. *E. coli* proteins (E) elute at 15-19 ml. B, electron micrograph of the spindle (S) fraction in A (scale bar: 100 nm).

The same result was observed with the human TPP II-G252R mutant, over-expressed in *E. coli* (clone hTPP II-*G252R*, Section 3.2.9). Intact spindles were formed upon concentration to ≥10 mg/ml by ammonium sulphate precipitation (purification approach II, Section 3.4.9), as revealed by size exclusion chromatography and electron microscopy in Figure 4.19.

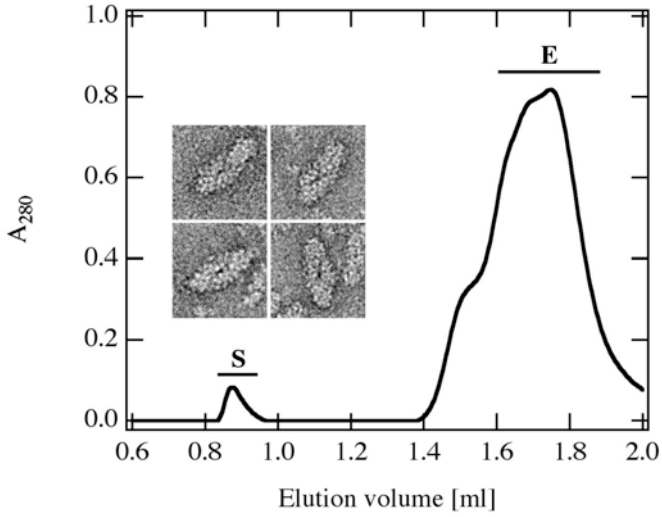

Figure 4.19. Size exclusion chromatography on Superose 6 (2.4 ml column) of human TPP II-G252R cell extract, after PEI precipitation and subsequent ammonium sulphate precipitation. Upon concentration, intact spindles (S) were formed. *E. coli* proteins (E) elute at 1.5-1.9 ml. Inset, gallery of hTPP II-G252R holocomplexes.

Taken together, the G260R mutation in *Drosophila* TPP II (or G252R in the human homologue) interfered with oligomerization, but it failed to produce a homogeneous oligomeric form. Moreover, at high enzyme concentrations of ≥10 mg/ml, the effect of the mutation was reversed and active spindles were formed.

4.6.1.2 Mutations in the conserved negatively charged clusters

The data shown above reveal that a single point mutation can weaken interactions between the subunits significantly. Therefore, it was attempted to enhance this attenuation by further point mutations. A number of residues, which form conserved and charged clusters (Figure 4.15), and therefore are likely to be exposed on the subunit interfaces, were exchanged with an oppositely charged residue or an Alanine. A collection of TPP II mutants carrying either a single point mutation or combinations of point mutations was generated (Table 4.4, Section 3.2.7). The point mutations were introduced into the dTPP II-Nmbp plasmid, in order to make use of the destabilizing effect of the MBP-tag, which abolished the inter-strand contacts (Section 4.5.3). The mutants were over-expressed in *E. coli* in soluble form and gave about the same expression yields, as judged by SDS-PAGE. In the cell extracts of the single point mutants the specific activity determined per μg of total protein were about the same as that of TPP II-Nmbp, except for the G260R mutant

which had only about 25% of the full activity. Also, three of the multiple mutants containing the G260R mutation exhibited about 25% activity and one mutant was inactive (Table 4.4). All other multiple mutants not containing the G260R mutation displayed roughly full specific activity (per μg of total protein) in the cell extract. The mutant proteins were purified by affinity chromatography to a concentration of 5 mg/ml and subsequently subjected to size exclusion chromatography in order to determine the assembly state. All the mutants eluted in a major peak close to the void volume, but displayed different assembly characteristics when scrutinized by electron microscopy (Figure 4.20). The E161K/E163A and the E224A/D227K mutants displayed a single stranded morphology similar to that of the TPP II-Nmbp (Figure 4.20A), whereas a combination of the G260R mutation with other mutations resulted in the formation of soluble aggregates (Figure 4.20B and C).

Table 4.4. Point mutations introduced to TPP II-Nmbp and their effect on TPP II activity. The specific activities in the cell extracts were calculated in relation to total protein, and compared to that of the TPP II-Nmbp (100 %), since the cell extracts of the mutants and TPP II-Nmbp contained about the same amount of TPP II (as judged by SDS-PAGE).

Mutations							Specific activity in the cell extract (%)
G260R	*E182A*	*E923A*	*E929A*	*E1313A*	*E161K/ E163A*	*E224A/ D227K*	
+							25
	+						100
		+					100
			+				100
				+			100
					+		100
						+	100
+						+	25
+	+					+	25
+	+	+				+	0

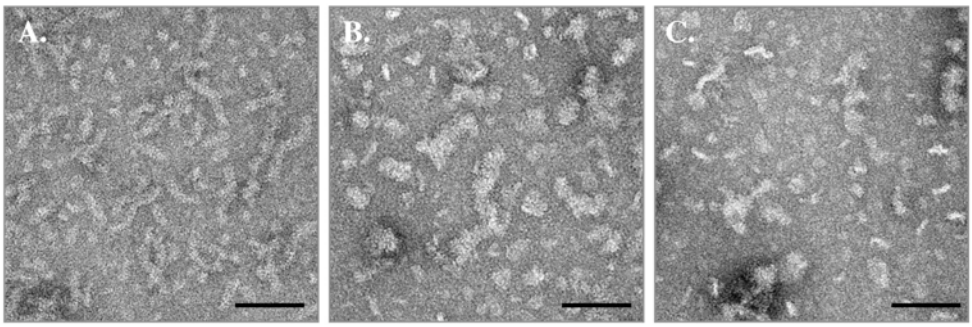

Figure 4.20. Electron micrographs of the purified mutant proteins. A, TPP II-E161K/E163A; B, TPP II-E224A/D227K/G260R; C, TPP II-E182A/E224A/D227K/G260R/E923A. Scale bars: 100 nm.

These results lead to the conclusion that the point mutations have a significant effect on the activity and structure of TPP II. The assembly was impaired irreversibly and amorphous, soluble aggregates were formed. Consequently, the aim to produce a homogeneous disassembly form of TPP II by introducing point mutations seems difficult to achieve without knowledge of the atomic structure of the enzyme.

4.6.1.3 Truncations at the C-terminus of TPP II

The C-terminus was chosen to be truncated for the following reasons: i) impaired assembly was observed in the C-terminally His_6-tagged TPP II (Section 4.5.2), suggesting that this region might be involved in complex formation. In addition, the conservation of the C-terminal two hydrophobic residues (LF) of TPP II is remarkable (see Figure 4.15); ii) the C-terminal domain is remote from the active site, whereas an N-terminal deletion would be very close to it and probably disrupt the catalytic core. To see whether the absence of the C-terminus will prevent assembly of the complexes, three truncation mutants lacking 59 (clone dTPP II-Nmbp-ΔC59), 82 (clone dTPP II-Nmbp-ΔC82), or 138 (clone dTPP II-Nmbp-ΔC138) residues at their C-termini were constructed (Sections 3.2.7.4, 3.4.11) and examined for their assembly characteristics. Since the C-terminal domain boundary had not been predicted at that time, the truncation points were selected so that large clusters are removed from the C-terminus. As determined by electron microscopy, the truncated proteins formed soluble aggregates but not distinct oligomers (data not shown). Interestingly, these mutants were inactive even though they carried the catalytic N-terminal domain. As the dimers were known to be the smallest active unit of TPP II (Seyit et al.,

2006; Tomkinson, 2000), the absence of activity was attributed to the lack of dimerization. The formation of amorphous, soluble aggregates indicates misassociation of the subunits, resulting from the absence of the C-terminal region.

4.6.2 Expression of TPP II domains

Due to the large subunit interfaces involved in complex formation, introducing a limited number of point mutations has not been sufficient to disassemble the complex. Also, large deletions at the C-terminus resulted in aggregation. Therefore, the separate expression and crystallization of the individual domains, was considered as an alternative to the full-length protein. The domain boundaries were predicted as indicated in Figure 4.21. According to this prediction, *Drosophila* TPP II is composed of at least three domains: N-terminal Subtilisin-like domain, central (mostly β-sheet) domain(s) and C-terminal (α-helical) domain.

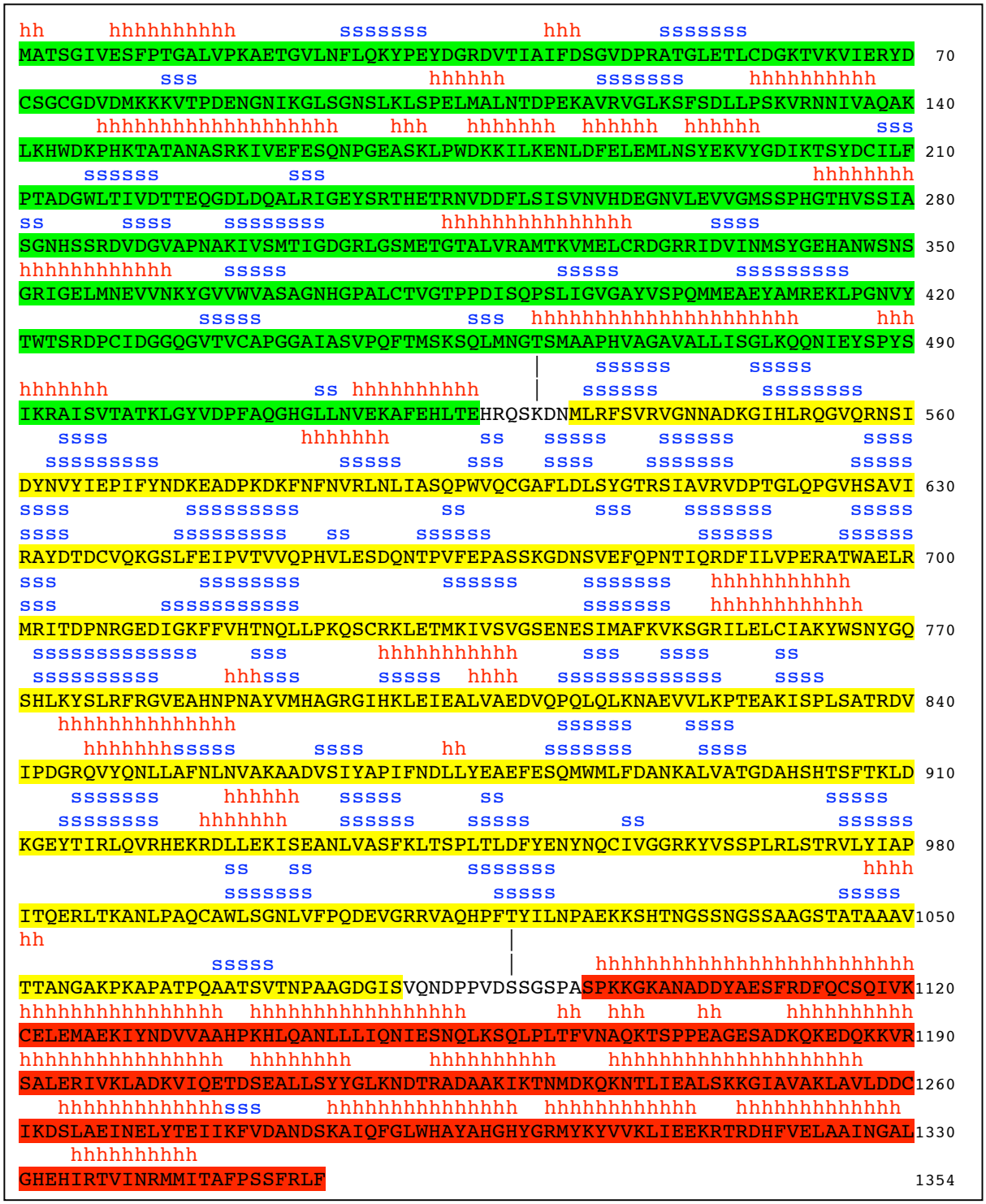

Figure 4.21. Prediction of the secondary structure and the domain boundaries of *Drosophila* TPP II (by Prof. Dr. Andrei Lupas – MPI for Developmental Biology, Tübingen, using the program HHpred at http://protevo.eb.tuebingen.mpg.de/toolkit/index.php?view=hhpred). Highlighted in green, N-terminal Subtilisin-like domain; highlighted in yellow, central domain(s); highlighted in red, C-terminal domain; h, α-helix; s, β-sheet.

4.6.2.1 Expression of the N-terminal domain of TPP II

Residue E526 was predicted to be located at the boundary of the N-terminal domain of *Drosophila* TPP II (Figure 4.21). Therefore, in order to truncate the rest of the gene and express the N-terminal domain separately, the *E526* codon in the dTPP II-Nmbp construct was mutated to a termination codon as described in Section 3.2.7.4. The expression construct is shown in Figure 4.22.

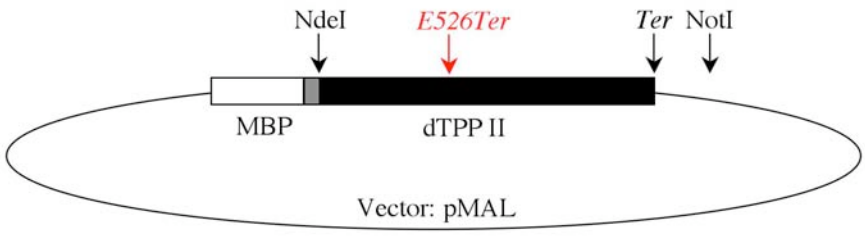

Figure 4.22. The dTPP II-Nmbp construct was mutated to express the N-terminal domain of *Drosophila* TPP II. The *E526Ter* mutation site is indicated in red. The grey box represents the sequence coding for a 26 amino acid linker ($TNSSSN_{10}LGIEGRISEFH$) between MBP and TPP II. Black arrows denote the NdeI and NotI restriction sites and the original termination codon (*Ter*).

The 57 kDa Subtilisin-like domain was expressed with an N-terminal maltose binding protein tag to promote solubility (Figure 4.23A). The fusion protein was over-expressed in soluble form in *E. coli* and purified to homogeneity (3 mg/ml, Figure 4.23B) by affinity chromatography (Section 3.4.11).

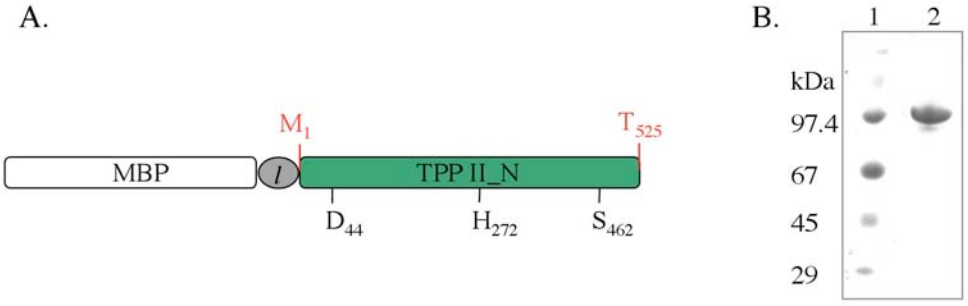

Figure 4.23. Expression and purification of the N-terminal (Subtilisin-like) domain of *Drosophila* TPP II. A, Schematic representation of the mbp-TPP II_N fusion protein; MBP, maltose-binding protein-tag; *l*, 26 amino acid linker between MBP and TPP II; TPP II_N, the N terminal domain between the residues M_1-T_{525}. D_{44}, H_{272} and S_{462}, the residues forming the active site, are located in the N-terminal domain of TPP II. B, SDS-gel; lane 1, marker; lane 2, purified 99,7 kDa mbp-TPP II_N fusion.

Although the Subtilisin-like domain carries the catalytically active residues, the domain did not have any peptidase activity when expressed separately. On a Superose 6 column, the protein eluted in the void volume, indicating aggregation. The electron microscopic investigation of the peak fraction revealed the presence of soluble aggregates not suitable for crystallization.

4.6.2.2 Expression of the C-terminal domain of TPP II

Residue S1095 was predicted to be located at the boundary of the C-terminal domain of *Drosophila* TPP II (Figure 4.21). The TPP II gene region starting with the *S1095* codon and ending with the original termination codon, was cloned in a pMAL vector as described in Section 3.2.8. The expression construct is shown in Figure 4.24.

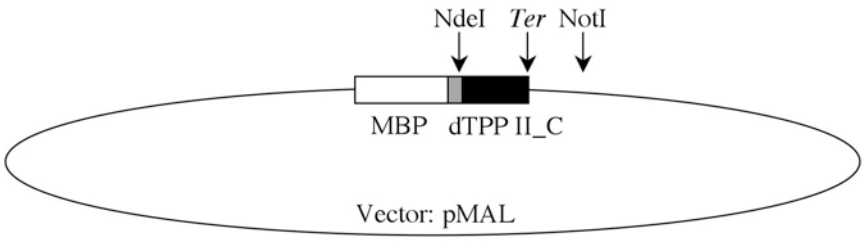

Figure 4.24. mbp-dTPP II_C plasmid used for expression of the C-terminal domain of *Drosophila* TPP II, with an N-terminal maltose-binding protein (MBP) tag. The grey box represents the 26 amino acid linker ($TNSSSN_{10}LGIEGRISEFH$) between MBP and TPP II. Arrows denote the NdeI and NotI restriction sites and the termination codon (*Ter*).

The 29.5 kDa C-terminal domain was expressed with a maltose-binding protein-tag at its N-terminus to promote solubility (Figure 4.25). The mbp-TPP II_C fusion (72.5 kDa) was over-expressed in soluble form in *E. coli*.

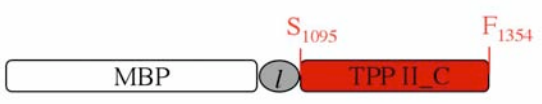

Figure 4.25. Schematic representation of the mbp-TPP II_C fusion protein. MBP, maltose-binding protein-tag; *l*, 26 amino acid linker between MBP and TPP II; TPP II_C, the C terminal domain between the residues S_{1095} and F_{1354}.

The fusion protein was purified by affinity chromatography (Section 3.4.11). The purified material was dialyzed overnight (Section 3.4.13) to remove the excess of maltose, and

subsequently separated on a 2.4 ml Superose 6 column. The chromatographic elution profile revealed two peaks (Figure 4.26). The peak fraction eluting at 0.9 ml, contained mainly aggregates. The second peak eluting at 1.75 ml contained the 72.5 kDa mbp-TPP II_C fusion protein. When mbp-TPP II_C was concentrated to 10 mg/ml, again approximately half of the total protein eluted in a non-assembled state, at 1.75 ml (Figure 4.26A).

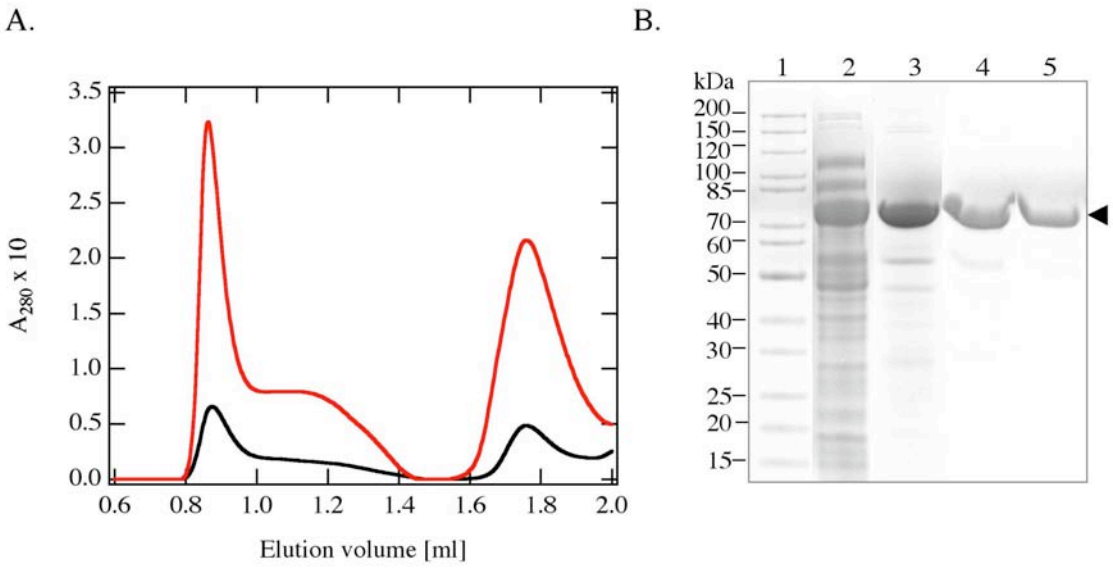

Figure 4.26. Purification of mbp-TPP II_C. A, Superose 6 chromatogram of the amylose eluate in panel B lane 3; black line, amylose resin eluate directly after purification, containing 1 mg/ml protein; red line, amylose eluate after dialysis and a subsequent concentration to 10 mg/ml. B, SDS-gel, lane 1, marker; lane 2, 2nd cell extract of *E. coli*; lane 3, amylose eluate; lane 4, fraction eluting at 0.9 ml in A; lane 5, peak eluting at 1.75 ml in A. Equal volumes of sample were loaded on lanes 4 and 5. The arrow denotes the 72.5 kDa mbp-TPP II_C band.

The inherent propensity of mbp-TPP II_C to form soluble aggregates could not be completely prevented; nevertheless, the concentrated (10 mg/ml) material was used in crystallization trials, but did not produce any crystals.

4.6.2.2.1 Disassembly of the mbp-TPP II_C aggregates

As treatment with PEI/pH 8.9 disassembled the TPP II complexes (Section 4.2.2), the same procedure was applied to the mbp-TPP II_C aggregates. The amylose resin eluate containing 5 mg/ml fusion protein (see Section 4.6.2.2), was incubated with 0.2 % PEI, at pH 8.9 for 10 min. Subsequently the sample was centrifuged and the supernatant subjected

to size exclusion chromatography on Superose 6 (2.4 ml column), which revealed complete disassembly of the aggregate peak (Figure 4.27). The sample was used for setting crystallization droplets but did not produce any crystals.

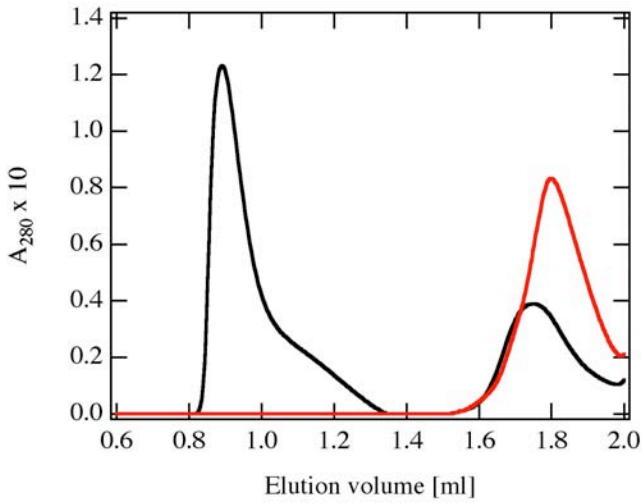

Figure 4.27. Size exclusion chromatography of dialyzed amylose column eluate containing 5 mg/ml mbp-TPP II_C, before (black line) and after (red line) polyethyleneimine treatment.

4.6.2.2.2 Factor Xa cleavage of mbp-TPP II_C

In order to obtain the untagged version of the C-terminal domain of TPP II, the MBP-tag was removed by cleavage with factor Xa. The fusion protein contained a factor Xa cleavage site, Ile-Glu-Gly-Arg, in the 26 amino acid linker (TNSSSN$_{10}$LGIEGRISEFH) between MBP and TPP II_C. mbp-TPP II_C was purified by affinity chromatography (Section 3.4.11) and subsequently, maltose was removed by dialysis (Section 3.4.13). The sample was treated with factor Xa at a w/w ratio of 1% the amount of fusion protein. The cleavage reaction was carried out at room temperature for 7 h, and went to completion generating two fragments corresponding to MBP (42 kDa) and TPP II_C with an apparent molecular mass of 29.5 kDa (Figure 4.28).

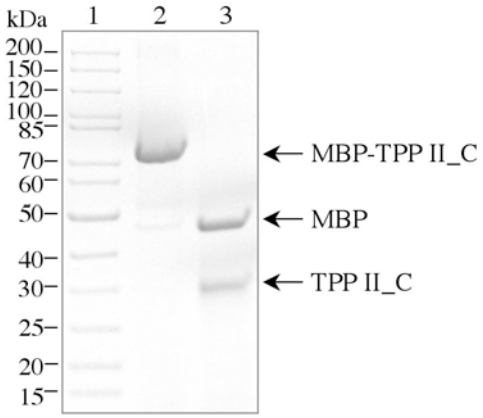

Figure 4.28. Release of the TPP II_C domain from the N-terminal MBP fusion, by proteolytic cleavage. SDS-gel, lane 1, marker; lane 2, affinity-purified MBP-TPP II_C; lane 3, TPP II_C, released from MBP by factor Xa cleavage.

After cleavage, partial purification of TPP II_C from MBP was achieved by passage through a second amylose affinity column. The concentration of TPP II_C to 5 mg/ml resulted in the formation of soluble aggregates. As the absence of MBP results in aggregation, its presence at the N-terminus of the C-terminal domain probably reduces the extent of misassembly by " shielding" the otherwise exposed hydrophobic surfaces.

4.6.3 Disassembly of TPP II by dialysis and cold treatment

Since introducing multiple mutations or deletions, or expressing the domains of TPP II separately, led to the formation of soluble aggregates, alternative disassembly methods were investigated, in which the amino acid sequence of TPP II was preserved. Previously, native human TPP II has been shown to disassemble upon dialysis against low ionic-strength buffer (Macpherson et al., 1987). Dialysis of the recombinant *Drosophila* TPP II against 25 mM Tris-HCl pH 7.5, 2 mM DTT and 5% glycerol at 4°C overnight, resulted in disassembly of the complexes into tetramers (Figure 4.29). Interestingly, the control incubated at 4°C overnight without dialysis showed significant disassembly as well (Figure 4.29). Therefore, the destabilization of the recombinant complex seems to occur as a result of both, cold treatment and dialysis. The dissociation into tetramers was also observed after overnight native PAGE at 4°C (Figure 4.29 inset).

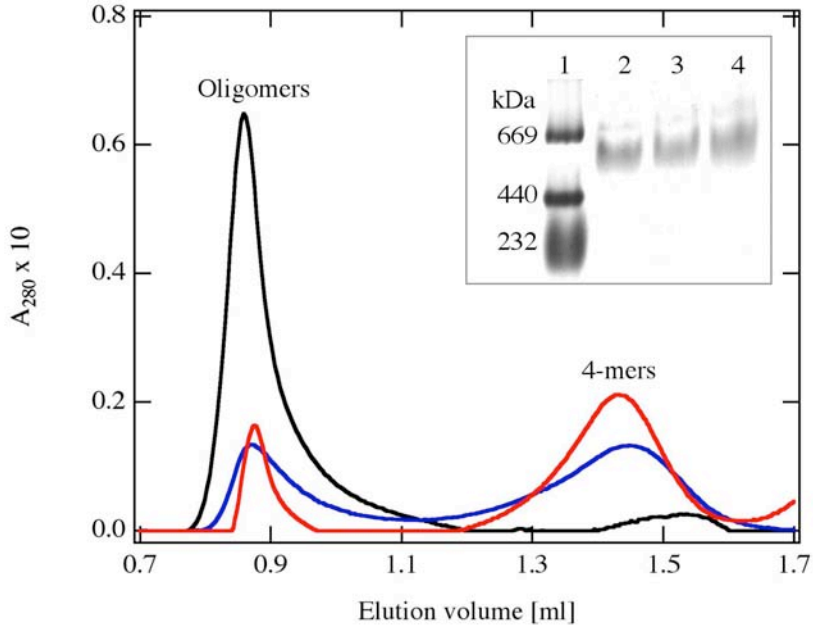

Figure 4.29. Size exclusion chromatogram showing the disassembly of TPP II oligomers (black line), into tetramers, after incubation at 4°C overnight (blue line), and after dialysis at 4°C overnight (red line). Inset, native-gel showing the disassembly into tetramers Lane 1, marker; lane 2, TPP II oligomers (black line); lane 3, sample incubated at 4°C overnight (blue line); lane 4, sample dialysed at 4°C overnight (red line).

The disassembly achieved by cold treatment was reversible, i.e. when concentrated to ≥ 5 mg/ml, the tetramers reassembled into higher oligomers of various size, thus could not be used for crystallization. Nevertheless, to take advantage of the effect of cold treatment on TPP II disassembly, the chemical disassembly methods described below were carried out at 4-0°C.

4.6.4 Chemical approaches to disassembly of TPP II

4.6.4.1 Disassembly of TPP II by reductive methylation of lysine residues

As mentioned above, the disassembly products of the G260R mutant of TPP II, as well as the tetramers resulting from the cold treatment and dialysis, reassembled upon concentration. To achieve irreversible disassembly, a more rigorous approach involving chemical modification was investigated. The objective was to use methylation to "seal" the subunit interfaces and prevent their oligomerization. Purified TPP II complexes at a

concentration of 1 mg/ml were methylated using the Jena methylation kit (Section 3.4.14). $1/5^{th}$ of the recommended reagent concentration was determined to be optimal for studying disassembly over time. After incubation for 5, 30, 40 and 90 min in the presence of formaldehyde (alkylation) and dimethylamine-borane (reduction), and subsequent quenching with ammonium sulphate, the specific activity decreased to 60, 25, 16 and 7% respectively. Size exclusion chromatography of the methylated samples indicated that the reduced activity was a result of disassembly. A disassembly peak corresponding to dimers was observed with the samples methylated for 30, 40 and 90 min (Figure 4.30A). Size exclusion chromatography of TPP II methylated for 30 or 40 min, revealed a prominent dimer peak that showed tailing on the high molecular mass side. TPP II methylated for 90 min, gave a more symmetrical dimer peak. This was an indication that the disassembly was complete and stalled at the dimer state, so that no further disassembly had occurred. The presence of dimers was confirmed by native PAGE, where no tetramers or monomers were observed (Figure 4.30B). The activity of the disassembly product was determined as 7%, which was in good agreement with the reported dimer activity of 8-10% (Seyit et al., 2006; Tomkinson, 2000). On the electron micrographs, the dimers appeared to be homogeneous in terms of particle size, as no aggregates or higher assemblies were observed (Figure 4.30C). On the other hand, they did not exhibit a well-defined structure in the 2D EM images, which can be attributed to a random orientation and/or random conformation of the dimers. The dimers obtained after 90 min of methylation did not reassemble when concentrated 15-fold (Figure 4.30B). Therefore, a scale-up of the methylation was performed to obtain material for crystallization. The methylated sample was dialyzed, concentrated to 5 mg/ml and used for crystallization trials, but no crystals were observed.

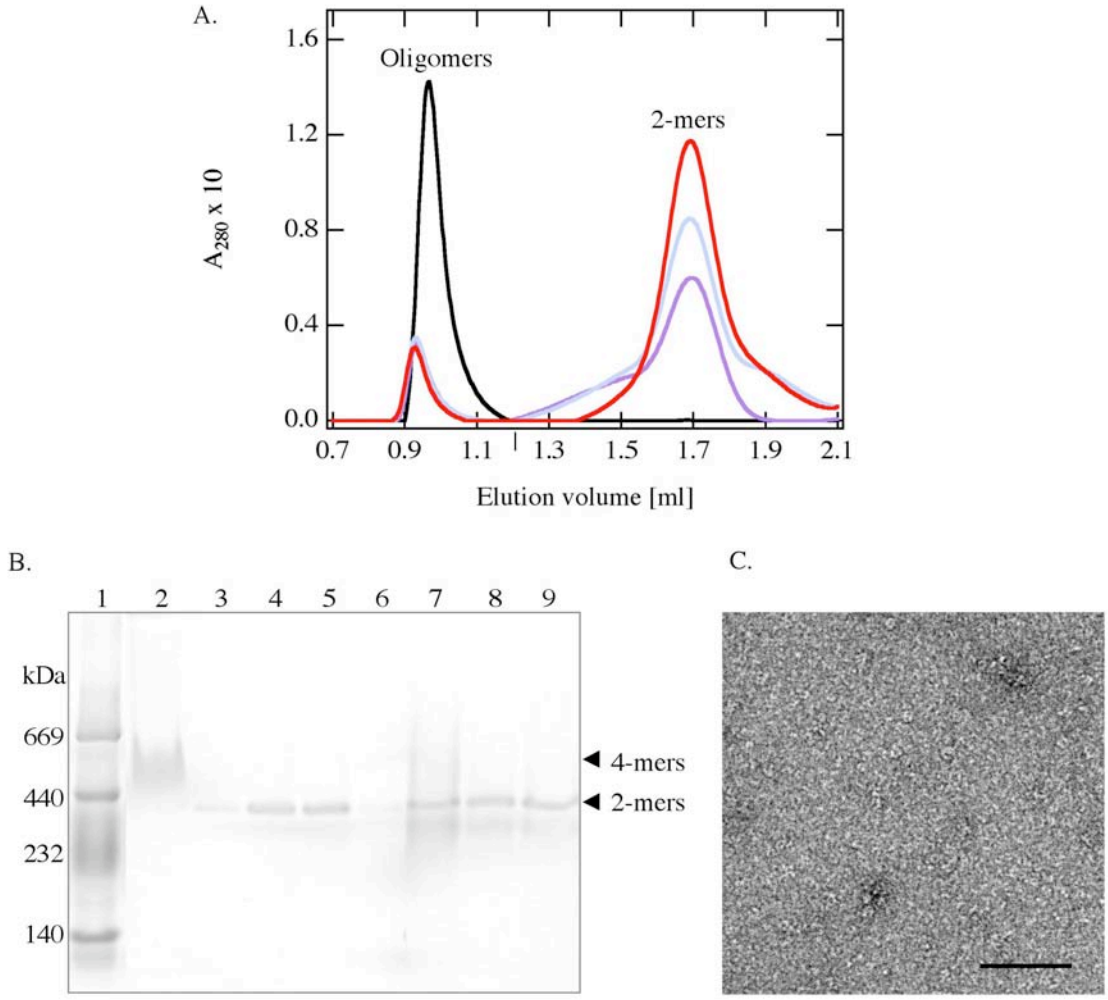

Figure 4.30. Disassembly of TPP II oligomers by methylation. A, size exclusion chromatography on Superose 6 of unmethylated TPP II oligomers (black line), and samples methylated for 30 min (purple line), 40 min (blue line) and 90 min (red line). B, native PAGE, lane 1, marker; lane 2, unmethylated TPP II oligomers (black line in A). Lanes 3, 4, 5, and 6, dimer peak fractions of 40 min sample, eluting at 1.60, 1.65, 1.70 and 1.75 ml respectively on Superose 6, equal volumes were loaded. Lane 7, TPP II methylated for 90 min (red line in A). Lane 8, dimer peak fraction of 90 min sample, eluting at 1.65 - 1.70 min. Lane 9, sample in lane 8 concentrated to 0.2 mg/ml. C, electron micrograph of the dimer peak fraction, scale bar: 100 nm.

4.6.4.2 Disassembly of TPP II by β-octyl glucoside treatment

The non-ionic detergent, β-octyl glucoside (OG, CMC: ~15 mM) has been shown to improve the crystallization behaviour of some soluble proteins (McPherson et al., 1986). This effect has been attributed to the ability of OG to prevent protein aggregation by diminishing nonspecific hydrophobic contacts between molecules.

TPP II complexes were treated with OG (Section 3.4.15) in order to determine the effect of OG on the disassembly. Purified TPP II at a concentration of 1 mg/ml (Figure 4.31A) was incubated with 20, 40 or 60 mM of OG at 0°C. Incubation overnight resulted in partial disassembly. When the incubation on ice was extended to four days, due to the cold sensitivity of the recombinant TPP II (see section 4.6.3), a significant disassembly into tetramers was observed even without OG (Figure 4.31B). On the other hand, at least 40 mM of OG was required for an almost complete disassembly of the oligomers into tetramers (Figure 4.31B). Increasing the concentration of OG from 40 to 60 mM, did not result in further disassembly (Figure 4.31B). A decrease of activity along with disassembly was observed (Figure 4.32). At 40 mM OG the tetramers retained ~60% of the activity of the spindles (21,000 ± 1,000 pmol x min^{-1} x μg^{-1}). This value is in good agreement with the tetramer activity determined in the absence of OG as 54% of the spindle activity (Seyit et al., 2006). The activity of the tetramers did not further decrease when the detergent concentration was increased to 60 mM (Figure 4.32), indicating a halt in disassembly at the tetramer stage.

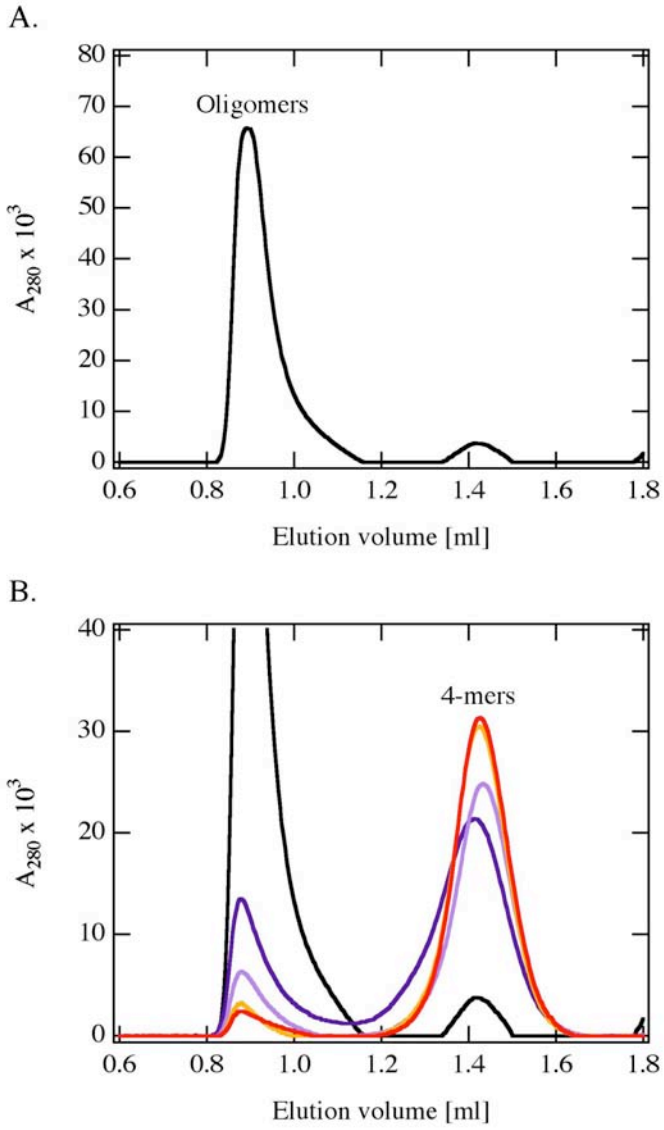

Figure 4.31. Disassembly of the TPP II oligomers into tetramers by treatment with β-octyl glucoside (OG). A, size exclusion chromatography of TPP II before OG treatment. B, size exclusion chromatography of TPP II oligomers (black line, same as in A); after incubation on ice for four days without OG (dark blue line); and after incubation on ice for four days in the presence of 20 mM OG (purple line), 40 mM OG (yellow line) and 60 mM OG (red line).

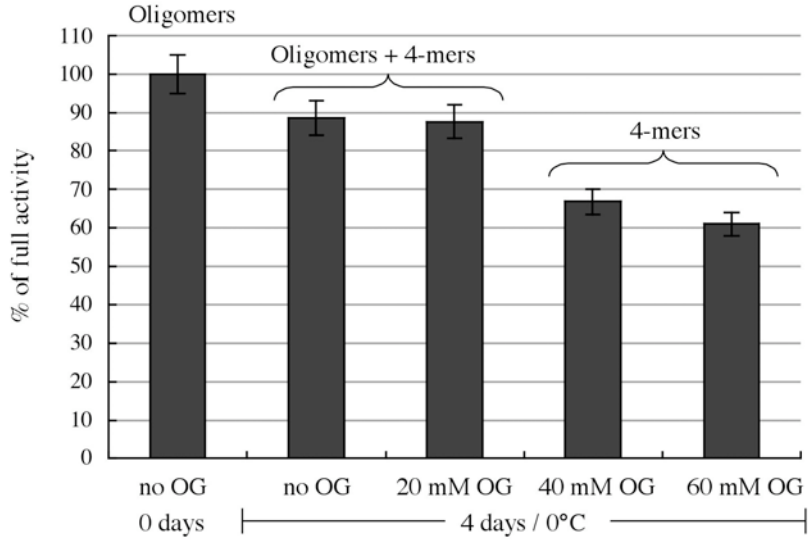

Figure 4.32. Decrease of specific activity upon disassembly of TPP II by β-octyl glucoside (OG) treatment. The specific activity of the oligomers (21,000 ± 1,000 pmol x min^{-1} x μg^{-1}) was taken as 100 %. Upon incubation at 0°C for 4 days, without OG or in the presence of 20 mM OG, the activity decreased to about 90 % and both oligomers and 4-mers were present as judged by size exclusion chromatography (see figure 4.31). After incubation in the presence of 40 and 60 mM OG, almost all of the oligomers disassembled into 4-mers, which were 60 % active.

In the presence of OG, the tetramers did not reassemble when concentrated up to 5 mg/ml, as judged by size exclusion chromatography (Figure 4.33A). In the electron micrographs, the tetramers appeared to be relatively homogenous in terms of particle size, as no aggregates or higher assemblies were observed (Figure 4.33B). Generally, the tetramers exhibited “trilobed” structures (Figure 4.33B).

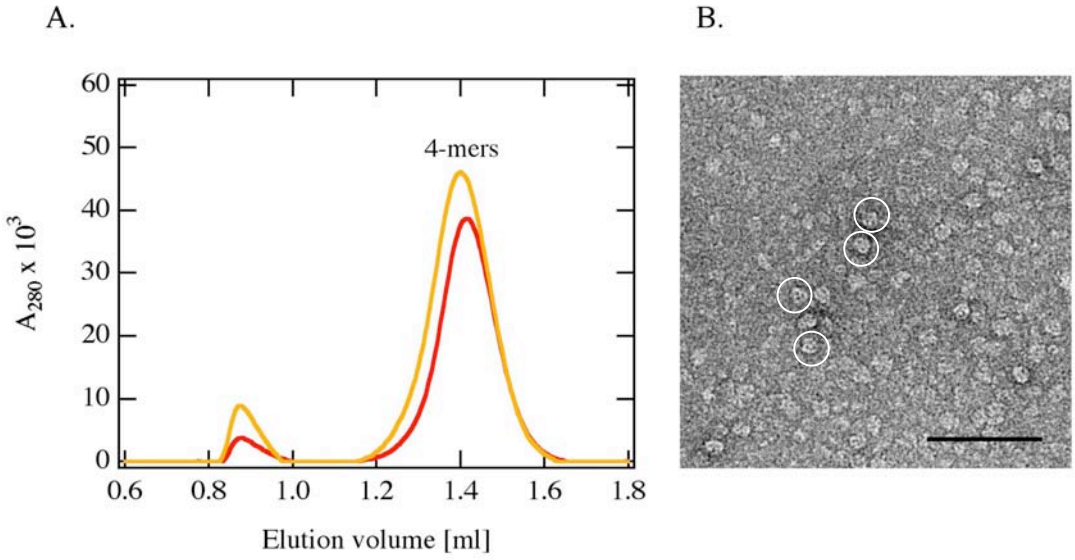

Figure 4.33. Concentration of TPP II tetramers in the presence of β-octyl glucoside. A, size exclusion chromatography, samples treated with 40 mM (yellow line) and 60 mM (red line) of β-octyl glucoside were concentrated to 5 and 3 mg/ml, respectively. B, electron micrograph of the tetramers after concentration (yellow line in A). Some of the tetramers showing a characteristic (trilobed) orientation are marked with circles. Scale bar: 100 nm.

Since the TPP II tetramers produced by β-octyl glucoside treatment, neither disassembled further nor reassembled upon concentration, they were good candidates for the crystallization experiments.

4.7 Crystallization of TPP II

4.7.1 Large-scale purification of TPP II

Wild type *Drosophila* TPP II to be used in the crystallization experiments was purified from *E. coli* using the purification approach II (Section 4.2.2), except that size exclusion chromatography was performed on a 330 ml Superose 6 column (Section 3.4.16). TPP II eluted in two adjacent peaks. The peak fractions were collected in two pools as shown in Figure 4.34A: p1 (eluate between 116-136 ml), contained 1 mg/ml TPP II and p2 (eluate between 136-148 ml), contained 1.5 mg/ml TPP II. SDS-PAGE of p1 and p2 (Figure 4.34B) and subsequent sequence analyses of the protein bands, revealed the presence of only TPP II (Section 4.7.2). Both of the p1 and p2 eluate pools exhibited the specific activity of spindles (21,000 ± 1,000 pmol x min^{-1} x μg^{-1}). The only noticeable difference

was the size of the TPP II oligomers, as shown by electron microscopy: p1, in addition to the spindles, contained over-long single strands (up to 300 nm, Figure 4.34C). These extended complexes, due to their larger Stokes radii, were partially separated from the spindles of the p2 peak (Figure 4.34D).

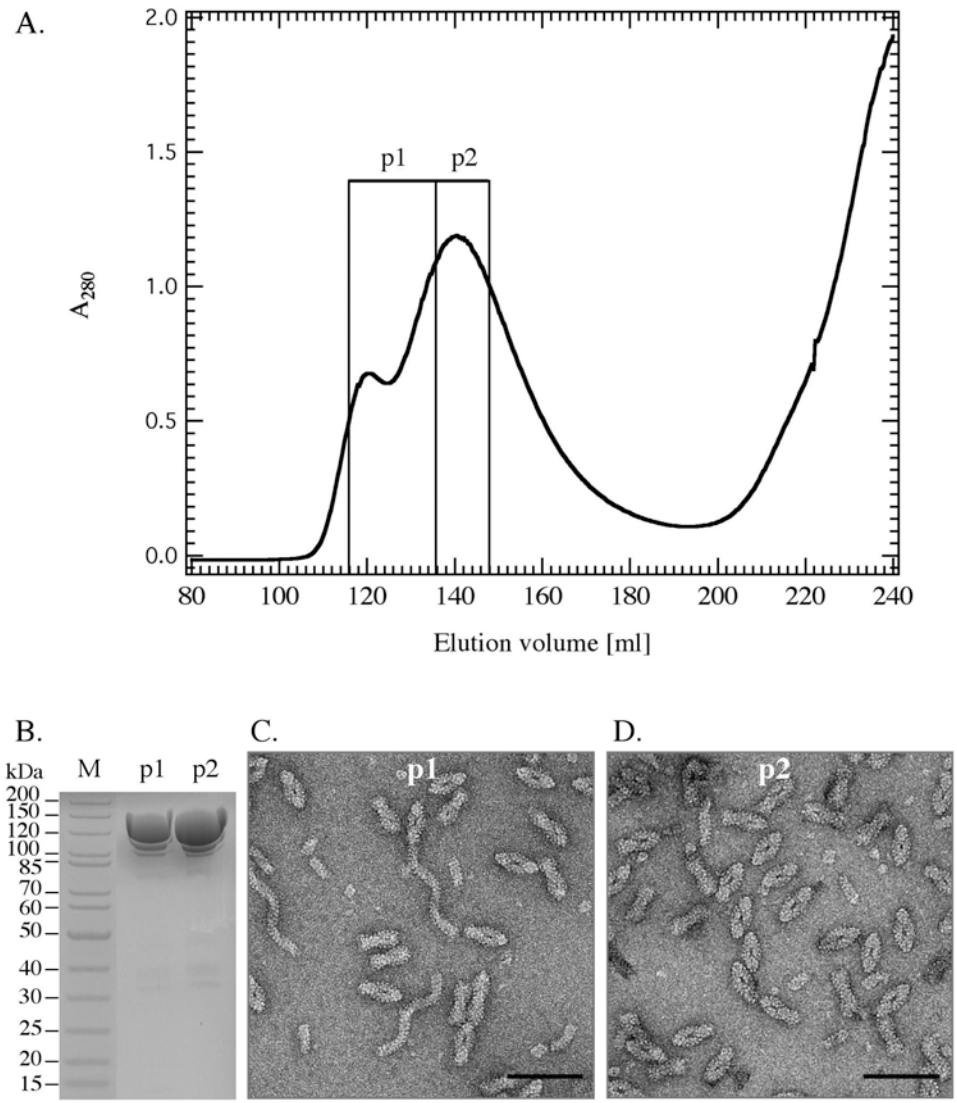

Figure 4.34. Large scale purification of TPP II for crystallization. A, size exclusion chromatography on Superose 6 (XK 26/70); p1 and p2 denote the pooled eluate fractions. B, SDS-gel of p1 and p2 in A. Equal volumes (25 µl) of p1 and p2 were loaded. C, electron micrograph of p1 fraction in A. D, electron micrograph of p2 fraction in A; scale bars: 100 nm.

Before being used in the crystallization experiments, the protein content of the TPP II preparation was analysed by mass spectrometry as described below in Section 4.7.2.

4.7.2 Analysis of the TPP II preparations by mass spectrometry

Mass spectrometry was performed to determine the purity of the TPP II preparations, and also to characterize the 115 kDa protein band accompanying the ~150 kDa TPP II band in the SDS-gels.

The size exclusion chromatography fractions eluting at 114-162 ml (see chromatogram in Figure 4.34A) were subjected to SDS-PAGE (Figure 4.35). The proteins detected in the overloaded lanes were tryptically digested and the resulting peptides were analyzed my mass spectrometry. The tryptic peptides of the 149 kDa TPP II (band #1 in Figure 4.35) are shown in Figure 4.36. Mass spectrometry of the intact enzyme was also preformed, which revealed a molecular mass of 148521 Da for the recombinant TPP II. The theoretical molecular mass (determined from the amino acid sequence) of full length TPP II is 148908 Da. However, when the mass of the N-terminal MATS residues is subtracted, a mass of 148518 Da is derived, which is the closest value to that obtained by mass spectroscopy.

The tryptic peptides of the 115 kDa fragment (band #2 in Figure 4.35) revealed a truncation at the C-terminus (Figure 4.37A). The missing C-terminal peptides were detected in the 31 kDa fragment (band #6 in Figure 4.35), as shown in Figure 4.37B. Mass spectrometry of the 115 and 31 kDa fragments revealed masses of 115439 and 30991 Da respectively. A C-terminal fragment starting with G1078 (Figure 4.37B) has a theoretical (determined from the amino acid sequence) mass of 30991 Da, which is the same as determined spectrometrically. For the N-terminal fragment, a mass of 115440 Da was calculated for the polypeptide chain between G4-N1054, which is almost the same as the spectrometrically determined mass of 115439 Da. The calculated and spectrometrically determined mass values matched exactly, when the mass of the N-terminal MATS residues was subtracted (see above). Since the 115 kDa band was present also in the native TPP II preparations (Rockel et al., 2002), apparently the same proteolytic cleavage occurs in *Drosophila* as well. The presence of an interdomain loop at this position is likely, because: i) the amino acid sequence shows the characteristics of a loop, ii) the region coincides with the non-conserved insert in *Drosophila* TPP II (see Figure 4.15), iii) it also coincides with the C-terminal domain boundary theoretically predicted by Prof. Dr. Andrei Lupas (Figure 4.21).

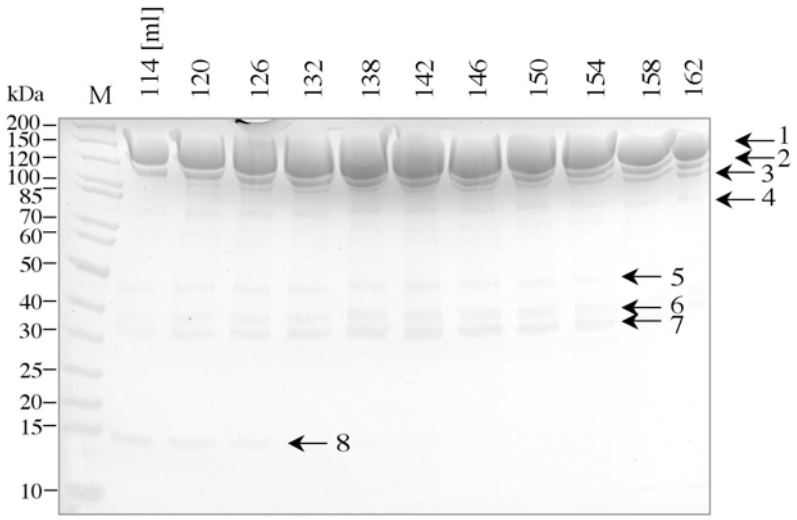

Figure 4.35. SDS-gel of the Superose 6 eluate fractions in Figure 4.34A. The elution volumes are indicated above each lane; M, marker. The numbered (1-8) electrophoretic bands represent proteolytic fragments of TPP II, as determined by mass spectrometry.

```
   1 MATSGIVESF PTGALVPKAE TGVLNFLQKY PEYDGRDVTI AIFDSGVDPR
  51 ATGLETLCDG KTVKVIERYD CSGCGDVDMK KKVTPDENGN IKGLSGNSLK
 101 LSPELMALNT DPEKAVRVGL KSFSDLLPSK VRNNIVAQAK LKHWDKPHKT
 151 ATANASRKIV EFESQNPGEA SKLPWDKKIL KENLDFELEM LNSYEKVYGD
 201 IKTSYDCILF PTADGWLTIV DTTEQGDLDQ ALRIGEYSRT HETRNVDDFL
 251 SISVNVHDEG NVLEVVGMSS PHGTHVSSIA SGNHSSRDVD GVAPNAKIVS
 301 MTIGDGRLGS METGTALVRA MTKVMELCRD GRRIDVINMS YGEHANWSNS
 351 GRIGELMNEV VNKYGVVWVA SAGNHGPALC TVGTPPDISQ PSLIGVGAYV
 401 SPQMMEAEYA MREKLPGNVY TWTSRDPCID GGQGVTVCAP GGAIASVPQF
 451 TMSKSQLMNG TSMAAPHVAG AVALLISGLK QQNIEYSPYS IKRAISVTAT
 501 KLGYVDPFAQ GHGLLNVEKA FEHLTEHRQS KDNMLRFSVR VGNNADKGIH
 551 LRQGVQRNSI DYNVYIEPIF YNDKEADPKD KFNFNVRLNL IASQPWVQCG
 601 AFLDLSYGTR SIAVRVDPTG LQPGVHSAVI RAYDTDCVQK GSLFEIPVTV
 651 VQPHVLESDQ NTPVFEPASS KGDNSVEFQP NTIQRDFILV PERATWAELR
 701 MRITDPNRGE DIGKFFVHTN QLLPKQSCRK LETMKIVSVG SENESIMAFK
 751 VKSGRILELC IAKYWSNYGQ SHLKYSLRFR GVEAHNPNAY VMHAGRGIHK
 801 LEIEALVAED VQPQLQLKNA EVVLKPTEAK ISPLSATRDV IPDGRQVYQN
 851 LLAFNLNVAK AADVSIYAPI FNDLLYEAEF ESQMWMLFDA NKALVATGDA
 901 HSHTSFTKLD KGEYTIRLQV RHEKRDLLEK ISEANLVASF KLTSPLTLDF
 951 YENYNQCIVG GRKYVSSPLR LSTRVLYIAP ITQERLTKAN LPAQCAWLSG
1001 NLVFPQDEVG RRVAQHPFTY ILNPAEKKSH TNGSSNGSSA AGSTATAAAV
1051 TTANGAKPKA PATPQAATSV TNPAAGDGIS VQNDPPVDSS GSPASPKKGK
1101 ANADDYAESF RDFQCSQIVK CELEMAEKIY NDVVAAHPKH LQANLLLIQN
1151 IESNQLKSQL PLTFVNAQKT SPPEAGESAD KQKEDQKKVR SALERIVKLA
1201 DKVIQETDSE ALLSYYGLKN DTRADAAKIK TNMDKQKNTL IEALSKKGIA
1251 VAKLAVLDDC IKDSLAEINE LYTEIIKFVD ANDSKAIQFA LWHAYAHGHY
1301 GRMYKYVVKL IEEKRTRDHF VELAAINGAL GHEHIRTVIN RMMITAFPSS
1351 FRLF
```

Figure 4.36. Amino acid sequence of *Drosophila* TPP II, and the matching tryptic peptides (bold red) of the 149 kDa protein in gel-band #1 in Figure 4.35.

A.

```
   1 MATSGIVESF PTGALVPKAE TGVLNFLQKY PEYDGRDVTI AIFDSGVDPR
  51 ATGLETLCDG KTVKVIERYD CSGCGDVDMK KKVTPDENGN IKGLSGNSLK
 101 LSPELMALNT DPEKAVRVGL KSFSDLLPSK VRNNIVAQAK LKHWDKPHKT
 151 ATANASRKIV EFESQNPGEA SKLPWDKKIL KENLDFELEM LNSYEKVYGD
 201 IKTSYDCILF PTADGWLTIV DTTEQGDLDQ ALRIGEYSRT HETRNVDDFL
 251 SISVNVHDEG NVLEVVGMSS PHGTHVSSIA SGNHSSRDVD GVAPNAKIVS
 301 MTIGDGRLGS METGTALVRA MTKVMELCRD GRRIDVINMS YGEHANWSNS
 351 GRIGELMNEV VNKYGVVWVA SAGNHGPALC TVGTPPDISQ PSLIGVGAYV
 401 SPQMMEAEYA MREKLPGNVY TWTSRDPCID GGQGVTVCAP GGAIASVPQF
 451 TMSKSQLMNG TSMAAPHVAG AVALLISGLK QQNIEYSPYS IKRAISVTAT
 501 KLGYVDPFAQ GHGLLNVEKA FEHLTEHRQS KDNMLRFSVR VGNNADKGIH
 551 LRQGVQRNSI DYNVYIEPIF YNDKEADPKD KFNFNVRLNL IASQPWVQCG
 601 AFLDLSYGTR SIAVRVDPTG LQPGVHSAVI RAYDTDCVQK GSLFEIPVTV
 651 VQPHVLESDQ NTPVFEPASS KGDNSVEFQP NTIQRDFILV PERATWAELR
 701 MRITDPNRGE DIGKFFVHTN QLLPKQSCRK LETMKIVSVG SENESIMAFK
 751 VKSGRILELC IAKYWSNYGQ SHLKYSLRFR GVEAHNPNAY VMHAGRGIHK
 801 LEIEALVAED VQPQLQLKNA EVVLKPTEAK ISPLSATRDV IPDGRQVYQN
 851 LLAFNLNVAK AADVSIYAPI FNDLLYEAEF ESQMWMLFDA NKALVATGDA
 901 HSHTSFTKLD KGEYTIRLQV RHEKRDLLEK ISEANLVASF KLTSPLTLDF
 951 YENYNQCIVG GRKYVSSPLR LSTRVLYIAP ITQERLTKAN LPAQCAWLSG
1001 NLVFPQDEVG RRVAQHPFTY ILNPAEKKSH TNGSSNGSSA AGSTATAAAV
1051 TTANGAKPKA PATPQAATSV TNPAAGDGIS VQNDPPVDSS GSPASPKKGK
1101 ANADDYAESF RDFQCSQIVK CELEMAEKIY NDVVAAHPKH LQANLLLIQN
1151 IESNQLKSQL PLTFVNAQKT SPPEAGESAD KQKEDQKKVR SALERIVKLA
1201 DKVIQETDSE ALLSYYGLKN DTRADAAKIK TNMDKQKNTL IEALSKKGIA
1251 VAKLAVLDDC IKDSLAEINE LYTEIIKFVD ANDSKAIQFG LWHAYAHGHY
1301 GRMYKYVVKL IEEKRTRDHF VELAAINGAL GHEHIRTVIN RMMITAFPSS
1351 FRLF
```

B.

```
1051 TTANGAKPKA PATPQAATSV TNPAAGDGIS VQNDPPVDSS GSPASPKKGK
1101 ANADDYAESF RDFQCSQIVK CELEMAEKIY NDVVAAHPKH LQANLLLIQN
1151 IESNQLKSQL PLTFVNAQKT SPPEAGESAD KQKEDQKKVR SALERIVKLA
1201 DKVIQETDSE ALLSYYGLKN DTRADAAKIK TNMDKQKNTL IEALSKKGIA
1251 VAKLAVLDDC IKDSLAEINE LYTEIIKFVD ANDSKAIQFG LWHAYAHGHY
1301 GRMYKYVVKL IEEKRTRDHF VELAAINGAL GHEHIRTVIN RMMITAFPSS
1351 FRLF
```

Figure 4.37. Amino acid sequence of *Drosophila* TPP II, and the matching tryptic peptides (bold red) of: A, 115 kDa fragment (gel-band #2 in Figure 4.35) and B, 31 kDa fragment (gel-band #6 in Figure 4.35). Residues S 1080 and S1095 (highlighted in grey) represent the end of the central domain and the start of the C-terminal domain respectively, according to the secondary structure predictions. Residues N 1054 and G1078 (highlighted in yellow) represent the end of the central domain and the start of the C-terminal domain respectively, as derived from the masses of the 115 kDa and 31 kDa TPP II fragments.

By mass spectrometry, all of the bands appearing in the SDS-gel in Figure 4.35 were shown to be TPP II fragments. As these fragments were observed in the Superose 6 fractions containing only holocomplexes, they must be products of proteolytic nicking which does not appear to affect the quaternary structure.

4.7.3 Preparation of TPP II tetramers and crystallization

TPP II tetramers to be used in the crystallization experiments were obtained by disassembling the oligomers prepared as described in Section 4.7.1. Size exclusion chromatography eluate pools p1 and p2 were both used in the crystallization studies, but here only the preparation in which p1 was used as a starting material and which resulted in formation of crystals is described. The oligomers (p1) were disassembled by treatment with 40 mM β-octyl glucoside (OG) at 0°C for eight days. The disassembly into tetramers was confirmed by size exclusion chromatography. The tetramers exhibited 56% of the spindle activity, which was in good agreement with the tetramer specific activities determined before (Section 4.6.4.2). To prevent reassembly, all the following steps were carried out in the presence of 40 mM OG. The tetramers were concentrated by ion exchange chromatography using a 1 ml HiTrap Q column (Section 3.4.16). The HiTrap Q eluate was pooled in two fractions: ep3-6, containing the front of the elution peak and having a TPP II concentration of 3.5 mg/ml and ep7-13, containing the tail of the elution peak with 2.3 mg/ml TPP II (Figure 4.38A). In order to minimize the buffer concentration and avoid an influence on the pH of the crystallization experiments, the samples were dialyzed against 25 mM Tris-SO_4 pH 7.5, 10 mM DTT, 5 % glycerol and 40 mM OG. After dialysis, the activity of the samples decreased from the initial 56% to about 25%. The decrease of activity was attributed to the low buffer concentration and/or to the absence of phosphate, since reduced activity was previously observed when potassium phosphate buffer at concentrations lower than 40 mM was used (data not shown).

To determine the oligomeric state of TPP II after concentration, aliquots of ep3-6 and ep7-13 were subjected to size exclusion chromatography. A single peak corresponding to tetramers was observed with both of the concentrated samples (Figure 4.38B), and the elution profile did not change after dialysis.

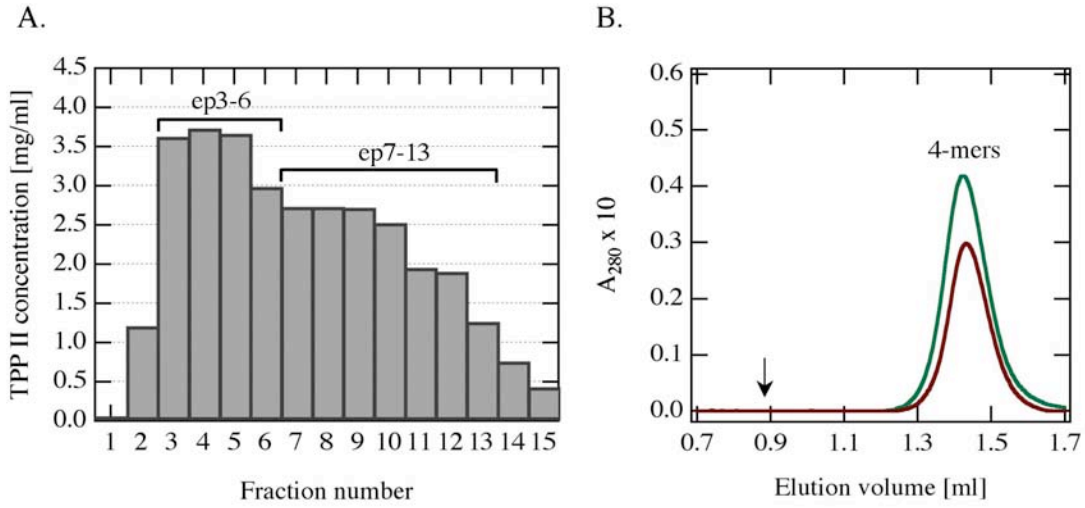

Figure 4.38 Concentration of TPP II tetramers by ion exchange chromatography, in the presence of β-octyl glucoside. A, HiTrap Q-eluate fractions; ep3-6, pool of fractions 3-6; ep7-13, pool of fractions 7-13. B, size exclusion chromatography of ep3-6 (green line) and ep7-13 (brown line) revealing the presence of tetramers. No oligomeric complexes (arrow) were observed.

The dialyzed fraction ep3-6, containing 3.5 mg/ml TPP II, was used for the crystallization experiments (Section 3.5.1), but did not produce crystals.

The dialyzed fraction ep7-13 was further concentrated to ~9.2 mg/ml by ultrafiltration using 100K MWCO centrifugal devices. No change in the specific activity was observed after this concentration step. The TPP II sample was analyzed by size exclusion chromatography, native PAGE and electron microscopy. In the well-resolved tetramer peak in Figure 4.39A, the presence of contaminating oligomeric forms can not be totally excluded. However, only tetramers were observed when the sample was analysed by native PAGE (Figure 4.39A inset). In the electron micrographs (Figure 4.39B) the tetramers displayed the characteristic trilobed orientation as shown before in Figure 4.33B.

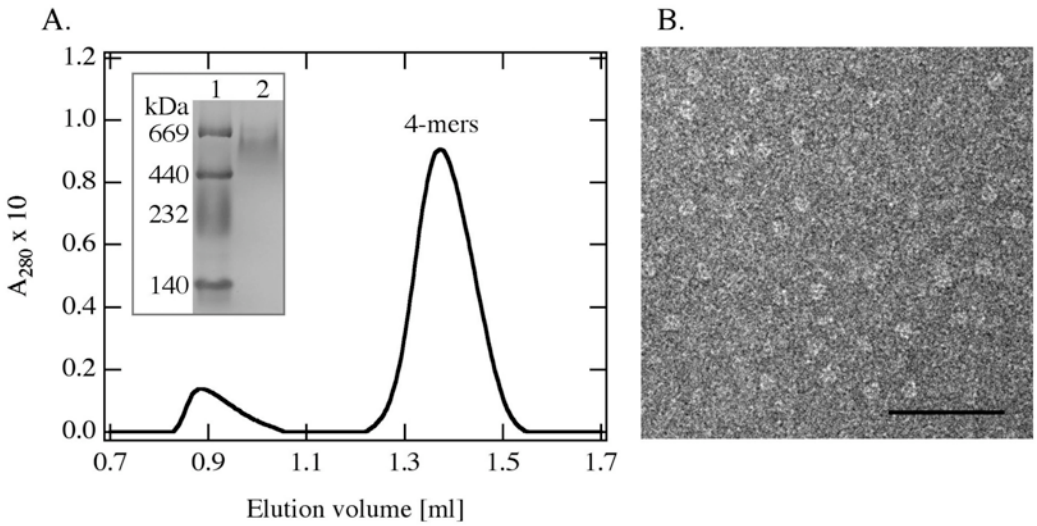

Figure 4.39. Sample ep7-13, containing TPP II tetramers at a concentration of ~9.2 mg/ml, used for crystallization. A, size exclusion chromatography; inset, native gel of ep7-13 (lane 2); lane 1, marker. B, electron micrograph of ep7-13; scale bar: 100 nm.

Sample ep7-13, containing TPP II tetramers at a concentration of 9.2 mg/ml, was used to set crystallization droplets (Section 3.5.1). After five months of incubation at 15°C, crystals of approximately 20 μm (Figure 4.40) grew in the setup where 5 % w/v PEG-2000 was used as precipitant. These crystals diffracted to about 20 Å resolution (Figure 4.40 C), which was not suitable for X-ray analysis. Nevertheless, establishment of an efficient protein expression/purification procedure and identification of the preliminary crystallization conditions is an essential starting point for obtaining better quality crystals of TPP II.

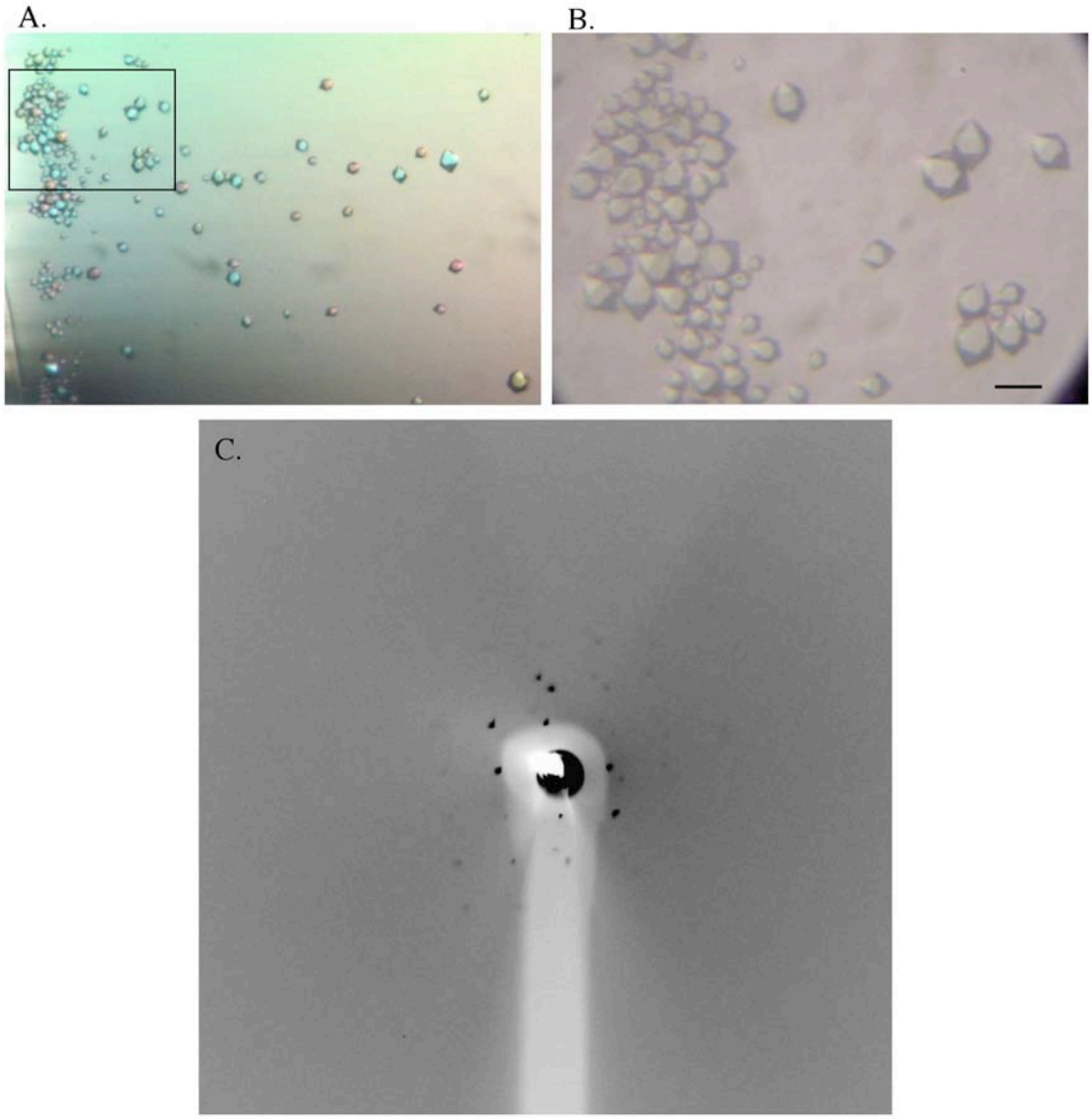

Figure 4.40. Crystallization of TPP II tetramers in the presence of β-octyl glucoside. A, crystals obtained after five months in hanging droplet containing 100 nl protein solution (9.2 mg/ml protein in 25 mM TrisSO_4 pH 7.5, 10 mM DTT, 5 % glycerol, 40 mM β-octyl glucoside) and 100 nl reservoir solution (5 % w/v PEG-2000), at 15°C. B, zoomed-in view of area enclosed by rectangle in A; scale bar: 20 μm. C, Diffraction pattern recorded at beamline PX10, SLS, by Dr. Kornelius Zeth – MPI for Developmental Biology, Tübingen. The resolution is ~ 20 Å.

5. Discussion

5.1 Over-expression of *Drosophila melanogaster* TPP II in *Escherichia coli*

In this study, a procedure for the recombinant expression of TPP II in *E. coli* was established. Previously, human embryonic kidney (HEK) 293 cells were used for the recombinant expression of TPP II, but the yields obtained were fairly low – about 0.5% of the total soluble protein (Renn et al., 1998). Moreover, the coexistence of native and recombinant TPP II subunits and their assembly into heterocomplexes led to data interpretation problems, especially in mutational studies (Hilbi et al., 2002; Tomkinson et al., 2002). These difficulties were overcome by over-expressing TPP II in *E. coli*. The expression yield of soluble TPP II in *E. coli* significantly depended on the conditions of cell growth and induction. Initially, the standard growth temperature of 37°C was used (data not shown), which did not yield soluble TPP II. Probably, the folding machinery of the cells could not cope with the rapid rate of protein production, leading to formation of inclusion bodies. Lower cultivation temperatures were expected to increase the yield of soluble protein in *E. coli*. Therefore, expression at 30, 25 and 18 °C (Section 4.1.1) was investigated. At 18°C, the amount of soluble TPP II was significantly higher than that obtained at 25 and 30 °C (Figure 4.2A). Thus, at low growth temperatures, the slower metabolism probably promoted the correct folding of the recombinant protein. The concentration of inducer (IPTG) was another parameter investigated for enhancing the solubility of the recombinant TPP II. Inducing the cells with 0.025 mM IPTG resulted in moderate expression levels (Figure 4.2B). When the IPTG concentration was increased to 1 mM, the amount of soluble protein was about the same as at 0.025 mM IPTG, but more insoluble protein was formed. The lower expression rate at 0.1 mM IPTG reduced the formation of insoluble protein, and gave the highest yield of soluble TPP II (Figure 4.2B). This result is in line with the conclusion on the temperature variation data.

In the expression experiments, Terrific broth (TB) was used as cultivation medium, which provided high cell densities. In the cultures grown in TB for 24 h, 4 fold higher cell densities were obtained, as compared to the cells grown in LB. Taken together, the

conditions chosen for routine expression of TPP II were: induction with 0.1 mM IPTG and growth in TB medium at 18°C for 24 h.

TPP II was found to associate with the cell debris after an initial cell disruption step. From the amino acid sequence of TPP II, no hydrophobic stretch compatible with a trans-membrane segment role was predicted. Thus, the nature of this binding is presently unknown. Interestingly, the same phenomenon was also observed in *Drosophila* eggs (Dr. Jürgen Peters unpublished data). The interaction must be fairly weak, since upon an additional homogenization step, the protein was released into the 2nd cell extract. This led to a substantial enrichment of the recombinant enzyme and provided a great ease in purification (see Section 5.2).

Under these conditions, TPP II expressed in soluble form amounted to ~10% of the total soluble protein in 2nd cell extract of *E. coli* (Section 4.2.2). For comparison, the native protein makes up ~0.05% of soluble protein in *Drosophila* egg lysate.

5.2 A novel approach to the purification of TPP II

Initially, TPP II was purified from *E. coli* using a purification method (approach I) involving three chromatographic steps (Section 4.2.1). Since only low yields of fully assembled complexes were obtained with this method, an alternative method (approach II) was developed (Section 4.2.2). The first step, PEI treatment of the 2nd cell extract of *E. coli*, was applied in order to remove the nucleic acids. Since addition of PEI increased the pH to 8.9, it resulted in disassembly of the TPP II oligomers into mainly tetramers. The disassembly products were reconstituted into predominantly spindles, upon concentration by ammonium sulphate precipitation. Owing to their high molecular mass of ≥6 MDa, the reassembled complexes were separated efficiently from all *E. coli* proteins by a single size exclusion chromatography step. The TPP II obtained was of high-purity as determined by SDS-PAGE and mass spectrometry. This simple and fast purification approach provided high amounts of recombinant protein – up to 50 mg of TPP II per preparation from 2.5 litres of *E. coli* culture – sufficient to be used in enzymological and structural characterization of TPP II.

5.3 Characterization of recombinant TPP II

5.3.1 Enzymological characterization of TPP II

H-Ala-Ala-Phe-aminomethyl-coumarin (AAF-AMC) has been a commonly used synthetic substrate for measuring the tripeptidase activity of TPP II (Geier et al., 1999; Glas et al., 1998; Hong et al., 2003; Seifert et al., 2003; Wang et al., 2000; Wray et al., 2002). The recombinant TPP II used in this study cleaved AAF-AMC with the same specific activity (21000 ± 1000 pmol x μg^{-1} x min^{-1}) as the native *Drosophila* TPP II (Rockel et al., 2005). The specific activity of mouse TPP II for AAF-AMC has been determined as 14700 pmol x μg^{-1} x min^{-1}, which is several orders of magnitude higher than that of the the tricorn protease (Tamura et al., 1996) or that of the 20S proteasome (51 pmol x μg^{-1} x min^{-1} with Suc-LLVY-AMC as substrate) (Geier et al., 1999).

The pH optimum of the recombinant enzyme was between 7.5 and 8.0, which is in agreement with the range determined as 7.5 - 7.8 for the native enzyme (Renn et al., 1998). The recombinant TPP II cleaved AAF-AMC with a K_m of 0.44 +/- 0.05 mM (Section 4.3). This value is in concurrence with the K_m of the native enzyme, which was determined as 0.47 +/- 0.07 mM (Seyit et al., 2006). This demonstrates that the TPP II complex formed in *E. coli* is not only morphologically but also functionally identical with the native complex.

5.3.2 Spindle formation is a self-assembly process

Spindle-shaped complexes of discrete length, displaying full activity, were formed in *E. coli*. Moreover, by ammonium sulphate precipitation, the spindles could also be reconstituted *in vitro* (Section 4.2.2). These observations indicate that spindle formation is a self-assembly process, which does not require length determining proteins or co-factors. Since *E. coli* does not express TPP II endogeneously, the co-purification of assembly-helper-proteins can be excluded. Therefore, the characteristic spindle shape of the TPP II complexes must be determined by the tertiary structure of component monomers only.

5.3.3 The spindle form stabilizes the activated state

When concentrated to ≥ 10 mg/ml, TPP II forms spindles with single or double stranded extensions (Figure 4.6). Thus, apparently, the length of component strands is not limited at

the spindle stage by sterical constrains. Since at close to physiological concentrations of 0.05 – 0.1 mg/ml the spindle conformation is, nevertheless, the preferred state of TPP II, spindles must be thermodynamically favoured (Seyit et al., 2006). The spindles showed higher resistance to GdnHCl treatment, than the single strands (Section 4.4). This provides evidence for the stabilization of the complexes upon formation of the inter-strand contacts. By electron microscopy it was shown that a double clamp – a resiprical interaction involving four dimeric subunits – is formed at each spindle pole (Rockel et al., 2005). In addition to the thermodynamic stability, such a clamp could also account for the kinetic stability of TPP II spindles (Rockel et al., 2005; Seyit et al., 2006).

In eukaryotic hosts, post-translational modifications might be involved in further stabilization of TPP II complexes. However, these modifications are apparently not crucial for the activation of the enzyme, since TPP II complexes obtained from *E. coli* displayed full activity.

5.3.4 His_6-tagging of TPP II monomers and its effect on assembly

In the presence of imidazole, although capable of spindle formation, the C-terminally His_6-tagged TPP II subunits displayed a higher propensity for dissociation than the untagged TPP II subunits (Section 4.5.2). Apparently, the addition of only 11 residues ($AAALEH_6$, corresponding to linker plus His_6-tag) at the C-terminus of TPP II polypeptide chain is sufficient to significantly alter the dissociation constants of the enzyme. Disassembly of the C-terminally tagged TPP II into dimers (Figure 4.11), suggested an involvement of the C-terminus in intra-strand contact formation. On the other hand, a His_6-tag at the N-terminus of TPP II did not impair the assembly of the complex (Section 4.5.1).

5.3.5 N-terminal maltose-binding protein tagging prevents spindle formation

The effect of an N-terminal bulky tag on complex formation was investigated. Maltose-binding protein (MBP) was chosen as a fusion partner for the following reasons: Firstly, unlike the N-terminal His_6-tag, which did not effect oligomerization (see above), the 42 kDa MBP is sufficiently large and thus more likely to introduce structural hindrance.

Secondly, MBP can be advantageous in terms of enhanced solubility, protection from proteolysis, improved folding and protein purification via affinity chromatography (Smyth et al., 2003).

The 192 KDa MBP-TPP II fusion was expressed as soluble protein in *E. coli* and purified by affinity chromatography (Section 4.5.3). The MBP fusion at the N-terminus of TPP II did not prevent the assembly of the subunits into single strands. However, as shown by electron microscopy (Figure 4.14B) no spindles were observed, demonstrating that the MBP-tag abolished the inter-strand contacts. This result shows that the N-terminal domains of TPP II subunits are oriented towards the inner side of the strands, where the strand-to-strands contacts are formed. Accordingly, the bulky parts of the segments in the 3D model in Figure 5.1 probably represent the N-terminal domains (Rockel et al., 2005).

The use of the MBP-tag enabled the isolation and characterization of unpaired single strands. The formation of the single strands demonstrated that strand assembly in principle can occur independently without prior formation of strand-to-strand contacts. When the MBP-tag was released by proteinase K cleavage (Rockel et al., 2005), spindles were formed. These observations allow speculations on an assembly mechanism of the complexes. The strands can grow separately and their length is determined by a combination of factors such as TPP II concentration and molecular crowding in the cell. When a sufficient number of monomers is reached, the two inter-strand contacts can be formed, leading to a stable spindle structure. This assembly model is supported by the fact that no “in-growth-spindles” of TPP II have been visualized so far, although it is also possible that those are formed only transiently and thus are not observed (Rockel et al., 2005).

Interestingly, the single strands had about the same specific molar activity for the hydrolysis of AAF-AMC as the wild-type spindles (Section 4.5.3). Thus, spindle formation does not have a detectable effect on the peptidase activity (Rockel et al., 2005).

5.4 Disassembly of the TPP II complexes for crystallization

Spindles are the predominant, but not the only oligomeric form observed in purified recombinant TPP II samples. As judged by electron microscopy, a significant amount of single strands and incomplete single strands co-exist with the spindles. Additionally, when TPP II is concentrated to ≥10 mg/ml, extended single strands, spindles with extensions at

the spindle poles and even multiple spindle complexes are also formed (Section 4.2.2, Figure 4.6). Owing to the linear concatameric architecture, the size of TPP II complexes is strongly concentration-dependent and not discrete. Due to this inherent heterogeneity in size, the oligomeric complexes were not suitable for crystallization. Therefore, a number of approaches for disassembling the oligomers into homogeneous and stable subunits were investigated systematically:

I) Mutational approach to disassembly
   a) Introduction of single or multiple point mutations
   b) Introduction of large C-terminal truncations
   c) Expression of the N- and C-terminal domains of TPP II separately

II) Disassembly by dialysis and cold treatment

III) Chemical approach to disassembly
   a) Reductive methylation of lysines
   b) β-octyl glucoside treatment

5.4.1 Mutational approach to disassembly

To overcome the obstacle of size heterogeneity, various mutational approaches to irreversibly prevent oligomerization, were investigated.

Homology alignments with other subtilases revealed an insert of ~200 amino acids within the catalytic domain of TPP II. A G252R mutation in this region was reported to prevent complex formation of human TPP II, and attempts to re-associate the mutant protein were unsuccessful (Tomkinson et al., 2002). Since the mutant protein was expressed in HEK 239 cells, due to the presence of endogenous wild type TPP II, the effect of this mutation could not be precisely established. Also, the recombinant mutant enzyme was suggested to form inactive dimers, but it was unknown whether these were formed by recombinant and endogenous monomers or if they were homo-dimers. To determine whether this mutation really can prevent assembly of TPP II irreversibly, the corresponding G260R mutation was introduced into *Drosophila* TPP II and the mutant protein was expressed in *E. coli*. In the cell extracts of *E. coli* the mutant protein occurred in various, enzymatically active assembly states, but unlike the wild type enzyme, no large numbers of spindles were observed (Section 4.6.1.1). This indicated that the assembly of the complexes was disfavoured as a result of the G260R mutation. However, upon concentration by

ammonium sulphate precipitation and subsequent size exclusion chromatography fully assembled and active spindles were observed as the dominating oligomeric form. The same result was obtained when the G252R mutant of human TPP II was over-expressed in *E. coli* and concentrated by ammonium sulphate precipitation. The concentration of TPP II from human cell culture (Tomkinson et al., 2002) may be inferred from volume activity data and the specific activity for human TPP II to be in the range of 0.1 - 0.5 mg/ml. This concentration is sufficient for the assembly of wild type TPP II but not the destabilized mutant protein complex. However, the concentration reached during ammonium sulphate precipitation of the recombinant *Drosophila* TPP II mutant (≥ 10 mg/ml) compensated for the reduced assembly constants of the G260R and G252R mutants (Seyit et al., 2006).

A homology model of the active site region of TPP II was built using the crystal structures of four subtilisn-like proteins (De Winter et al., 2005). According to this model, the 200 aa insert seems to be located at the surface of the N-terminal domain (De Winter et al., 2005). Therefore, it may participate in contact formation between the bulky (N-terminal) domains of TPP II subunits (see Figure 5.1).

Since a single residue exchange had a critical destabilizing effect on TPP II complexes, the point mutational approach for disassembly was pursued further. Single and multiple point mutations were introduced into MBP-tagged TPP II. Selected charged and conserved residues (Figure 4.15), which were considered likely to be involved in inter-subunit contact formation were mutated. Mutations other than G260R did not appear to have a destabilizing effect. However, when they were introduced in combination with the G260R mutation, both activity and structure were impaired irreversibly, and soluble, amorphous aggregates were formed (Figure 4.20).

The 3D model of TPP II complexes in Figure 5.1 points out three levels of assembly interactions: intra-dimer (between two monomers), inter-dimer (between the dimers in a strand) and inter-strand (between the two strands in a spindle). By introducing a MBP-tag, the inter-strand interaction was abolished. However, large subunit surfaces seem to be involved in formation of the inter-dimer and intra-dimer contacts (see Figure 5.1), and thus, without knowledge of the 3D structure it is not possible to predict the combination of the key residues. Therefore, instead of introducing point mutations, the effect of large C-terminal truncations (59, 82 or 138 residues) was investigated. The truncated variants of TPP II formed soluble aggregates, probably because of the new hydrophobic surfaces

introduced upon truncation. Interestingly, although the truncated proteins contained the catalytic domain, they were inactive. As the dimers are the smallest active unit (Seyit et al., 2006; Tomkinson, 2000) of TPP II, the loss of activity might have resulted from the lack of dimerization. Just like the truncation mutants, separately expressed catalytic, N-terminal domain (residues 1-526) was also inactive and aggregated. Therefore, the C-terminal domain appears to be essential for the formation of the active enzyme and its presence is a prerequisite for correct folding and assembly of TPP II.

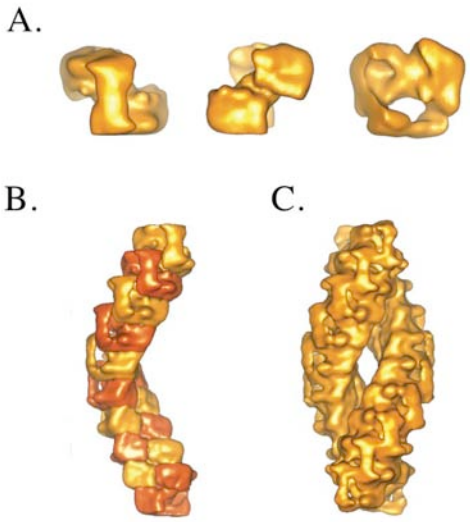

Figure 5.1. Surface representations of TPP II showing the different stages of oligomerization (Rockel et al., 2006). A, different orientations of a computationally excised dimer. B, computationally excised single strand. The segments (dimers) are shown in altering colouring to emphasize their interdigitation. C, TPP II holocomplex.

5.4.2 Disassembly by dialysis and cold treatment

TPP II purified from human erythrocytes has been reported to disassemble when dialysed against low ionic strength buffer, at 4°C (Macpherson et al., 1987). The size of the disassembly products decreased with increasing dialysis time. The disassembly was attributed to the low ionic strength and/or low glycerol concentration of the buffer (Macpherson et al., 1987). Disassembly upon dialysis at 4°C was observed with the recombinant *Drosophila* TPP II, as well (Section 4.6.3), resulting in tetramers. Interestingly, disassembly into tetramers also occurred when recombinant TPP II was incubated at 4°C without dialysis, or when it was subjected to native PAGE at 4°C.

Therefore, recombinant TPP II oligomers appear to be cold labile. It is as yet unclear why the major disassembly product of the recombinant *Drosophila* TPP II is the tetramer, whereas human TPP II disassembles into mainly dimers (Harris and Tomkinson, 1990; Tomkinson, 2000).

The disassembly of human TPP II has been shown to be reversible, since the low oligomeric forms could be reassociatead *in vitro*, in a concentration dependent manner (Tomkinson, 2000). The same behaviour was observed with recombinant *Drosophila* TPP II. When concentrated to ~5 mg/ml, the disassembly products resulting from the cold treatment reassembled into complexes. Thus, to achieve irreversible disassembly, chemical modification of TPP II was investigated.

5.4.3 Chemical approach to disassembly

Introducing multiple mutations or deletions into the polypeptide chain of TPP II led to the formation of soluble aggregates. Therefore, in order to preserve the native tertiary structure it seems necessary to use full length, wild type TPP II for further disassembly experiments. However, the disassembly achieved by introducing the G260R mutation or by cold treatment is reversible, and depended on the protein concentration. Thus, the aim of the chemical approach was to prevent assembly irreversibly by modifying the molecular interactions of the subunits. Beneficially, unlike the mutational approach, the chemical modification approach does not require previous knowledge of the 3D structure of the protein.

5.4.3.1 Disassembly by reductive methylation of lysines

Lysines are found predominantly on the surface of proteins (Baud and Karlin, 1999). Therefore, methylation of lysine side chains was exploited with the aim to reduce their interactions and prevent assembly of the subunits. The methylation reaction can be carried out in a highly specific manner, so that no new heterogeneity is introduced to the protein (Rayment, 1997). Moreover, methylation of the accessible side chains and the N-terminal amino group has been shown to promote crystal growth, as a result of altering the surface properties of proteins. The technique has been critical for obtaining X-ray quality crystals of the myosin subfragment-1 (Rayment et al., 1993) and has been successfully applied to

several other proteins as well (Kurinov et al., 2000; Kurinov and Uckun, 2003; Rypniewski et al., 1993).

Disassembly into dimers was observed when reductive methylation of TPP II complexes was carried out for 30, 40 and 90 min. The best result was obtained when the reactions were carried out for 90 min, as judged from the symmetric size exclusion chromatography peak and native-gel (Figure 4.30) of the methylated TPP II. The disassembly was accompanied by a decrease of specific activity to 7% of the full spindle activity. This value is close to the expected dimer specific activity, which is 8-10% of that of the holocomplexes (Seyit et al., 2006; Tomkinson, 2000).

The structure of methylated lysozyme has been shown to be essentially identical to that of the native protein (Rypniewski et al., 1993). According to this, and from the presence of enzymatic activity, at the present degree of methylation, the native structure of TPP II dimers is probably preserved.

According to the size exclusion chromatography and native-gel data in Figure 4.30, methylated TPP II seems to be homogeneous in terms of size. In the electron micrographs, although similar in size, disassembled particles do not display a uniform conformation. This may be due to the random orientation and/or conformational flexibility of the dimers (see Figure 5.1A).

It is important to note that a variable degree of modification can introduce additional heterogeneity into the protein. Therefore, to ensure that a homogeneous population of protein is achieved at the end of the process, a quantitative amino acid analysis is necessary to determine the number of non-, mono-, di-, and tri-methylated lysine residues.

Attempts to crystallize the methylated TPP II dimers did not yield crystals. Nevertheless, since the disassembly achieved by reductive methylation was irreversible even at high TPP II concentrations (~5 mg/ml), the approach is worth further investigation.

5.4.3.2 Disassembly by β-octyl glucoside treatment

β-octyl glucoside (OG) has been commonly used in the crystallization of membrane proteins. It binds to the hydrophobic regions of the membrane proteins and provides their solubility in an aqueous environment. OG was successfully used in the crystallization of soluble proteins as well (McPherson et al., 1986), where it minimized non-specific hydrophobic interactions and aggregation. Also, OG inhibited the *in vitro* self-assembly of

tubulin into microtubules (Andreu, 1982). Thus, in this study, OG was used to establish whether it could disassemble TPP II oligomers by modifying the hydrophobic interactions between the subunits. OG was chosen for the advantages of having a defined chemical structure, small uniform micelles, high water solubility and high critical micelle concentration (CMC: ~15 mM). As revealed by size exclusion chromatography in Figure 4.31, TPP II complexes efficiently disassembled into tetramers when treated with OG at a concentration of 40 mM (≥ 2 CMC). At this concentration saturation must have been reached since the detergent was in large molar excess over TPP II (24 x 10^3 mol OG per mol TPP II tetramer). In the presence of OG, the tetramers exhibited specific activity corresponding to ~60% of the full spindle activity. This was in good agreement with the expected tetramer activity, which was determined as 54% in the absence of OG (Seyit et al., 2006). Therefore, OG apparently does not have an adverse effect on the native structure of the tetramers.

It is important to note that i) the cold sensitivity of recombinant TPP II, which leads to disassembly even in the absence of OG (see Section 5.4.2), must have facilitated or perhaps enabled the effect of OG and ii) the degree of disassembly critically depended on the length of incubation time, confirming that disassembly is a slow process as shown previously (Seyit et al., 2006).

The disassembled tetramers did not reassemble when concentrated to 5 mg/ml in the presence of OG, as judged by size exclusion chromatography (Figure 4.33). On the electron micrographs, unlike in the "non-chemical" disassembly attempts, the majority of methylated TPP II particles seem to be homogenous in size and no higher oligomers or amorphous aggregates are observed. Consequently, the disassembly of the oligomers by OG treatment seems to be a promising approach for obtaining stable TPP II subunits of a discrete size.

5.5 Crystallization of TPP II

5.5.1 TPP II tetramers as candidates for crystallization

The major disassembly product of human TPP II is the dimer (Harris and Tomkinson, 1990; Tomkinson, 2000). Recombinant *Drosophila* TPP II disassembled into dimers upon

C-terminal His_6-tagging and methylation, whereas upon PEI/pH 8.9, cold or OG treatment, the most abundant disassembly state was the tetramer. Tetramers are good candidates for crystallization for the following reasons: Firstly, tetramers contain the structural information of both, how the monomers are connected in a dimer, and how dimers are connected in a TPP II strand (Figure 5.2). Secondly, according to the proposed activation model (Seyit et al., 2006), tetramers contain two fully active monomers, whereas dimers have monomers with only basal activity (Figure 5.2). Thus, tetramers also contain the structural information of how the active sites are arranged in the TPP II oligomers. Thirdly, the 3D model of a single strand (Figure 5.2 inset) shows that the tetramers have much larger contact area between the bulky domains of the subunits, compared to the dimers. Consequently, tetramers are expected to be conformationally more stable than dimers.

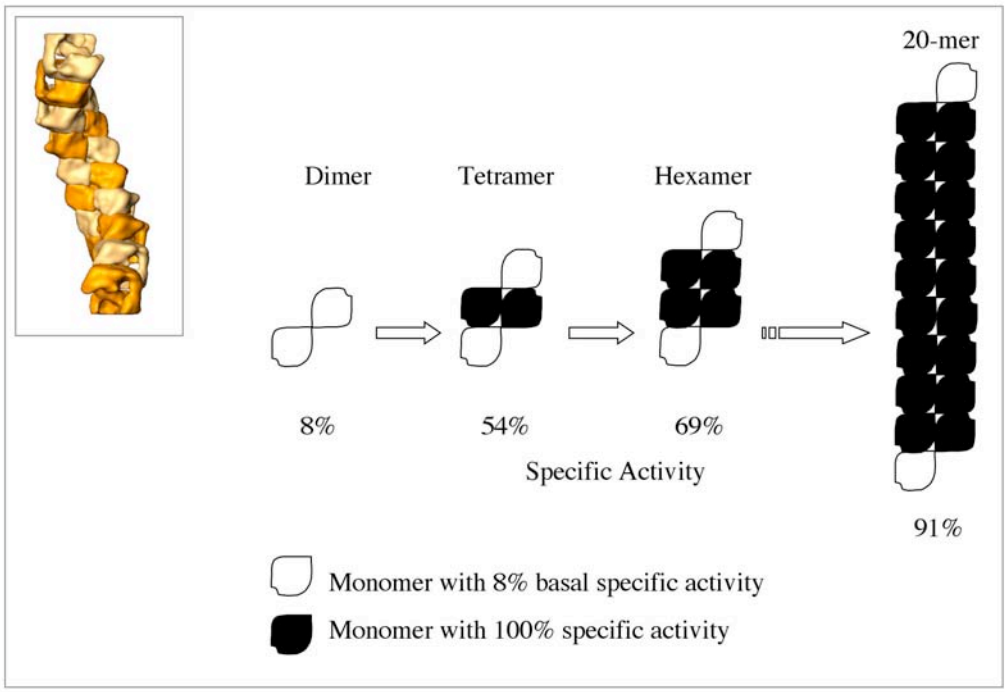

Figure 5.2. Structural organization of TPP II subunits and their equilibrium specific activities (Seyit et al., 2006). The tetramer is the smallest assembly form to contain fully active monomers. Schematic representations were derived from the 3D-model (inset) of a TPP II single strand.

5.5.2 Crystallization of TPP II tetramers

TPP II to be used in the crystallization experiments was prepared as described in Section 4.7.1, and shown to be of high-purity by mass spectrometry (Section 4.7.2). As a result of

the mass spectrometrical analysis of a 115 kDa fragment of TPP II, a region adjacent to the C-terminal domain boundary was found to be susceptible to proteolytic cleavage, without affecting the tertiary structure of the TPP II complexes. The cleavage was observed not only with recombinant TPP II but also with the native enzyme purified from *Drosophila* (Rockel et al., 2002). The region where the cleavage occurs coincides with a C-terminal loop present only in *Drosophila* TPP II and not in other homologues (Figure 4.15). Presently, it is not possible to predict how the cleavage of this loop might affect crystallization of TPP II. Proteolytic nicking may result in disordering some regions but need not necessarily hamper crystallization. It might even have a positive effect if disordered loops, which are exposed on the surface of the TPP II complexes, are eliminated by proteolysis.

Following purity assessment of TPP II, the next step of sample preparation for the crystallization experiments was the disassembly of the TPP II oligomers into tetramers by treatment with OG. This approach enabled concentration of TPP II to 9.2 mg/ml, without leading to re-association (Figure 4.39). It is presently unknown how OG prevents oligomerization. Probably, OG "shields" the hydrophobic contact regions of the subunits. OG saturation must be obtained at 12g OG / g protein (when 40 mM OG was used), since increasing the OG to 18g OG / g protein did not result in further disassembly. Even when TPP II tetramers were concentrated to 9.2 mg/ml, OG was in large molar excess over TPP II (26×10^2 mol OG per mol TPP II tetramer).

Crystals of TPP II were obtained from a solution containing polyethylene glycol 2000 (PEG-2000) as precipitating agent. Besides disassembly, the presence of OG might have aided crystal formation as well. It was demonstrated that the inclusion of OG was beneficial in improving crystal growth, and in some cases, in obtaining new crystal forms of soluble proteins (McPherson et al., 1986). In the same study, the authors have found that the effect of OG is more pronounced when PEG is used as precipitant in the crystallization drops, which is in accordance with the result obtained with TPP II. In addition to the crystals shown in Figure 4.40, some microcrystals were also observed when PEG-2000 or PEG-4000 were used as precipitant. Better crystals might be obtained by a more comprehensive search for optimal conditions using various concentrations of OG and PEG.

6. Literature

Andreu, J. M. (1982). Interaction of tubulin with non-denaturing amphiphiles. EMBO Journal *1*, 1105-1110.

Balow, R. M., and Eriksson, I. (1987). Tripeptidyl peptidase II in haemolysates and liver homogenates of various species. Biochemical Journal *241*, 75-80.

Balow, R. M., Ragnarsson, U., and Zetterqvist, O. (1983). Tripeptidyl aminopeptidase in the extralysosomal fraction of rat liver. Journal of Biological Chemistry *258*, 11622-11628.

Balow, R. M., Tomkinson, B., Ragnarsson, U., and Zetterqvist, O. (1986). Purification, substrate specificity, and classification of tripeptidyl peptidase II. Journal of Biological Chemistry *261*, 2409-2417.

Baud, F., and Karlin, S. (1999). Measures of residue density in protein structures. Proceedings of the National Academy of Sciences of the United States of America *96*, 12494-12499.

Baumeister, W., Walz, J., Zühl, F., and Seemüller, E. (1998). The proteasome - paradigm of a self-compartmentalizing protease. Cell *92*, 367-380.

Book, A. J., Yang, P. Z., Scalf, M., Smith, L. M., and Vierstra, R. D. (2005). Tripeptidyl peptidase II. An oligomeric protease complex from Arabidopsis. Plant Physiology *138*, 1046-1057.

Borissenko, L., and Groll, M. (2005). Crystal structure of TET protease reveals complementary protein degradation pathways in prokaryotes. Journal of Molecular Biology *346*, 1207-1219.

Breslin, H. J., Miskowski, T. A., Kukla, M. J., De Winter, H. L., Somers, M. V. F., Roevens, P. W. M., and Kavash, R. W. (2003). Tripeptidyl-peptidase II (TPP II) inhibitory activity of (S)-2,3-dihydro-2-(1H-imidazol-2-yl)-1H-indoles, a systematic SAR evaluation. Part 2. Bioorganic & Medicinal Chemistry Letters *13*, 4467-4471.

Breslin, H. J., Miskowski, T. A., Kukla, M. J., Leister, W. H., De Winter, H. L., Gauthier, D. A., Somers, M. V., Peeters, D. C., and Roevens, P. W. (2002). Design, synthesis, and tripeptidyl peptidase II inhibitory activity of a novel series of (S)-2,3-dihydro-2-(4-alkyl-1H-imidazol-2-yl)-1H-indoles. Journal of Medicinal Chemistry *45*, 5303-5310.

Burri, L., Servis, C., Chapatte, L., and Levy, F. (2002). A recyclable assay to analyze the NH2-terminal trimming of antigenic peptide precursors. Protein Expression and Purification *26*, 19-27.

Chand, A., Wyke, S. M., and Tisdale, M. J. (2005). Effect of cancer cachexia on the activity of tripeptidyl-peptidase II in skeletal muscle. Cancer Letters *218*, 215-222.

Ciechanover, A. (2005). Proteolysis: from the lysosome to ubiquitin and the proteasome. Nature Reviews Molecular Cell Biology *6*, 79-86.

Ciehanover, A., , Hod, Y., , and Hershko, A. (1978). A heat-stable polypeptide component of an ATP-dependent proteolytic system from reticulocytes. Biochemical and Biophysical Research Communications *81*, 1100-1105.

De Vos, W. M., Voorhorst, W. G., Dijkgraaf, M., Kluskens, L. D., Van der Oost, J., and Siezen, R. J. (2001). Purification, characterization, and molecular modeling of pyrolysin and other extracellular thermostable serine proteases from hyperthermophilic microorganisms. Methods in Enzymology *330*, 383-393.

De Winter, H., Breslin, H., Miskowski, T., Kavash, R., and Somers, M. (2005). Inhibitor-based validation of a homology model of the active-site of tripeptidyl peptidase II. Journal of Molecular Graphics & Modelling *23*, 409-418.

Ganellin, C. R., Bishop, P. B., Bambal, R. B., Chan, S. M., Leblond, B., Moore, A. N., Zhao, L., Bourgeat, P., Rose, C., Vargas, F., and Schwartz, J. C. (2005). Inhibitors of tripeptidyl peptidase II. 3. Derivation of butabindide by successive structure optimizations leading to a potential general approach to designing exopeptidase inhibitors. Journal of Medicinal Chemistry *48*, 7333-7342.

Gavioli, R., Frisan, T., Vertuani, S., Bornkamm, G. W., and Masucci, M. G. (2001). c-myc overexpression activates alternative pathways for intracellular proteolysis in lymphoma cells. Nature Cell Biology *3*, 283-288.

Geier, E., Pfeifer, G., Wilm, M., Lucchiari-Hartz, M., Baumeister, W., Eichmann, K., and Niedermann, G. (1999). A giant protease with potential to substitute for some functions of the proteasome. Science *283*, 978-981.

Glas, R., Bogyo, M., McMaster, J. S., Gaczynska, M., and Ploegh, H. L. (1998). A proteolytic system that compensates for loss of proteasome function. Nature *392*, 618-622.

Harris, J. R., and Tomkinson, B. (1990). Electron-Microscopic and Biochemical-Studies on the Oligomeric States of Human Erythrocyte Tripeptidyl Peptidase .2. Micron and Microscopica Acta *21*, 77-89.

Hasselgren, P. O., Wray, C., and Mammen, J. (2002). Molecular regulation of muscle cachexia: It may be more than the proteasome. Biochemical & Biophysical Research Communications *290*, 1-10.

Herberts, C., Reits, E., and Neefjes, J. (2003). Proteases, proteases and proteases for presentation. Nature Immunology *4*, 306-308.

Hilbi, H., Jozsa, E., and Tomkinson, B. (2002). Identification of the catalytic triad in tripeptidyl-peptidase II through site-directed mutagenesis. Biochimica Et Biophysica Acta-Proteins and Proteomics *1601*, 149-154.

Hong, X., Lei, L., and Glas, R. (2003). Tumors acquire inhibitor of apoptosis protein (IAP)-mediated apoptosis resistance through altered specificity of cytosolic proteolysis. Journal of Experimental Medicine *197*, 1731-1743.

Kisselev, A. F., Akopian, T. N., Woo, K. M., and Goldberg, A. L. (1999). The sizes of peptides generated from protein by mammalian 26 and 20 S proteasomes - Implications for understanding the degradative mechanism and antigen presentation. Journal of Biological Chemistry *274*, 3363-3371.

Kloetzel, P. M. (2004). Generation of major histocompatibility complex class I antigens: functional interplay between proteasomes and TPPII. Nature Immunology *5*, 661-669.

Kloetzel, P. M., and Ossendorp, F. (2004). Proteasome and peptidase function in MHC-class-I-mediated antigen presentation. Current Opinion in Immunology *16*, 76-81.

Kurinov, I. V., Mao, C., Irvin, J. D., and Uckun, F. M. (2000). X-ray crystallographic analysis of pokeweed antiviral protein-II after reductive methylation of lysine residues. Biochemical & Biophysical Research Communications *275*, 549-552.

Kurinov, I. V., and Uckun, F. M. (2003). High resolution X-ray structure of potent anti-HIV pokeweed antiviral protein-III. Biochemical Pharmacology *65*, 1709-1717.

Levy, F., Burri, L., Morel, S., Peitrequin, A. L., Levy, N., Bachi, A., Hellman, U., Van den Eynde, B. J., and Servis, C. (2002). The final N-terminal trimming of a subaminoterminal proline-containing HLA class I-restricted antigenic peptide in the cytosol is mediated by two peptidases. Journal of Immunology *169*, 4161-4171.

Macpherson, E., Tomkinson, B., Balow, R. M., Hoglund, S., and Zetterqvist, O. (1987). Supramolecular structure of tripeptidyl peptidase II from human erythrocytes as studied by electron microscopy, and its correlation to enzyme activity. Biochemical Journal *248*, 259-263.

McPherson, A., Koszelak, S., Axelrod, H., Day, J., Williams, R., Robinson, L., McGrath, M., and Cascio, D. (1986). An experiment regarding crystallization of soluble proteins in the presence of beta-octyl glucoside. Journal of Biological Chemistry *261*, 1969-1975.

Princiotta, M. F., Schubert, U., Chen, W., Bennink, J. R., Myung, J., Crews, C. M., and Yewdell, J. W. (2001). Cells adapted to the proteasome inhibitor 4-hydroxy- 5-iodo-3-nitrophenylacetyl-Leu-Leu-leucinal-vinyl sulfone require enzymatically active proteasomes for continued survival. Proceedings of the National Academy of Sciences of the United States of America *98*, 513-508.

Qiagen (2003). The QIAexpressionist, 5th edn, Qiagen.

Rayment, I. (1997). Reductive alkylation of lysine residues to alter crystallization properties of proteins. Methods in Enzymology *276*, 171-179.

Rayment, I., Rypniewski, W. R., Schmidt-Base, K., Smith, R., Tomchick, D. R., Benning, M. M., Winkelmann, D. A., Wesenberg, G., and Holden, H. M. (1993). Three-dimensional structure of myosin subfragment-1: a molecular motor. Science *261*, 50-58.

Reits, E., Neijssen, J., Herberts, C., Benckhuijsen, W., Janssen, L., Drijfhout, J. W., and Neefjes, J. (2004). A major role for TPPII in trimming proteasomal degradation products for MHC class I antigen presentation. Immunity *20*, 495-506.

Renn, S. C. P., Tomkinson, B., and Taghert, P. H. (1998). Characterization and cloning of tripeptidyl peptidase ii from the fruit fly, drosophila melanogaster. Journal of Biological Chemistry *273*, 19173-19182.

Rockel, B., Bosch, J., and Baumeister, W. (2006). Structural studies of large, self-compartmentalizing proteases, Vol 2 (Weinheim, WILEY-VCH).

Rockel, B., Peters, J., Kühlmorgen, B., Glaeser, R. M., and Baumeister, W. (2002). A giant protease with a twist: the TPP II complex from Drosophila studied by electron microscopy. Embo Journal *21*, 5979-5984.

Rockel, B., Peters, J., Muller, S. A., Seyit, G., Ringler, P., Hegerl, R., Glaeser, R. M., and Baumeister, W. (2005). Molecular architecture and assembly mechanism of Drosophila tripeptidyl peptidase II. Proceedings of the National Academy of Sciences of the United States of America *102*, 10135-10140.

Rose, C., Vargas, F., Facchinetti, P., Bourgeat, P., Bambal, R. B., Bishop, P. B., Chan, S. M. T., Moore, A. N. J., Ganellin, C. R., and Schwartz, J. C. (1996). Characterization and inhibition of a cholecystokinin-inactivating serine peptidase. Nature *380*, 403-409.

Rypniewski, W. R., Holden, H. M., and Rayment, I. (1993). Structural consequences of reductive methylation of lysine residues in hen egg white lysozyme - an x-ray analysis at 1.8-angstrom resolution. Biochemistry *32*, 9851-9858.

Sambrook, J., Fritsch, E. F., and Maniatis, T. (2001). Molecular Cloning (Cold Spring Harbour, NY, Cold Spring Harbour Laboratory Press).

Saveanu, L., Carroll, O., Hassainya, Y., and van Endert, P. (2005). Complexity, contradictions, and conundrums: studying post-proteasomal proteolysis in HLA class I antigen presentation. Immunological Reviews *207*, 42-59.

Schagger, H., and von Jagow, G. (1987). Tricine-sodium dodecyl sulfate-polyacrylamide gel electrophoresis for the separation of proteins in the range from 1 to 100 kDa. Analytical Biochemistry *166*, 368-379.

Schoenheimer, R. (1942). The Dynamic State of Body Constituents, Harvard University Press, Cambridge, MA.

Seifert, U., Maranon, C., Shmueli, A., Desoutter, J. F., Wesoloski, L., Janek, K., Henklein, P., Diescher, S., Andrieu, M., de la Salle, H., *et al.* (2003). An essential role for tripeptidyl peptidase in the generation of an MHC class I epitope. Nature Immunology *4*, 375-379.

Seyit, G., Rockel, B., Baumeister, W., and Peters, J. (2006). Size matters for the tripeptidylpeptidase II complex from Drosophila - The 6-MDa spindle form stabilizes the activated state. Journal of Biological Chemistry *281*, 25723-25733.

Siezen, R. J., and Leunissen, J. A. M. (1997). Subtilases - the superfamily of subtilisin-like serine proteases. Protein Science *6*, 501-523.

Smyth, D. R., Mrozkiewicz, M. K., McGrath, W. J., Listwan, P., and Kobe, B. (2003). Crystal structures of fusion proteins with large-affinity tags. Protein Science *12*, 1313-1322.

Spurlino, J. C., Lu, G. Y., and Quiocho, F. A. (1991). The 2.3-A resolution structure of the maltose- or maltodextrin-binding protein, a primary receptor of bacterial active transport and chemotaxis. Journal of Biological Chemistry *266*, 5202-5219.

Tamura, T., Tamura, N., Cejka, Z., Hegerl, R., Lottspeich, F., and Baumeister, W. (1996). Tricorn protease - the core of a modular proteolytic system. Science *274*, 1385-1389.

Tenzer, S., Peters, B., Bulik, S., Schoor, O., Lemmel, C., Schatz, M. M., Kloetzel, P. M., Rammensee, H. G., Schild, H., and Holzhutter, H. G. (2005). Modeling the MHC class I pathway by combining predictions of proteasomal cleavage, TAP transport and MHC class I binding. Cellular & Molecular Life Sciences *62*, 1025-1037.

Tomkinson, B. (1994). Characterization of cDNA for murine tripeptidyl-peptidase II reveals alternative splicing. Biochemical Journal *304*, 517-523.

Tomkinson, B. (1995). Characterization of cDNA for murine tripeptidyl-peptidase II reveals alternative splicing.[erratum for Biochem J. 1994 Dec 1;304 (Pt 2):517-23; PMID: 7998988]. Biochemical Journal *306*, 15.

Tomkinson, B. (2000). Association and dissociation of the tripeptidyl-peptidase II complex as a way of regulating the enzyme activity. Archives of Biochemistry and Biophysics *376*, 275-280.

Tomkinson, B. (2004). Tripeptidyl-peptidase II. In Handbook of Proteolytic Enyzmes, A. J. Barrett, N. D. Rawlings, and J. F. Woessner, eds. (London, Elsevier), pp. 1882-1885.

Tomkinson, B., Hansen, M., and Cheung, W. F. (1997). Structure-function studies of recombinant murine tripeptidyl-peptidase II: the extra domain which is subject to alternative splicing is involved in complex formation. FEBS Letters *405*, 277-280.

Tomkinson, B., and Jonsson, A. K. (1991). Characterization of cDNA for human tripeptidyl peptidase II: the N-terminal part of the enzyme is similar to subtilisin. Biochemistry *30*, 168-174.

Tomkinson, B., Laoi, B. N., and Wellington, K. (2002). The insert within the catalytic domain of tripeptidyl-peptidase II is important for the formation of the active complex. European Journal of Biochemistry *269*, 1438-1443.

Tomkinson, B., and Lindas, A. C. (2005). Tripeptidyl-peptidase II: A multi-purpose peptidase. International Journal of Biochemistry & Cell Biology *37*, 1933-1937.

Tomkinson, B., Wernstedt, C., Hellman, U., and Zetterqvist, O. (1987). Active site of tripeptidyl peptidase II from human erythrocytes is of the subtilisin type. Proceedings of the National Academy of Sciences of the United States of America *84*, 7508-7512.

Walz, J., Tamura, T., Tamura, N., Grimm, R., Baumeister, W., and Koster, A. J. (1997). Tricorn protease exists as an icosahedral supermolecule in vivo. Molecular Cell *1*, 59-65.

Wang, E. W., Kessler, B. M., Borodovsky, A., Cravatt, B. F., Bogyo, M., Ploegh, H. L., and Glas, R. (2000). Integration of the ubiquitin-proteasome pathway with a cytosolic oligopeptidase activity. Proceedings of the National Academy of Sciences of the United States of America *97*, 9990-9995.

Wang, W. Y., and Malcolm, B. A. (1999). Two-stage PCR protocol allowing introduction of multiple mutations, deletions and insertions using QuikChange (TM) site-directed mutagenesis. Biotechniques *26*, 680-682.

Wilson, C., Gibson, A. M., and McDermott, J. R. (1993). Purification and characterization of Tripeptidylpeptidase II from post-mortem human brain. Neurochemical Research *18*, 743-749.

Wray, C. J., Tomkinson, B., Robb, B. W., and Hasselgren, P. O. (2002). Tripeptidyl-peptidase II expression and activity are increased in skeletal muscle during sepsis. Biochemical and Biophysical Research Communications *296*, 41-47.

York, I. A., Bhutani, N., Zendzian, S., Goldberg, A. L., and Rock, K. L. (2006). Tripeptidyl peptidase II is the major peptidase needed to trim long antigenic precursors, but is not required for most MHC class I antigen presentation. Journal of Immunology *177*, 1434-1443.

7. Acknowledgements

I would like to express the deepest appreciation to Prof. Dr. Wolfgang Baumeister for his trust and for the opportunity to work in his department.

Special thanks should be given to Dr. Jürgen Peters and Dr. Beate Rockel for the invaluable support and guidance during this work.

I would also like to thank Prof. Dr. Bing Jap for the collaboration on the TPP II project and for his supervision during my stay in Berkeley.

I gratefully acknowledge Mrs. Brigitte Kühlmorgen for the many electron microscopy images of TPP II.

Many thanks to Prof. Dr. Andrei Lupas and Dr. Peter Zwickl for their scientific support and advice and to Dr. Kornelius Zeth for the constructive discussions and ideas.

I also owe many thanks to the colleagues at Max Planck Institute for the pleasant working atmosphere.

I am most grateful to my parents and my brother for their endless love and support.
Sevgili aileme, sonsuz sevgi ve destekleri için en içten tesekkürler.